DESIGN OF FUZZY LOGIC CONTROLLER FOR ANTI-SWAY CONTROL OF TOWER CRANE UNDER DISTURBANCE

MSC THESIS

WELDAY MEBRAHTU GEBRESLASSIE

HAWASSA UNIVERSITY, HAWASSA, ETHIOPIA

JULY, 2020

DESIGN OF FUZZY LOGIC CONTROLLER FOR ANTI-SWAY CONTROL OF TOWER CRANE UNDER DISTURBANCE

WELDAY MEBRAHTU GEBRESLASSIE

A THESIS SUBMITTED TO THE
DEPARTMENT OF ELECTRICAL AND COMPUTER ENGINEERING,
HAWASSA INSTITUTE OF TECHNOLOGY,

SCHOOL OF GRADUATE STUDIES

HAWASSA UNIVERSITY

HAWASSA, ETHIOPIA

IN PARTIAL FULFILLMENT OF THE

REQUIREMENTS FOR THE

DEGREE OF

MASTER OF SCIENCE IN ELECTRICAL AND COMPUTER ENGINEERING
(CONTROL AND INSTRUMENTATION ENGINEERING)

JULY, 2020

Declaration

I hereby declare that this MSc thesis entitled **"Design of Fuzzy Logic Controller for Anti-Sway Control of Tower Crane under Disturbance"** is my original work and has not been presented for a degree in any other university, and will not be presented by me to any other university for similar or any other degree award, and all sources of material used for this thesis have been duly acknowledged.

Name: Welday Mebrahtu

Signature: _____

This MSc thesis entitled **"Design of Fuzzy Logic Controller for Anti-Sway Control of Tower Crane under Disturbance"** has been submitted for examination with my approval as thesis advisor.

Name: Dr.-Ing. Gebremichael Teame

Signature: _____

Place and Date of Submission: _____

Examiners' Approval Sheet

We, the undersigned, members of the Board of Examiners of the final open defense by **Mr. Welday Mebrahtu** Id. No: **PGCon/037/09**, have read and evaluated his/her thesis entitled **"Design of Fuzzy Logic Controller for Anti-Sway Control of Tower Crane under Disturbance"**, and examined the candidate. This is, therefore, to certify that the thesis has been accepted in partial fulfillment of the requirements for the degree.

Mr. Muluken Regassa	_____	_____
Name of Chair Person	Signature	Date
Dr.-Ing. Gebremichael Teame	_____	_____
Name of Major Advisor	Signature	Date
Mr. Yeshitla Hailu	_____	_____
Name of Internal Examiner	Signature	Date
Dr.Eskinder Anteneh.	_____	_____
Name of External Examiner	Signature	Date
_____	_____	_____
SGS Approval	Signature	Date

Acknowledgment

For most the glory goes to the **ALMIGHTY GOD** for all His blessings; through Him all things are possible. In Him, I put my trust for protection and guidance.

My thanks also go to Hawassa University Institute of Technology and Adigrat University, for giving me the opportunity to take my MSc program in Control and Instrumentation Engineering.

I express my deepest gratitude my advisor **Dr.-Ing. Gebremichael Teame** for initiating this study and giving me his time and advices throughout this thesis work. His fruitful suggestions and careful review of the draft have made the production of this thesis possible. It was a great pleasure for me to conduct this thesis work under his advising.

I would like to thank the members of Control and Instrumentation chair of the department of Electrical and Computer Engineering for providing me with an excellent atmosphere throughout the study of my MSc program and for doing this thesis work.

I wish to thank my family for always standing on my side and providing me with consistent support and continuous inspiration throughout my years of study. Without their support, the accomplishment of this MSc program and thesis work is impossible.

Lastly but not the least, I would like to thank my best friend **Hiluf Nigus**, who always willing to help and give his best suggestions and comments.

Thank you all

Welday Mebrahtu

Abstract

Tower cranes are widely used in constructions and loading unloading systems due to restricted human capability to transport numerous types of loads. Furthermore, in order to transport the load in minimum time from one position to another, load oscillation or sway angle will occur. This undesirable sway causes inaccurate positioning of the load, longer time of task completion, difficult automation by the human operator and damage to the system or the operating environment. This thesis presents the design of optimal motion planning, PID controller and fuzzy logic controller (FLC) for the sway angle control of tower crane system with friction. The optimal motion planning is an algorithm to determine optimal time for acceleration, constant velocity, and deceleration for trolley and jib motions when they are driven under trapezoidal velocity time curve. This algorithm considers the trolley and jib initial positions, final positions and system nature. The Newton's second law is used to drive the mathematical model of tower crane or rotary crane system and the simulation results are done using MATLAB/Simulink environment. Simulation results are presented in trolley and jib optimal time trajectory tracking capability and load sway angle reduction. The FLC is compared with the classical PID controller in terms of the trolley and jib optimal time velocity, acceleration, magnitude of sway angle, rate of change of sway angle and displacement profile tracking performance under the effect of various trolley displacements. It has been seen that the fuzzy logic controller gives better performance in minimizing the sway angle and tracking the optimal time references of tower crane system than the classical PID controller.

Keywords: *Tower Crane, Anti-Sway, Motion Control, Fuzzy Logic Controller, Tracking Control*

Table of Contents

List of Figures

List of Tables

List of Abbreviations

AC	Alternating current
CC	Cohen-Coon
CHR	Chien–Hrones–Reswick
COG	Centroid of Gravity
DC	Direct current
DOF	Degree of freedom
FIS	Fuzzy inference system
FLC	Fuzzy logic controller
GUI	Graphical user interface
KE	Kinetic energy
LN	Large Negative
LP	Large Positive
LQR	Linear quadratic regulator
MF	Membership function
MN	Medium Negative
MOM	Mean of Maximum
PE	Potential energy
PID	Proportional-integral-derivative
SN	Small Negative
SP	Small Positive
ZN	Ziegler-Nichols
Z	Zero
3D	Three dimensional

CHAPTER ONE

Introduction

1.1. Background

The crane systems are the most commonly used tools in the industries, warehouse, shipping yards, construction sites, mining sites, power plants, among others, to perform manipulations or guides products to be transported from one place to another [1, 2]. The ever increasing need of products of huge sizes, as well as the emergence of high risers, inspires the use of modern systems particularly crane systems to conveniently execute various tasks within the shortest possible time.

The first cranes were invented by the Ancient Greeks and Romans for lifting heavy loads and such an early crane was driven by human or animal power [3]. They were believed to have made practical and effective use of the crane for constructing tall buildings.

In general cranes can be categorized regarding their mechanical structures, dynamics and applications as overhead cranes, tower cranes and boom cranes [4].

An overhead crane system consists of a hoisting mechanism such as flexible cable and hook, a support mechanism such as trolley rafter and moving mechanisms which are hoist, bridge and a cart or trolley. The hoisting mechanism has two main functions. It picks up the load from initial place and places the load at the target destination and evades the hindrances in the path by lifting up and lowering down the load. The function of the support mechanism is to guide and support the suspension point along with the cart and the bridge around the crane workspace. Overhead cranes are commonly used in ports and factories for loading and unloading heavy shipments and risky materials. Overhead cranes can be classified as indoor overhead cranes and outdoor overhead cranes. Figure 1.1 indicates the commonly used indoor overhead crane system.

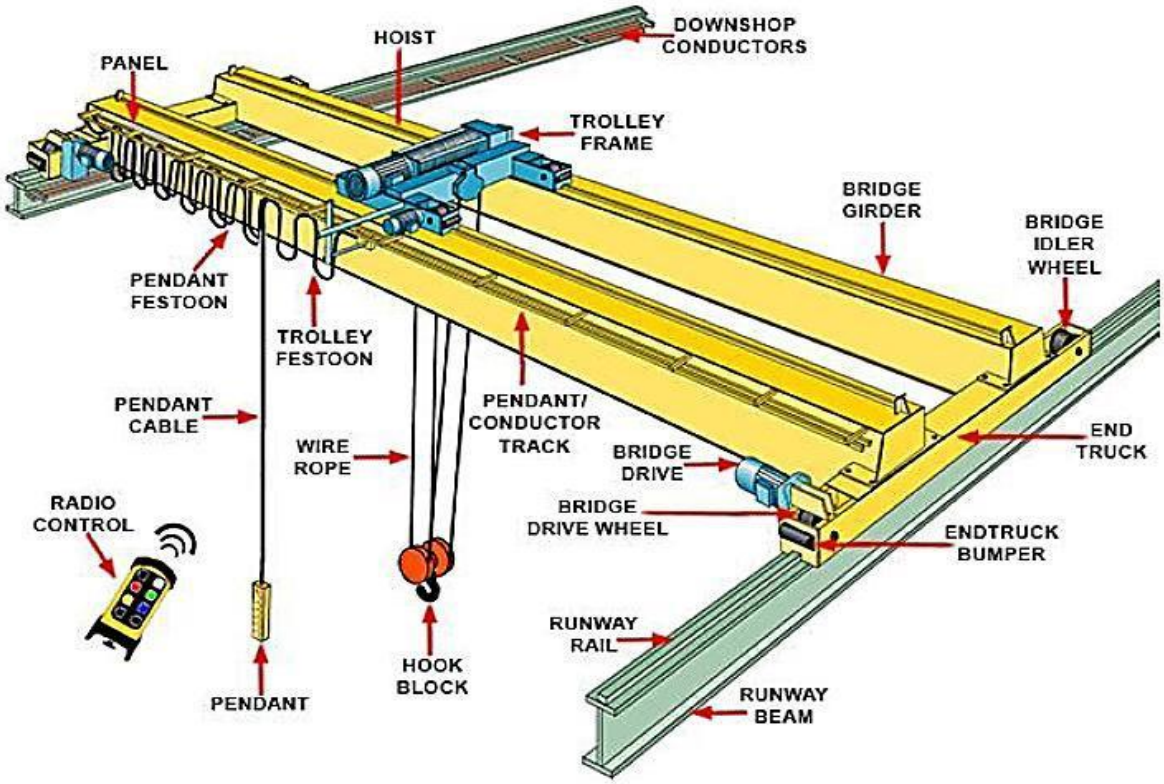

Figure 1.1: Indoor overhead crane system [5]

Figure 1.2 shows the outdoor overhead crane also known as gantry cranes which consist of a trolley which moves along a horizontal rail or jib. Usually the jib is supported by pairs of legs at both ends. Because of their simple operation and less cost, gantry cranes are commonly used in the shipping yards, industries, mining sites and transport industries [6].

Figure 1.2: Gantry crane systems [7]

A rotary (also tower) cranes, consist of jib that moves (rotates) horizontally about a fixed vertical support. The cart can move either linearly as the case of gantry or rotates within the operating range of the crane. As shown in Figure 1.3 the load is connected to the cart or trolley by a set of cables or ropes. Because of this additional flexibility, rotary cranes are commonly used in the construction sites and transport industry [8].

Figure 1.3: Tower crane systems [9]

Boom cranes as shown in Figure 1.4, consists of a rotating base where the boom is connected. The payload is attached to the tip of the boom by a set of cables and pulleys. As the base rotates, the boom tip can be placed at any point horizontally within the reach of the crane. Boom cranes offers more flexibility than gantry crane and tower cranes of the same capacity. They are usually mounted on ships or harbor pavements to transfer cargo between offshore structures and ships [8].

Figure 1.4: Boom crane systems [10]

However, those systems suffered greatly from undesired deflection and swaying during the process. Conversely, these detrimental phenomenon, significantly posed problems to the systems, resulting to inaccurate positioning of the load, unease of operation by the human operator and in some cases even cause a destruction to the system [1, 11].

Still, the need to provide suitable working condition for the human operator and also to minimized maintenance cost due to system failure, thousands of researchers engaged in studying the dynamic behavior of the crane system and proposed various control strategies in order to achieve optimum performance of the crane systems [12]. In this thesis work, a tower crane system is considered.

1.2. Statement of the Problem

A crane is a type of machine, generally fitted out with a hoist cables, chains, and sheaves, that can be used for transportation of heavy loads and hazardous materials in factories, shipyards, high building construction, nuclear installations and harbors. Generally, cranes are mostly employed in construction, transport and manufacturing industries for the transferring of materials, loading and unloading of goods and assembling of heavy equipment respectively. The major concern with the operation of tower crane systems is to transport, load and unload the load easily from one point to another as fast as possible. However, the critical issue that hinders the efficiency of the tower crane system is the swaying of the load. There are many factors and disturbances that initiate the load sway angles such as wind, speed of the trolley and jib controlled by the operators, inefficient control system and the complex effect of the tower crane movement on the load. This persistent

swaying constitutes; inaccurate positioning of the load, longer time of task completion, difficult automation by the human operator and damage to the system or the operating environment. Therefore, the tower crane system needs a proper automatic anti-sway control system in order to reduce the sway immediately at destination without human interruption. In this thesis an optimal motion planning followed by fuzzy logic controller is designed to diminish the unfavorable load sway angle, to maintain the specified position and to have an optimal time to enhance both efficiency and safety of the system.

1.3. Objectives

1.3.1. General Objective

The main objective of this thesis is to design fuzzy logic controller for anti-sway control of tower crane system.

1.3.2. Specific Objectives

The specific objectives of this thesis are;

- To develop mathematical model of the tower crane system
- To design an optimal time reference trajectories for the tower crane system
- To design PID controller for anti-sway control of tower crane system
- To design FLC controller for anti-sway control of tower crane system
- To compare FLC with PID controller.

1.4. Scope

This thesis mainly focuses on the design of fuzzy logic controller based on seven linguistic variables, triangular MF, COG defuzzification method and Mamdani type FIS for the anti-sway control of tower crane under disturbance. Apart from this the study, design and analysis of the mathematical model of 2D tower crane system and the drive system, developing an optimal time motion planning algorithm, simulating and investigating the dynamic performance of the tower crane system are held. The fuzzy logic controller is compared with the conventional PID controller. The optimal motion planning algorithm and the fuzzy logic controller are developed on Matlab M-file script and Matlab/Simulink respectively.

1.5. Methodology

The methodology followed in this thesis is presented as follows:

- Literature reviewing relevant theses which have inputs for the thesis.
- Developing the mathematical model of tower crane system using Newton's second law.
- Developing minimum time optimization and terminal control problem.
- Designing of PID controller for the tower crane system using MATLAB auto tuning method.
- Developing fuzzy logic controller design using Mamdani type fuzzy inference system using Matlab/Simulink.
- Simulating the closed-loop, PID and FLC controlled system using MATLAB/Simulink.
- Testing, comparison of PID and FLC using time domain performance analysis techniques.
- Concluding and recommending the overall thesis work.

1.6. Thesis Organization

This thesis contains six chapters, and this introduction makes the first chapter of the thesis. The rests are described below.

Chapter two deals with the literature review of different journals, conference papers and others.

Chapter three deals with the mathematical modeling of tower crane system with friction and optimal motion planning based on desired position coordinate.

Chapter four is concerned with the design of controller for the tower crane system. It includes PID controller and fuzzy logic controller design with optimal input coordinate as desired input reference.

Chapter five presents the simulation results and discussions of tower crane system. It includes M-file Matlab program, Simulink model of the system using PID controller and fuzzy logic controller techniques.

Chapter six which is the last chapter and it draws the conclusion and recommendation.

CHAPTER TWO

Literature Review

This section gives an overview of the research that has been performed in the field of tower crane sway control. A number of researchers have investigated the control of tower cranes based on open loop and closed loop control systems [13-15]. Next, we summarize some of this recent work.

2.1. Open loop controllers

Parker *et al.* [15, 16] applied several input shaping techniques to bring the load to settle at the desired motion profile. However, these techniques could not reduce developed sways less than 10°.

Smith A.D. [17] used filtering methods such as notch and low-pass filtering to reduce the load sway angles by filtering out the natural frequencies of the tower crane fluctuation from the trolley motion. The major drawback of these methods is that they slow down the response of the system due to the filtering effects.

Furthermore, the input shaping and filtering methods are open-loop controllers and these controllers are poor to handle the external disturbances and model uncertainty.

2.2. Closed loop controllers

Golafshani and Aplevich [18] used a bang-bang controller to track the time optimal trajectories generated for the arm, trolley or cart, and the rope length and to reduce the load sway angle. But, in their research output the sway is still not zero.

A. H. HAILU [19] designed an optimal motion planning and hybrid (adaptive-PID) for the anti-sway control of a crane system. However, the author designed the controller for 3D overhead crane system not for tower crane system and also he didn't consider external disturbance such as wind.

A. A. Al-Mousa [6] designed Fuzzy Logic controller and Time-Delayed Position Feedback Control to control position, sway angle and also develops a trapezoidal velocity time path for the trolley and jib part of the tower crane system. But, the author didn't determine the optimal time of acceleration, constant velocity and deceleration for the tower crane system i.e. the whole operation of the tower crane system is executed at different time. This may reduce the efficiency of the tower

crane and cause a safety problem to the human operator. Besides, the author didn't consider an external disturbance.

An inverse dynamics was designed to control the sway angle of the tower crane system. But, the load sway angle was not reduced to zero at destination using these techniques and also the author didn't consider external disturbance [20].

A delayed feedback controller was designed to control both the load sway angle and the position of gantry and tower crane systems [21]. However, these techniques are time consuming and they don't diminish the load sway angle at the destination. In addition to this the author didn't consider external disturbance.

A hybrid LQR and input shaping techniques were designed to control the jib position and the load sway angle due to the rotation of the jib part of the tower or rotary crane system [22]. However, the authors did not consider the trolley position and the load sway angle due to the displacement of the trolley.

A gain scheduling feedback controller was used to control the load sway angle of the tower crane system [23]. But, the author considers the DC motor model as constant gain and the reference of the controller was not optimal.

F. Altaf [24] developed an Event-Triggered Control for multiple 3D Tower Cranes. However, the author uses a step input as a reference to the controller and also the sway angle at the destination is not reduced to zero. In addition to this the author doesn't develop an optimal motion planning to optimize the time of acceleration, constant velocity and deceleration.

The authors in [25] designed a robust FLC to control the load sway angle of a crane system. However, these authors applied fuzzy logic controller to control gantry crane system which is completely different in structure, dynamics and application from the tower crane system and also they didn't consider external disturbances.

The authors in [26] designed FLC for sway and position control of an automatic overhead crane system. The authors compared the performance of FLC with LQR and the performance of FLC is

better than the LQR. But, the authors designed the controllers for indoor overhead crane system not for tower crane system and they didn't consider external disturbance.

Hurteau and Desantis [27] designed a microprocessor based adaptive controller and the gains of the controllers are adjusted according to the cable length. However, if the cable length varies in undesired way, degradation of the system performance happens.

Nally and Tarbia [28] applied a distributed fuzzy logic controller to reduce the load sway angles ensued during the operation of cranes. Then again, the authors implemented the controller for overhead crane system load sway angle control not for tower crane system.

This thesis proposes a solution to the previous work gaps by using fuzzy logic controller to reduce the load oscillation or sway at the desired position with minimum time. In addition the controller uses optimal time trajectory which includes velocity, acceleration, displacement, sway angle and rate of change of sway angle profiles. Fuzzy logic controller is one of the recent developing methods in control that gains more popularity due to the following reasons. First, while applying traditional control, one needs to know about the model and the objective function formulated in precise terms. This makes it very difficult to apply in many cases. Second, by applying a fuzzy logic controller for control we can utilize the human experience and knowhow for designing a controller. Third, the fuzzy logic controller rules, basically the IF-THEN rules, can be best utilized in designing a controller.

CHAPTER THREE

System Modeling

The control mechanism of any mechanical system starts from mathematical modeling. As the motion of tower crane system is dynamic in nature due to the load variation which result in turn variation in other parameters, the variation in speed which also affects the angle and the position. So, to model the nonlinear behavior of tower crane is difficult without considering the following assumptions to simplify the complexity of the design. Few assumptions are given to arrive at a simplified model of the tower crane in this chapter. This chapter also presents a complete description of the tower crane system modeling that includes modeling the optimal control system which is used to generate optimal time references for the tower crane system, modeling of the trolley and jib with load motion and modeling of the DC motor system. To derive a set of equations of motion that model the tower crane system dynamics, we use the newton's law. Therefore, the details of the tower crane system modeling are presented as follows.

3.1. Tower Crane Modeling

A tower crane system consists of a trolley that moves radially along a rotating jib. The jib rotates and traces an angle $\gamma(t)$ in a circular plane. The combined movements of the jib and the trolley enable positioning of the trolley and consequently the load over any point in the work space. The load attached to the end of the lift-line can move freely in three dimensions. The variation in the length of the hoisting cable is important for picking up the load, putting it down, and moving it away from obstacles. As shown in Figure 3.1, the structure of the crane consists of

a) A tower that holds the jib of the crane; it is responsible for the rotational motion of the crane.
b) A base that is usually fixed to the ground to prevent any oscillations.
c) A jib that is mounted to the tower.
d) A trolley that slides over the jib in a translational direction.
e) A suspension system of cables and pulleys. In the very general case, the length of the cable can be changed during load transport or at least at the pickup and end points. The process of changing the cable length is called hoisting.

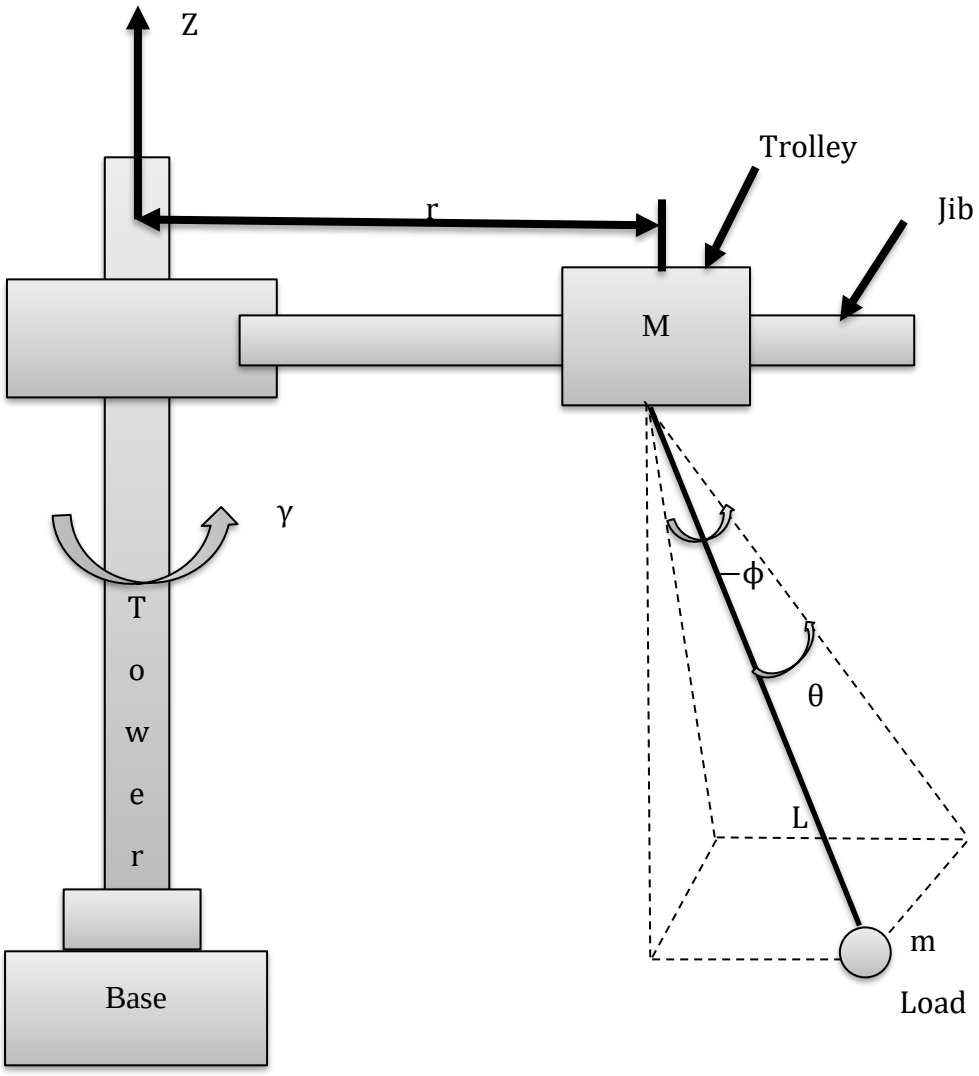

Figure 3.1: Structure of tower crane system

The loads swaying are characterized by two angles, Φ and θ. The angle Φ is the angle which the cable makes with the z-axis in the $x - z$ plane. The out-of-plane angle θ is the angle which the cable makes with the xz-plane. The two sway angles happen due to linear displacement of the trolley and the rotation of the jib or arm respectively. So, it is clear that, the objective of the controller is to move the load while keeping Φ and θ as small as possible as shown in Figure 3.1.

The tower crane modeling includes modeling of the trolley and jib motions, modeling of a motor that drives the trolley and jib and modeling the optimal control system. Therefore, the details of the tower crane system modeling are described as follows.

3.1.1. Modeling of Trolley and Jib

Consider the trolley load motion shown in Figure 3.2. The trolley motion of the tower crane system follows a trapezoid path. The forces exerted to the trolley will produce a horizontal sliding movement along the respective directions and when the trolley attached to the load with weightless flexible cable in turn it results in load oscillation. The load is attached to the trolley with the massless cable and develops a sway angle along $x - z$ plane due to the displacement of the tower crane's trolley and the rotation of the tower crane's jib. The sway angles in x-axis and z-axis are represented by $\Phi(t)$ and $\theta(t)$ respectively. Hence, from the Figure 3.2 the trolley system can be modeled as follows.

From the principle of energy transformation i.e. the potential and kinetic energy, we can derive our necessary equations at the minimum and maximum sway positions of the load [19]. The kinetic energy equation of the trolley and the load at the minimum sway angle are given by:

$$\mathrm{KE(trolley)} = \frac{1}{2}\mathrm{Mv}^2$$

$$\mathrm{KE(load)} = \frac{1}{2}\mathrm{mv}^2$$

$$\mathrm{KE(total)} = \mathrm{KE(trolley)} + \mathrm{KE(load)} = \frac{1}{2}(\mathrm{m} + \mathrm{M})\mathrm{v}^2 \tag{3.1}$$

where m is mass of the load, M is mass of the trolley and v is the velocity of the trolley.

From the vertical component i.e. the potential energy equation:

$$\mathrm{PE} = \mathrm{mgh} \tag{3.2}$$

where g is the acceleration due to gravity and h is the height in meters (m).

The kinetic energy at the minimum position and the potential energy at the maximum sway angle are equal. Hence, for $h > 0$

$$\frac{1}{2}\mathrm{mv}^2 = \mathrm{mgh}$$

$$\frac{1}{2}\mathrm{v}^2 = \mathrm{gh} \rightarrow \quad \mathrm{v} = \sqrt{2\mathrm{gh}}$$

$$\mathrm{h} = \frac{\mathrm{v}^2}{2\mathrm{g}} \tag{3.3}$$

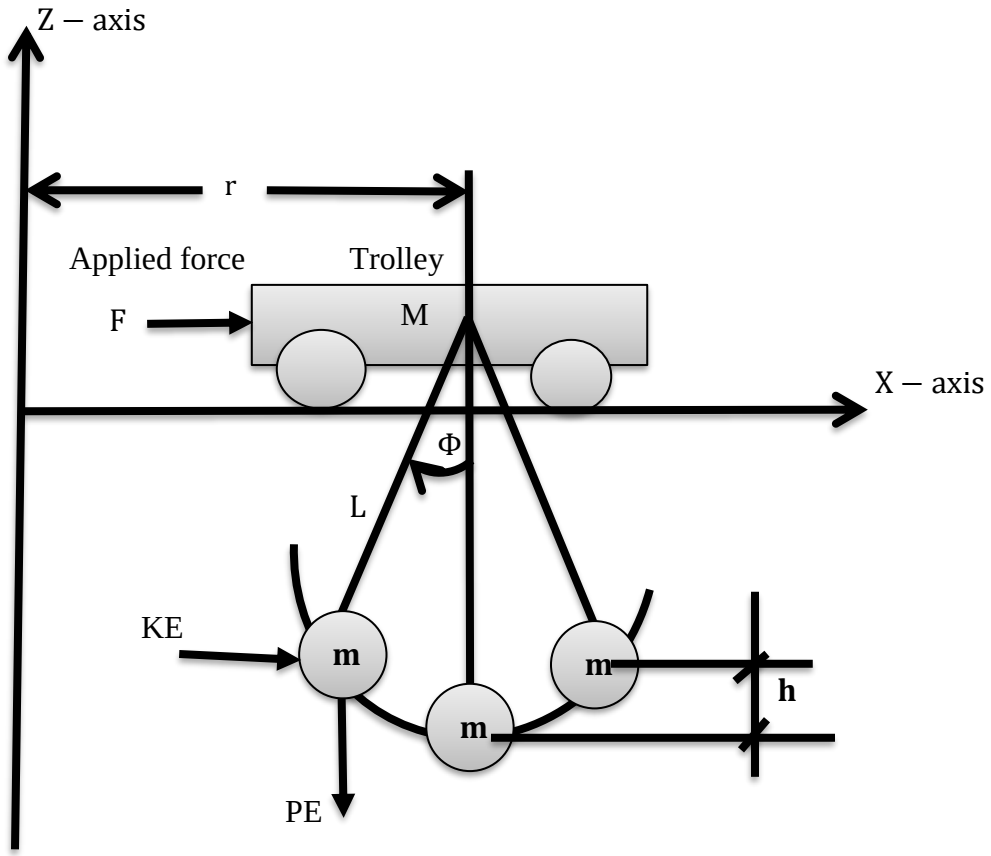

Figure 3.2: Trolley-load motion free body diagram

From Figure 3.2 the sway angle of the load can also be derived as follows:

$$L - h = L\cos\Phi(t)$$

$$\cos\Phi(t) = 1 - \frac{h}{L} = 1 - k \tag{3.4}$$

where $\Phi(t)$ is the sway angle of the load and k is the ratio of the height to the length of the cable.

From (3.4) we can calculate the maximum sway angle of the load as:

$$\Phi(t) = \cos^{-1}\left(\frac{L-h}{L}\right) = \cos^{-1}(1-k) \tag{3.5}$$

By substituting (3.3) into (3.5) we get

$$\Phi(t) = \cos^{-1}\left(1 - \frac{v^2(t)}{2gL}\right) \tag{3.6}$$

Equation (3.5) shows that the sway angle is optimized by varying the values of k where, k is a constant constraint which is dependent on the policy or specification of the system. The sway angle at the destination can be reduced to zero if we design an optimal motion planning, where the system is driven under trapezoidal velocity-time curve as shown in Figure 3.3. An optimal motion

planning is an algorithm to determine optimal time for acceleration, constant velocity, and deceleration for trolley and jib motions when they are driven under trapezoidal velocity time curve. This algorithm includes the trolley and jib initial positions, final positions and system nature. The output of the algorithm is used as a reference for the controller.

If we design an optimal motion planning algorithm, the trolley must accelerate from rest position, and after a certain time the trolley move with constant velocity v_{f1} then after come to rest, at the final destination the crane has to decelerate with velocity of v_{f2}. Finally, the crane come to rest i.e. v_{f2} will be zero.

In similar way, we can formulate the parameters from motion of the jib using kinetic and potential energy equation. The kinetic energy of the jib is given by;

$$\mathrm{KE(jib)} = \frac{1}{2}\mathrm{M_j v^2}$$

$$\mathrm{KE(total)} = \mathrm{KE(trolley)} + \mathrm{KE(load)} + \mathrm{KE(jib)} = \frac{1}{2}(\mathrm{M_j} + \mathrm{m} + \mathrm{M})\mathrm{v^2} \quad (3.7)$$

where $\mathrm{M_j}$ is the mass of the jib.

When we model the jib, easily the same procedures will be followed. The only difference is mass of the jib includes the mass of the trolley and load i.e. the mass of the jib is the summation of the jib mass itself and both the trolley and load mass. The kinetic energy at the minimum position and the potential energy at the maximum sway angle are equal. Therefore, for the jib load motion the sway angle is given by;

$$\theta(\mathrm{t}) = \cos^{-1}(1 - \mathrm{k}) = \cos^{-1}\left(1 - \frac{\mathrm{v^2(t)}}{2\mathrm{gL}}\right) \quad (3.8)$$

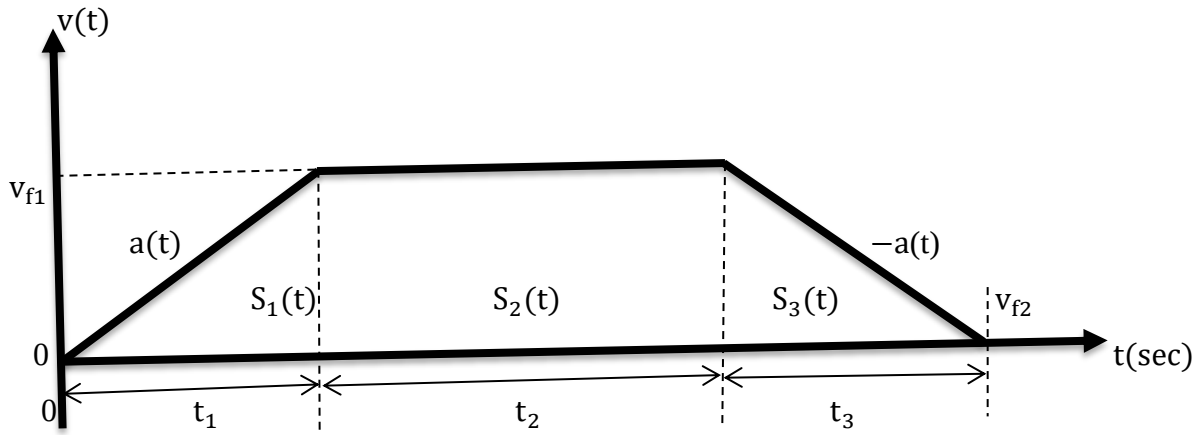

Figure 3.3: Trapezoidal velocity-time curve

Assume that the time of acceleration is equal to the time of deceleration i.e. $t_1 = t_3$, and the total displacement of trolley will be:

$$S(t) = S_1(t) + S_2(t) + S_3(t) \tag{3.9}$$

where:

$S_1(t)$: The distance covered during acceleration.

$S_2(t)$: The distance covered during constant velocity i.e. $a(t) = 0$

$S_3(t)$: The distance covered during deceleration.

$S(t)$: Total displacement covered by the trolley

$a(t)$: The maximum acceleration

t_1, t_3:The acceleration and deceleration times

t_2:The time at the maximum velocity

v_0, v_{f1}, v_{f2}: Initial and final velocity

The velocity, acceleration and the rate of change of sway angle of the trolley and jib can be calculated as follows respectively:

$$v_i(t) = \frac{dS_i(t)}{dt}, \qquad a_i(t) = \frac{dv_i(t)}{dt}, \qquad \dot{\Phi}(t) = \frac{d\Phi(t)}{dt}, \qquad \dot{\theta}(t) = \frac{d\theta(t)}{dt} \tag{3.10}$$

where a_i, v_i, Φ, θ , F_i and S_i are the acceleration, velocity, sway angle, force and displacement of the trolley and jib along x and z-axis respectively.

At the initial state all the above quantities translational velocity, acceleration, the rate of change of the sway angle and the applied force are all zeros i.e. ($a_i = 0$, $v_i = 0$, $\Phi = 0$, $\theta = 0$, $F_i = 0$) which we consider as the initial possible constrains. By differentiating both sides of (3.6), we can derivate the equation for the rate of change of the sway angle:

$$\frac{d}{dt}(\cos\Phi) = \frac{d}{dt}\left(1 - \frac{v^2}{2gL}\right)$$

$$-\sin\Phi\frac{d\Phi}{dt} = -\frac{v}{gL}\frac{dv}{dt} \tag{3.11}$$

Rearranging (3.11), we get;

$$\frac{d\Phi}{dt} = \frac{v}{gL\sin\Phi}\frac{dv}{dt} \tag{3.12}$$

From the free body diagram of Figure 3.2 we can calculate $\sin\Phi$

$$(L\sin\Phi)^2 = L^2 - (L-h)^2$$

$$L^2\sin^2\Phi = L^2 - L^2 + 2Lh - h^2$$

$$\sin^2\Phi = \frac{2Lh - h^2}{L^2} \quad \rightarrow \quad \sin\Phi = \frac{\sqrt{2Lh - h^2}}{L} = \sqrt{k(2-k)} \tag{3.13}$$

This angle parameter helps for setting constraints which in turn necessary to put constraints for the optimization control mechanisms. Therefore, (3.12) becomes:

$$\frac{d\Phi}{dt} = \frac{v}{gL\sin\Phi}\frac{dv}{dt} = \frac{v}{g\sqrt{2Lh - h^2}}\frac{dv}{dt}, \qquad v = \sqrt{2gh}$$

$$\frac{d\Phi}{dt} = \frac{v}{gL\sin\Phi}\frac{dv}{dt} = \frac{\sqrt{2gh}}{g\sqrt{2Lh - h^2}}\frac{dv}{dt}$$

$$\frac{d\Phi}{dt} = \frac{1}{\sqrt{g\left(L - \frac{v^2}{4g}\right)}}\frac{dv}{dt} = \frac{1}{\sqrt{g\left(L - \frac{v^2}{4g}\right)}}a \tag{3.14}$$

Similarly, the rate of change of sway angle of the jib is derived in a similar manner to the rate of change of sway angle of the trolley by differentiating both sides of (3.8). Therefore, it is given by;

$$\frac{d\theta}{dt} = \frac{1}{\sqrt{g\left(L - \frac{v^2}{4g}\right)}}\frac{dv}{dt} = \frac{1}{\sqrt{g\left(L - \frac{v^2}{4g}\right)}}a \tag{3.15}$$

Therefore, from (3.14) and (3.15) we can conclude that the change in sway angle along x-axis and z-axis is due to acceleration. In addition to this, we have also $L - \frac{v^2}{4g} > 0$ and $L - \frac{v^2}{4g} \neq 0$. This

implies that $v^2 < 4gL$ and the sway angle are being affected by the cable length and velocity of the trolley and jib respectively.

From Figure 3.3, we can see how the sway angle is being affected by the cable length and the velocity of the trolley.

$$v_{f1} = v_0 + a_1 t_1 = a t_1$$
$$h = \frac{v^2}{2g} = \frac{(a t_1)^2}{2g} \tag{3.16}$$

Therefore, the rate change of the sway angle will be:

$$\frac{d\Phi}{dt} = \frac{1}{\sqrt{g\left(L - \frac{{v_{f1}}^2}{4g}\right)}} \frac{dv}{dt} = \frac{1}{\sqrt{g\left(L - \frac{{v_{f1}}^2}{4g}\right)}} a \tag{3.17}$$

Since $\frac{dv_x}{dt} = a_x$, that is the acceleration is the time derivative of velocity.

where a_x is the acceleration in x-direction. Thus, the trolley rate of change of the sway angle will be:

$$\frac{d\Phi}{dt} = \frac{1}{\sqrt{g\left(L - \frac{{v_{f1x}}^2}{4g}\right)}} \frac{dv_x}{dt} = \frac{1}{\sqrt{g\left(L - \frac{{v_{f1x}}^2}{4g}\right)}} a_x \tag{3.18}$$

Similarly, for the jib the rate of change of sway angle is given by;

$$\frac{d\theta}{dt} = \frac{1}{\sqrt{g\left(L - \frac{{v_{f1z}}^2}{4g}\right)}} \frac{dv_z}{dt} = \frac{1}{\sqrt{g\left(L - \frac{{v_{f1z}}^2}{4g}\right)}} a_z \tag{3.19}$$

3.1.2. Translational Displacement Equation

The displacement of the trolley in the x-axis is the area covered in the trapezoidal curve as shown in Figure 3.3. From (3.7) we have:

$$S(t) = S_1(t) + S_2(t) + S_3(t)$$
$$S(t) = \frac{1}{2} a_x(t) {t_1}^2 + v_{f1x} t_2 + \frac{1}{2} a_x(t) {t_3}^2 \tag{3.20}$$

The maximum velocity of the trolley is given by;

$$v_{f1x}(t) = v_0 + a_{1x}(t) t_1 \tag{3.21}$$

Since the trolley starts from rest ($v_0 = 0$) and its time of acceleration and deceleration are equal i.e. $t_1 = t_3$ equation (3.20) becomes;

$$S(t) = \frac{1}{2} v_{f1x} t_1 + v_{f1x} t_2 + \frac{1}{2} v_{f1x} t_3$$

$$S(t) = v_{f1x} t_1 + v_{f1x} t_2 \ = v_{f1x}(t_1 + t_2)$$

$$S(t) = a t_1 (t_1 + t_2) \qquad (3.22)$$

3.1.3. Radial Displacement Equation

The jib motion follows a trapezoidal curve path. A trapezoidal angular velocity profile of the jib along the z-axis is shown in Figure 3.4. The area under the curve is the total angular distance moved. The slopes of the initial and final ramp are the maximum angular acceleration and deceleration. The top level of the trapezoid is the maximum angular velocity.

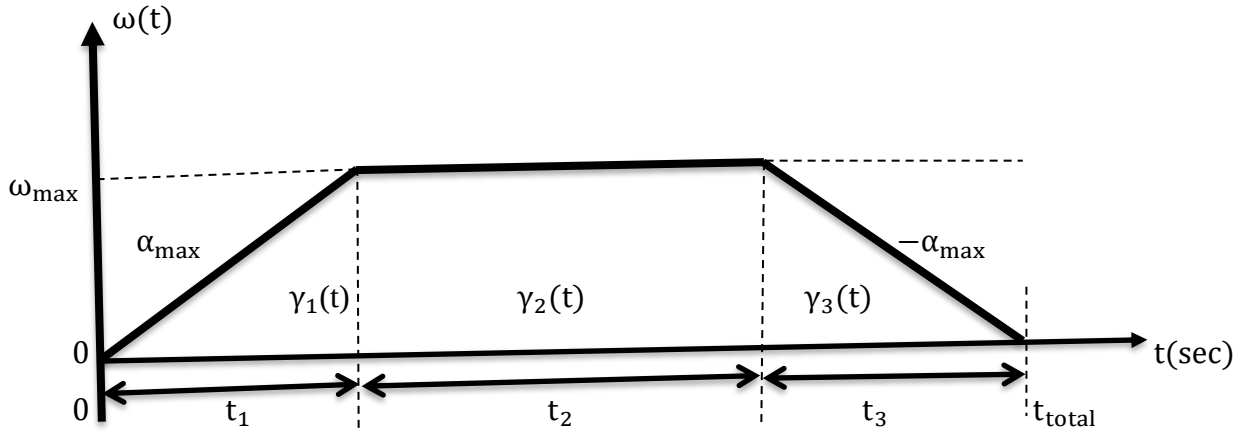

Figure 3.4: Jib trapezoidal angular velocity-time curve

where

$\omega_{max}(t)$: The maximum angular velocity of the jib

$\alpha_{max}(t)$:The maximum angular acceleration of the jib

t_1, t_3:The acceleration and deceleration times

t_2:The time at the maximum velocity

t_{total}: The total motion time

$$t_1 \ = \ t_3 = \frac{\omega_{max}}{\alpha_{max}}$$

$$t_{total} \ = t_1 + \ t_2 + \ t_3 \qquad (3.23)$$

From Figure 3.4 the total angular displacement of the jib is given by:

$$\gamma(t) = \gamma_1(t) + \gamma_2(t) + \gamma_3(t)$$

$$\gamma(t) = \frac{1}{2} t_1 \omega_{max} + t_2 \omega_{max} \ + \frac{1}{2} t_3 \omega_{max} \ = \omega_{max} \ (t_1 + \ t_2)$$

$$\gamma(t) = \alpha_{max} t_1 \ (t_1 + \ t_2) \tag{3.24}$$

Equation (3.22) represents the translational displacement of the trolley along x-axis. Equation (3.24) represents the angular displacement of the jib along z-axis. When the trolley moves radially from one point to another point, while the jib is rotating the combined motion of the trolley and the jib rotation form an arc. From figure 3.4 the radial displacement of the jib in fully 360° rotation of the jib along z- axis is given by:

$$S_z(t) = \frac{\gamma(t)}{360^{\circ}} 2\pi r = \frac{\pi r(t)\gamma(t)}{180^{\circ}} \tag{3.25}$$

where:

$S_z(t)$: Radial displacement of the jib along z-axis

$\gamma(t)$: The angle that the jib rotates

$r(t)$: Radius of the jib or trolley displacement in the x-axis

3.1.4. Time Optimization

The optimization techniques are used to find a set of design parameters $x = \{x_1, x_2, \dots, x_n\}$, that can in some way be defined as optimal. In a simple case this might be the minimization or maximization of some system characteristic that is dependent on x. In a more advanced formulation the objective function, f(x), to be minimized or maximized, might be subjected to constraints in the form of equality constraints, $G_i(x) = 0 \ (i = 1, \dots, m_e)$; inequality constraints, $G_i(x) \leq 0 \ (i = m_e + 1, \dots, m)$; and/or parameter bounds, x_l, x_u.

A general problem description is stated as

$$\underset{x \in R^n}{\text{minimize}} \ f(x) \tag{3.26}$$

subjected to

$$G_i(x) = 0, \qquad i = 1, \dots, m_e$$
$$G_i(x) \leq 0 \qquad i = m_e + 1, \dots, m$$
$$x_l \leq x \leq x_u$$

where x is the vector of design parameters ($x \in R^n$), f(x) is the objective function that returns a scalar value and the vector function G(x) returns the value of the equality and inequality constraints evaluated at x.

In our case we consider the optimization method to determine the optimal time of acceleration, constant velocity and deceleration both trolley and jib because these moving parts of the tower

crane system are needed to be arrived at the destination as fast as possible with zero sway angle of the load. Since the destination of the load is known, the load will attain faster or slower depending on the velocity of the trolley and jib. That means, the faster the velocity the higher the sway angle will have in the tower crane and vice versa. The objective functions and constraints considered in our case are derived in a similar way with author in [19]. From Figure 3.3 the distance is a quadratic function of time intervals. Therefore, from the quadratic equation of (3.22) we can solve for the time as:

$$at_1{}^2 + at_1t_2 - S = 0$$

$$t_1 = \frac{-at_2 \pm \sqrt{a^2t_2{}^2 + 4aS}}{2a} = -\frac{t_2}{2} \pm \frac{1}{2}\sqrt{t_2{}^2 + \frac{4S}{a}}$$

From the above equation we can develop constraints:

$$t_2 > 0, t_1 > 0, a > 0, S > 0$$

$$t_2{}^2 + \frac{4S}{a} \geq 0 \text{ and } \sqrt{t_2{}^2 + \frac{4S}{a}} > t_2$$

$$\frac{S}{a} > 0$$

Objective function for the time of acceleration or deceleration along x and z-axis

$$\underset{t_1}{\text{minimize}} \left(\frac{|Sx| * t1x + |Sz| * t1z}{|Sx| + |Sz|}\right), \sqrt{2 * K * g * l} * \left(\frac{Sx}{ax * (Sx + Sz)} + \frac{Sz}{az * (Sx + Sz)}\right) \quad (3.27)$$

subjected to

$$ax > 0, az > 0, t1x, t1z > 0, Sx > 0, Sz > 0.$$

Objective function for the time of constant velocity along x and z-axis:

$$\underset{t_2}{\text{maximize}} \left(\frac{Sx}{ax * t1} - t1, \quad \frac{Sz}{az * t1} - t1\right) \quad (3.28)$$

subjected to

$$ax > 0, az > 0, t1 > 0, Sx > 0, Sz > 0.$$

Assume the trapezoidal velocity-time curve of Figure 3.3 for trolley motion along x-axis starts at 0 sec, the acceleration, velocity and displacement of the trolley can be summarized as below:

$$S(t) = \begin{cases} \frac{1}{2}at^2, & 0 \le t \le t_1 \\ v_{f1x}t, & t_1 \le t \le t_1 + t_2 \\ \frac{1}{2}at_1{}^2 + v_{f1x}t_2 + \frac{1}{2}a(t - t_1 - t_2)^2, & t_1 + t_2 \le t \le t_1 + t_2 + t_3 \end{cases} \quad (3.29)$$

$$v(t) = \begin{cases} at, & 0 \le t \le t_1 \\ v_{f1x}(t), & t_1 \le t \le t_1 + t_2 \\ v_{f1x}(t) - at, & t_1 + t_2 \le t \le t_1 + t_2 + t_3 \\ 0, & t_1 + t_2 + t_3 \le t \end{cases} \quad (3.30)$$

$$a(t) = \begin{cases} a(t), & 0 \le t \le t_1 \\ 0, & t_1 \le t \le t_1 + t_2 \\ -a(t), & t_1 + t_2 \le t \le t_1 + t_2 + t_3 \\ 0, & t_1 + t_2 + t_3 \le t \end{cases} \quad (3.31)$$

From equation of (3.24) we can solve for the acceleration time t_1 as:

$$\alpha_{max}t_1{}^2 + \alpha_{max}t_1t_2 - \gamma = 0 \quad (3.32)$$

$$t_1 = \frac{-\alpha_{max}t_2 \pm \sqrt{\alpha_{max}{}^2t_2{}^2 + 4\alpha_{max}\gamma}}{2\alpha_{max}} = -\frac{t_2}{2} \pm \frac{1}{2}\sqrt{t_2{}^2 + \frac{4\gamma}{\alpha_{max}}} \quad (3.33)$$

From equation (3.33) we can develop constraints for optimization problem:

$$t_2 > 0, t_1 > 0, \alpha_{max} > 0, \gamma > 0$$

$$t_2{}^2 + \frac{4\gamma}{\alpha_{max}} \ge 0 \text{ and } \sqrt{t_2{}^2 + \frac{4\gamma}{\alpha_{max}}} > t_2$$

$$\frac{\gamma}{\alpha_{max}} > 0 \rightarrow \gamma > 0 \quad (3.34)$$

Assume the jib rotation in the z-axis starts at 0 sec; the acceleration, velocity and displacement of the jib are described as follows.

$$\gamma(t) = \begin{cases} \frac{1}{2}\alpha_{max}t^2, & 0 \le t \le t_1 \\ \frac{1}{2}\alpha_{max}t_1{}^2 + \omega_{max}(t - t_1), & t_1 \le t \le t_1 + t_2 \\ \frac{1}{2}\alpha_{max}t_1{}^2 + \omega_{max}t_2 + \frac{1}{2}\alpha_{max}(t - t_1 - t_2)^2, & t_1 + t_2 \le t \le t_1 + t_2 + t_3 \\ \gamma_{end} & t_1 + t_2 + t_3 \le t \end{cases} \quad (3.35)$$

$$\omega(t) = \begin{cases} \alpha_{max} t\,, & 0 \le t \le t_1 \\ \omega_{max}(t), & t_1 \le t \le t_1 + t_2 \\ \omega_{max} - \alpha t\,, & t_1 + t_2 \le t \le t_1 + t_2 + t_3 \\ 0 & t_1 + t_2 + t_3 \le t \end{cases} \quad (3.36)$$

$$\alpha(t) = \begin{cases} \alpha_{max}\,, & 0 \le t \le t_1 \\ 0, & t_1 \le t \le t_1 + t_2 \\ -\alpha_{max}, & t_1 + t_2 \le t \le t_1 + t_2 + t_3 \\ 0, & t_1 + t_2 + t_3 \le t \end{cases} \quad (3.37)$$

Equations (3.35) to (3.37) represent the rotational motion of the jib and we convert these equations into radial motion using equation (3.25). The translational motion of the trolley and the rotational motion of the jib execute at the same time or the translational and radial times of the system are equal. Equations (3.1) to (3.37) are used in the optimization algorithm to generate the optimal time trajectories i.e. velocity, acceleration, sway angle and rate of change of sway angle for the tower crane in the x-z plane.

3.2. Modeling of Tower Crane with Friction

To derive the equations of motion, one needs to define clearly the tower crane system parameters. In this thesis the mathematical model of the tower crane is done by splitting into two subsystems. These are trolley and jib subsystems. For this research, only two dimensional tower cranes are considered. As shown in Figures 3.5 and 3.6 r is the horizontal position of the trolley, L is the length of the cable, Φ is the sway angle of the load, M and m are the mass of the trolley and load respectively. The trolley and load are considered as point masses and assumed to move in two dimensional x-z planes. Furthermore, the elongation of the cable due to the tension force is also ignored. Since certain amount of applied force F pushes trolley to move along x- direction, large sway angle appears which needs to be minimized to as small as possible. In this thesis Newton's second law is applied for deriving the dynamic equations of the tower crane. Here, trolley and load model is derived based on Newton's second law. The dynamics of the system is analyzed by splitting into two parts, which are trolley and load. For both trolley and load, the free body diagram considered for mathematical derivation is shown in Figures 3.5 and 3.6 respectively.

A simplified model of the tower crane motions based on the following assumptions is developed in this thesis.

- The tower crane members are rigid.

- The hook and the load together as well as the trolley are considered as point masses.
- Friction exists between the trolley and the jib motions.
- The trolley and the load move in the x-z plane and the length of suspension cable is constant.

Note that T is assumed to be the longitudinal force caused by the cable. The cable is assumed to be thin and massless, which means that its gravitational effect, moment of inertia etc. that may give an effect to this rigid body can be neglected. Using kinetics characteristics, which relates the force and acceleration, the following equation can be derived:

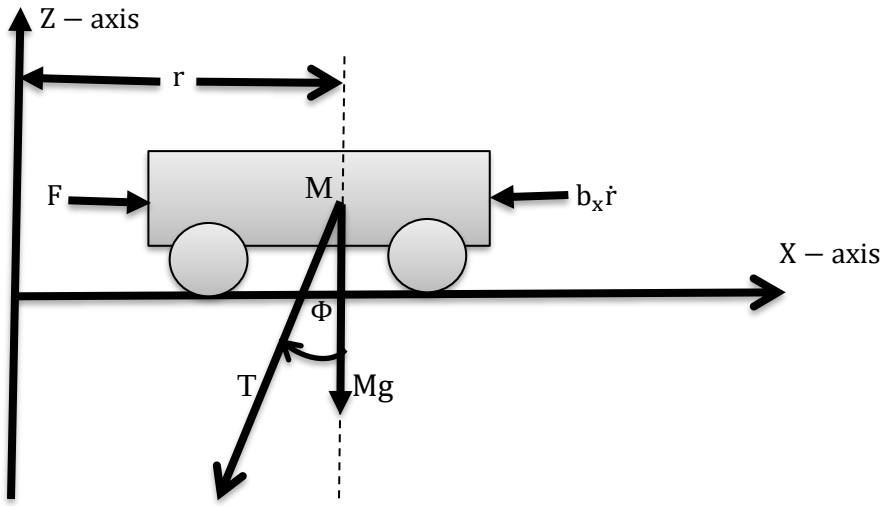

Figure 3.5: Trolley free body diagram

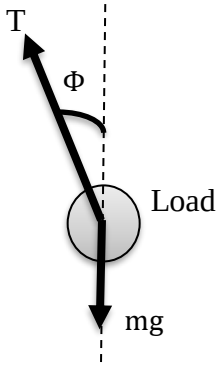

Figure 3.6: Load free body diagram

(i) Trolley, horizontal:

According to Newton's second law the sum of all horizontal forces acting on the trolley are equal to the net force i.e.

$$M\frac{d^2r}{dt^2} = F + T\sin\Phi - b_x\dot{r} \tag{3.38}$$

where b_x is the viscous frictional coefficient in the x-direction.

(ii) Trolley, vertical: taking positive forces downwards.

$$T\cos\Phi + Mg = 0 \tag{3.39}$$

(iii) Load, horizontal:

$$m\frac{d^2(r + L\sin\Phi)}{dt^2} = -T\sin\Phi \tag{3.40}$$

(iv) Load, vertical: taking positive forces downwards.

$$m\frac{d^2(L\cos\Phi)}{dt^2} = -T\cos\Phi + mg \tag{3.41}$$

From equations (3.38) and (3.40),

$$M\frac{d^2r}{dt^2} = F - m\frac{d^2(r + L\sin\Phi)}{dt^2} - b_x\dot{r}$$

$$M\frac{d^2r}{dt^2} + m\frac{d^2(r + L\sin\Phi)}{dt^2} + b_x\dot{r} = F \tag{3.42}$$

From equations (3.40) and (3.41),

$$m\frac{d^2(L\cos\Phi)}{dt^2} = m\left(\frac{\cos\Phi}{\sin\Phi}\right)\left(\frac{d^2(r + L\sin\Phi)}{dt^2}\right) + mg$$

$$m\frac{d^2(L\cos\Phi)}{dt^2}\sin\Phi - m\left(\frac{d^2(r + L\sin\Phi)}{dt^2}\right)\cos\Phi = mg\sin\Phi \tag{3.43}$$

where

$$\frac{d^2(r + L\sin\Phi)}{dt^2} = \ddot{r} + L\ddot{\Phi}\cos\Phi - L\dot{\Phi}^2\sin\Phi \tag{3.44}$$

$$\frac{d^2(L\cos\Phi)}{dt^2} = -L\ddot{\Phi}\sin\Phi - L\dot{\Phi}^2\cos\Phi \tag{3.45}$$

Summarizing equations (3.42), (3.43), (3.44), and (3.45) yields

$$(M + m)\ddot{r} + b_x\dot{r} + mL\ddot{\Phi}\cos\Phi - mL\dot{\Phi}^2\sin\Phi = F \tag{3.46}$$

$$\ddot{r}\cos\Phi + L\ddot{\Phi} = -g\dot{\Phi}\sin\Phi \tag{3.47}$$

Referring to equations (3.46) and (3.47), the following nonlinear equations of motions the trolley systems along x-axis are derived as:

$$\ddot{r} = \frac{1}{(M+m)}\left(F + mL\ddot{\Phi}\cos\Phi + mL\dot{\Phi}^2\sin\Phi - b_x\dot{r}\right) \quad (3.48)$$

$$\ddot{\Phi} = \frac{1}{L}\left(\ddot{r}\cos\Phi - g\dot{\Phi}\sin\Phi\right) \quad (3.49)$$

The jib is the rotating part of the tower crane and its dynamics are derived in a similar way as the trolley system using Newton's second law for rotational system. Therefore, the nonlinear equations of motions for the jib system are derived as:

$$(J + (m+M)r^2)\ddot{\gamma} + b_\gamma\dot{\gamma} + mLr(-\dot{\theta}^2\sin\theta + \ddot{\theta}\cos\theta) = T_\gamma \quad (3.50)$$

$$\ddot{\theta} = \frac{1}{L}\left(-r\ddot{\gamma}\cos\theta - g\dot{\theta}\sin\theta\right) \quad (3.51)$$

Substituting equation (3.49) into (3.48) we get the trolley force dynamics along x-axis as

$$(M+m)\ddot{r} + b_x\dot{r} - m\ddot{r}\cos^2\Phi + mL\dot{\Phi}^2\sin\Phi + mg\dot{\Phi}\cos\Phi\sin\Phi = F \quad (3.52)$$

where F is the mechanical force that derives the trolley machine along x-axis and Φ is the sway angle due to the movement of the tower crane's trolley along x-axis.

Similarly, substituting equation (3.51) into (3.50) the external torque of the jib system is given by:

$$(J + (M+m)r^2)\ddot{\gamma} + b_\gamma\dot{\gamma} - mrL\dot{\theta}^2\sin\theta - mrg\dot{\theta}\sin\theta\cos\theta - mr^2\ddot{\gamma}\cos^2\theta = T_\gamma \quad (3.53)$$

where T_γ is the external driving torque for the jib rotational motion along z-axis, J is the moment of inertia of the jib along z-axis, b_γ is the viscous frictional coefficient in the γ -direction and θ is the sway angle due to the rotation of the tower crane's jib along z-axis.

To obtain a state model for the trolley represented by (3.52), let us take the state variables as

$$\left.\begin{aligned} x_1 &= r \\ x_2 &= \dot{r} \\ x_3 &= \Phi \\ x_4 &= \dot{\Phi} \end{aligned}\right\} \text{ trolley state variables and } u_1 = F \text{ as input variable}$$

Then, the state equations of the trolley are

$$\left.\begin{aligned} \dot{x}_1 &= x_2 \\ \dot{x}_2 &= \frac{-b_x x_2 + m\dot{x}_2\cos^2 x_3 - mL{x_4}^2\sin x_3 - mgx_4\cos x_3\sin x_3 + u_1}{(M+m)} \\ \dot{x}_3 &= x_4 \\ \dot{x}_4 &= \frac{1}{L}(\dot{x}_2\cos x_3 - gx_4\sin x_3) \end{aligned}\right\} \quad (3.54)$$

Similarly, to obtain a state model for the jib represented by (3.53), let us take the state variables as

$$\left.\begin{aligned} x_5 &= \gamma \\ x_6 &= \dot{\gamma} \\ x_7 &= \theta \\ x_8 &= \dot{\theta} \end{aligned}\right\} \text{ jib state variables and } u_2 = T_\gamma \text{ as input variable}$$

Then, the state equations of the jib are

$$\left.\begin{aligned} \dot{x}_5 &= x_6 \\ \dot{x}_6 &= \frac{-b_\gamma x_6 + m x_1 L \dot{x}_8{}^2 \sin x_7 + m x_8 x_1 g \sin x_7 \cos x_7 + m x_1{}^2 \dot{x}_6 \cos^2 x_7 + u_2}{\left(J + (M+m) x_1{}^2\right)} \\ \dot{x}_7 &= x_8 \\ \dot{x}_8 &= \frac{1}{L}(-x_1 \dot{x}_6 \cos x_7 - g x_8 \sin x_7) \end{aligned}\right\} \quad (3.55)$$

To find the equilibrium points, we set $\dot{x}_1 = \dot{x}_2 = \dot{x}_3 = \dot{x}_4 = \dot{x}_5 = \dot{x}_6 = \dot{x}_7 = \dot{x}_8 = 0$ and solve for $x_1, x_2, x_3, x_4, x_5, x_6, x_7$ and x_8:

The equilibrium points are located at $(0,0,n\pi,0,0,0,n\pi,0)$, for $n = 0, \pm 1, \pm 2, \ldots$. From the physical description of the trolley and jib, it is clear that the trolley and jib have only two equilibrium positions corresponding to the equilibrium points $(0,0,0,0,0,0,0,0)$ and $(0,0,\pi,0,0,0,\pi,0)$. Other equilibrium points are repetitions of these two positions, which correspond to the number of full sways the load would make before it rests at one of the two equilibrium positions.

3.3. Tower Crane Model Linearization Using Simple Assumption

The dynamic model of the tower crane system represented by equations (3.52) and (3.53), contains nonlinear functions of $\cos\theta, \cos\Phi, \sin\Phi$ and $\sin\theta$. So, these nonlinearities are linearized by expanding the nonlinear function into a Taylor series at the equilibrium point, i.e. in the static operation mode to eliminate higher order nonlinear model. At equilibrium point the system does not oscillate very far from its equilibrium position (i.e. $\Phi = \theta = 0$). In this case we can expand $\cos\Phi$, $\sin\Phi, \cos\theta$ and $\sin\theta$ into Taylor series around the equilibrium points (i.e. around $\Phi = \theta = 0$). We obtain

$$\sin\Phi = \Phi - \frac{\Phi^3}{3!} + \frac{\Phi^5}{5!} - \frac{\Phi^7}{7!} + \frac{\Phi^9}{9!} - \cdots = \sum_{n=0}^{\infty} (-1)^n \frac{\Phi^{2n+1}}{(2n+1)!} \quad (3.56)$$

$$\cos\Phi = 1 - \frac{\Phi^2}{2!} + \frac{\Phi^4}{4!} - \frac{\Phi^6}{6!} + \frac{\Phi^8}{8!} - \cdots = \sum_{n=0}^{\infty} (-1)^n \frac{\Phi^{2n}}{(2n)!} \tag{3.57}$$

where Φ is the sway angle in radian.

For sufficiently small sway angle equations (3.56)-(3.57) are approximated to:

$$\sin\theta \cong \theta, \sin\Phi \cong \Phi, \cos\Phi \cong 1, \cos\theta \cong 1, \dot{\Phi}\Phi \cong 0, \dot{\theta}\theta \cong 0 \tag{3.58}$$

Using the above assumptions, the nonlinear mathematical equations (3.52) and (3.53) are linearized around its equilibrium point as follows and therefore, the following equations have been obtained.

$$M\ddot{r} + b_x\dot{r} = F \tag{3.59}$$

$$(J + Mr^2)\ddot{\gamma} + b_\gamma\dot{\gamma} = T_\gamma \tag{3.60}$$

Since, the trolley and jib are driven by DC motors the force, F and torque, T_γ are calculated from the physical properties of the motor.

3.4. Modeling of DC Motor

Electric motors can be classified by their functions as servomotors, gear motors, and so forth, and by their electrical configurations as DC and AC motors [29]. An extra categorization can be made as single phase and poly-phase with synchronous and induction motors in terms of their operating principles for AC motors, and permanent Magnet and shunt DC motors for DC motors. Any motor can be used in a servo system and the common ones are DC and AC motors. DC motor is a common actuator in many mechanical systems and industrial applications such as industrial robots, educational robots, and different types of cranes [30]. DC motors are preferable in industrial application because they have better starting torque compare to AC motors, although they are more costly than AC motors [31].

The DC motors are either armature-controlled with fixed field or field-controlled with fixed armature current and also they require an appreciable amount of shaft power. The DC motor is a common actuator that provides rotary motion in control systems [32].

The tower crane is driven by three DC motors. One motor is used to rotate the jib of the tower crane; second motor is used for the linear displacement of the trolley while the last motor is used for lifting and lowering of the payload. But, in this thesis we consider only two motors which are used for the linear displacement of the trolley and for rotating the jib of the tower crane.

To perform the simulation of the tower crane system, an appropriate model needs to be established. In this thesis the general model for any DC servo system containing dc motor; gearbox and inertial load is derived. The mathematical modeling of DC motor with load coupled through gear can be derived by taking the basic equations of the electrical, mechanical and coupling equations of a DC motor as shown in Figure 3.7. In our case the loads are the trolley and jib. In this thesis similar motor are considered for both the trolley and the jib actually they are not identical because the jib includes the mass of the load and the trolley including its mass. The capacity of the motor that drives the jib is greater than the motor that drives the trolley.

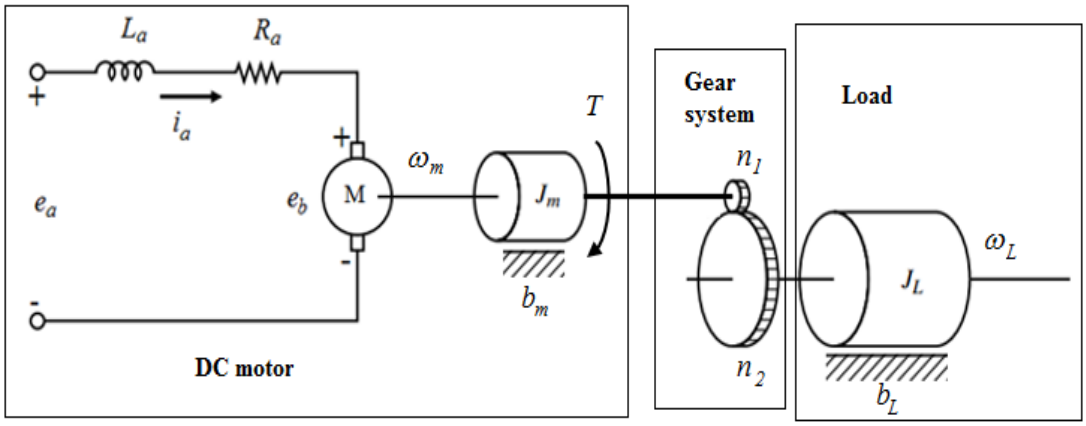

Figure 3.7: Armature-controlled DC servo motor with load coupled through gear [33]

In order to model the DC servo motor shown in Figure 3.7, we define parameters and variables as follows.

R_a=armature-winding resistance (Ω)

L_a= armature-winding inductance (H)

i_a =armature-winding current (A)

i_f = field current (A)

e_a= applied armature voltage (V)

e_b= back emf generated by the motor (V)

K_b= Emf constant (V.sec/rad)

T_m = torque delivered by the motor (Nm)

J_m= moment of inertia of the motor (Kgm^2)

b_m = viscous-friction coefficient of the motor (N.m.sec/rad)

J_L= moment of inertia of the load (Kgm^2)

b_L = viscous-friction coefficient of the load (N.m.sec/rad)

T_L = torque delivered by the load (Nm)

n = gear ratio

The magnetic flux, φ between the stator and the rotor is given by the linear relation:

$$\varphi = k_f i_f \tag{3.61}$$

where k_f is a constant and i_f is the stator current.

The torque T_m is developed by the motor is given by the relation:

$$T_m = k_m i_a \varphi \tag{3.62}$$

where k_m is the armature coil constant. Substituting equation (3.61) into (3.62), the torque now has the form

$$T_m = K_i i_a \tag{3.63}$$

where K_i is a torque constant.

The speed of an armature controlled DC servo motor is controlled by the armature voltage e_a, which is supplied by a power supply (or amplifier). The Kirchhoff's law of voltages for the rotor network is

$$e_a(t) = R_a i_a + L_a \frac{di_a}{dt} + e_b(t) \tag{3.64}$$

The back emf $e_b(t)$ is proportional to the angular velocity. Thus, with a back emf constant K_b, we have

$$e_b = K_b \frac{d\theta_m}{dt} = K_b w_m \tag{3.65}$$

where θ_m is the angular position of the motor. Applying the Laplace transform to equation (3.64) with zero initial conditions, the armature current is

$$I_a(s) = \frac{E_a(s) - E_b(s)}{L_a s + R_a} = \frac{E_a(s) - K_b s\theta_m(s)}{L_a s + R_a} \tag{3.66}$$

Since, the shaft torque T_m is used for driving load against the inertial and frictional torque therefore,

$$T_m = K_i i_a = J_m \frac{dw_m}{dt} + b_m w_m + T \tag{3.67}$$

T is the torque that drives the load through the gears. The motor torque and motor speed are related to the load torque and speed of load through the gear system. The ratio of the angular velocity of the gears is inversely proportional to the ratio of the number of teeth, while the ratio of torques is directly proportional to the ratio of the number teeth. Thus, it is expressed as

$$\frac{w_L}{w_m} = \frac{n_1}{n_2} = \frac{T}{T_L} = n = \text{constant} \tag{3.68}$$

Then the toque T is related to the load torque T_L through the gear ratio as

$$T = nT_L \tag{3.69}$$

Now, consider the load torque T_L, it is expressed as

$$T_L = J_L \frac{dw_L}{dt} + b_L w_L \tag{3.70}$$

Taking the Laplace transform of equation (3.70)

$$T_L(s) = (J_L s + b_L)\Omega_L(s) \tag{3.71}$$

Substituting $w_m = \frac{w_L}{n}$ and equation (3.69) and (3.71) into (3.67) yields

$$K_i I_a(s) = (J_m s + b_m)\frac{\Omega_L(s)}{n} + n\,(J_L s + b_L)\Omega_L(s) \tag{3.72}$$

$$nK_i I_a(s) = (J_e s + b_e)\Omega_L(s) \tag{3.73}$$

where $J_e = J_m + n^2 J_L$ is the equivalent inertia of the motor and load referred to the armature and $b_e = b_m + n^2 b_L$ is the equivalent damping of the motor and load referred to the armature. Then the overall transfer function that relates the load speed with the armature voltage by rearranging equation (3.66) and (3.73) is

$$\frac{\Omega_L(s)}{E_a(s)} = \frac{nK_i}{(J_e s + b_e)(L_a s + R_a) + K_i K_b} \tag{3.74}$$

The equivalent block diagram of the DC motor with load coupled through gear can be represented based on equation (3.74) as shown in figure 3.8.

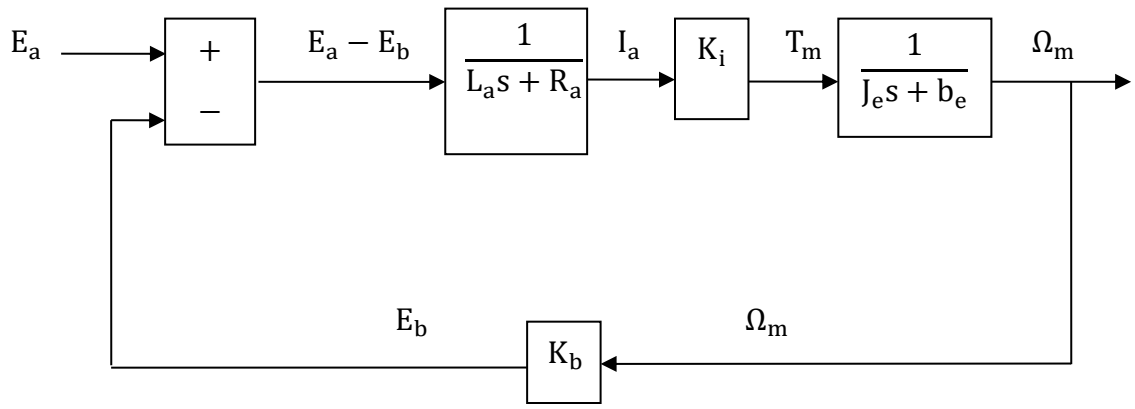

Figure 3.8: Equivalent block diagram of a DC motor with load coupled through gear

The model (3.74) describes any DC servo rotational system but the trolley system of the crane has translational motion along the jib so few terms need to be modified. Since trolley translates along the jib so its speed can be written as:

$$v_t(t) = v(t) = \dot{r}(t) = r_p \omega_L \tag{3.75}$$

where

$v_t(t)$: Translational speed of trolley along the jib

ω_L: Rotational speed of gearbox output shaft driving trolley

r_p: Radius of pulley attached to trolley and together with belt it transforms the rotational motion into translational motion

Taking Laplace transform of equation (3.75)

$$V_t(s) = V(s) = r_p \Omega_L(s) \tag{3.76}$$

Substituting equation (3.74) in to equation (3.76), the transfer function for trolley system from the armature voltage, $E_a(s)$ to the trolley speed, V(s) is given by:

$$\frac{V(s)}{E_a(s)} = \frac{nK_i r_p}{(J_e s + b_e)(L_a s + R_a) + K_i K_b} \tag{3.77}$$

The jib or arm is the rotating part of the tower crane system. So, its angular velocity is given by:

$$V_z(s) = \Omega_L(s) = s\gamma(s) \tag{3.78}$$

Therefore, the transfer function for jib system from the armature voltage, $E_a(s)$ to the jib speed, $V_z(s)$ is given by:

$$\frac{V_z(s)}{E_a(s)} = \frac{nK_i}{(J_e s + b_e)(L_a s + R_a) + K_i K_b} \tag{3.79}$$

Force balance equation for trolley leaving out load due to motor plus gearbox is given by:

$$F = M\dot{v}(t) + b_x v \tag{3.80}$$

From (3.77) $\dot{v}(t)$ can be derived as:

$$\dot{v}(t) = \frac{1}{J_e R_a + L_a b_e}\left(nK_i r_p e_a - J_e L_a \ddot{v} - (R_a b_e + K_i K_b)v\right) \tag{3.81}$$

Substituting equation (3.81) into equation (3.80) we get:

$$F = \frac{M}{J_e R_a + L_a b_e}\left(nK_i r_p e_a - J_e L_a \ddot{v} - (R_a b_e + K_i K_b)v\right) + b_x v \tag{3.82}$$

Substituting equation (3.82) into equation (3.59) gives the velocity model of the trolley system.

$$M\ddot{r} + b_x \dot{r} = \frac{M}{J_e R_a + L_a b_e}\left(nK_i r_p e_a - J_e L_a \ddot{v} - (R_a b_e + K_i K_b)v\right) + b_x v \tag{3.83}$$

Rearranging equation (3.83) gives the trolley velocity equation:

$$\ddot{v} + \left(\frac{J_e R_a + L_a b_e}{J_e L_a}\right)\dot{v} + \left(\frac{R_a b_e + K_i K_b}{J_e L_a}\right)v = \frac{nK_i r_p e_a}{J_e L_a} \tag{3.84}$$

Similarly, from equation (3.70) we have

$$T_\gamma = J\,\dot{v}_z + b_\gamma v_z \tag{3.85}$$

where $\dot{\gamma} = w_L = v_z$

Using equation (3.79) $\dot{v}_z$ can be calculated as

$$\dot{v}_z(t) = \frac{1}{J_e R_a + L_a b_e}(nK_i e_a - J_e L_a \ddot{v}_z - (R_a b_e + K_i K_b)v_z) \tag{3.86}$$

Substituting (3.86) into equation (3.85) gives

$$T_\gamma = \frac{J}{J_e R_a + L_a b_e}(nK_i e_a - J_e L_a \ddot{v}_z - (R_a b_e + K_i K_b)v_z) + b_\gamma v_z \tag{3.87}$$

Substituting equation (3.87) into equation (3.60) gives the velocity model of the jib system.

$$(J + Mr_p{}^2)\ddot{\gamma} = \frac{J}{J_e R_a + L_a b_e}(nK_i e_a - J_e L_a \ddot{v}_z - (R_a b_e + K_i K_b)v_z) \tag{3.88}$$

Rearranging equation (3.88) gives the jib velocity equation:

$$\ddot{v}_z + \left(\frac{(J + Mr_p{}^2)(J_e R_a + L_a b_e)}{J_e L_a}\right)\dot{v}_z + \left(\frac{R_a b_e + K_i K_b}{J_e L_a}\right)v_z = nK_i e_a \tag{3.89}$$

With the parameters of the DC motor and trolley shown in Table 3.1, and substituting these parameter values into equation (3.84) describing the dynamic behavior of the trolley become

$$\ddot{v} + 0.9405\dot{v} + 14.66v = 19.0405e_a \tag{3.90}$$

Applying Laplace transform to equation (3.90). Therefore, the transfer functions from the output V to the input E_a describing the dynamic behavior of the trolley become:

$$s^2V(s) + 0.9405sV(s) + 14.66V(s) = 19.0405E_a(s) \tag{3.91}$$

By rearranging equation (3.91) we get

$$\frac{V(s)}{E_a(s)} = \frac{19.0405}{s^2 + 0.9405s + 14.66} \tag{3.92}$$

Similarly, with the parameters of the DC motor and jib shown in Table 3.1, and substituting these parameter values into equation (3.89) describing the dynamic behavior of the jib become:

$$\ddot{v}_z + 0.9405\dot{v}_z + 14.66v_z = 476.017e_a \tag{3.93}$$

Applying Laplace transform to equation (3.93). Therefore, the transfer functions from the output V to the input E_a describing the dynamic behavior of the jib become:

$$s^2V_z(s) + 0.9405sV(s) + 14.66V(s) = 476.017E_a(s) \tag{3.94}$$

By rearranging equation (3.94) we get

$$\frac{V_z(s)}{E_a(s)} = \frac{476.017}{s^2 + 0.9405s + 14.66} \tag{3.95}$$

Table 3.1: Trolley and Jib motor parameters [24, 34, 35]

Parameter	Value
Rated power	3.7 KW
Rated motor speed, N	1750 rpm
Rated terminal voltage	240 V
R_a	11.4 Ω
L_a	0.1214 H
K_b	0.0045 V sec/rad
K_T	1.28 Nm/A
J_m	0.02215 Kgm^2
B_m	0.00295 Nm sec/rad
J_L	0.022 Kgm^2
B_L	0.0005 Nm sec/rad
N	100
M	0.7Kg
J	50Kgm^2
r_p	0.04m

CHAPTER FOUR

Controller Design

Different controllers are used in the control of the tower crane system. The purpose of the control systems used is to make the value of the response of the plant to follow the reference signal. Any difference between the desired signal value in the system and the existing system output value is considered as a fault. This fault is tried to be reduced via the controller applied to the system.

4.1. Proportional-Integral-Derivative (PID) Controller Design

A PID controller is implemented in almost all industrial processes because it is simple and robust. The main function of PID controller is to minimize the error between the actual output and reference input. It calculates the error between the measured process variable and desired set point and then gives a corrective action to adjust the process according to the set point and to keep the error as low as possible. The proportional term gives reaction based on the current error; the integral value determines the action based on the sum of recent errors and derivative value gives the reaction based on the rate at which error changes. The combined action of these three parameters helps in generating a control signal to adjust the process or plant to the desired value. The general equation of PID controller is:

$$u(t) = K_p \left[e(t) + \frac{1}{T_i} \int_0^t e(\tau) d\tau + T_d \frac{de(t)}{dt} \right] \tag{4.1}$$

where K_p is the proportional gain, T_i is the integral time constant, T_d is the derivative or rate time constant.

By adjusting the controller gains we can obtain a control action based on the plant requirements. The output of the PID controller is dependent on the responsiveness of controller towards the error, the degree at which the controller goes beyond the set point and the system oscillations.

Taking the Laplace transform of equation (4.1) gives,

$$U(s) = \left(K_p + K_d s + \frac{K_i}{s} \right) E(s) \tag{4.2}$$

where $K_i = \frac{K_p}{T_i}$ is the integral gain and $K_d = K_p T_d$ is the derivative gain.

The variable E(s) in equation (4.2) represents the tracking error. This error signal will be sent to the PID controller and both the derivative and the integral of this error signal are computed by the

controller. In practical applications, the pure derivative action is never used, due to the "derivative kick" produced in the control signal for a step input, and to the undesirable noise amplification. It is usually replaced by a first-order low pass filter. Thus, the Laplace transformation representation of the approximate PID controller can be written as

$$U(s) = K_p\left[1 + \frac{1}{T_i s} + \frac{T_d s}{1 + s\frac{T_d}{N}}\right]E(s) \tag{4.3}$$

where N is the filter coefficient.

The system performance can be evaluated by performance criteria parameters; the overshoot M_p, rise time t_r, settling time t_s and steady-state error e_{ss}.

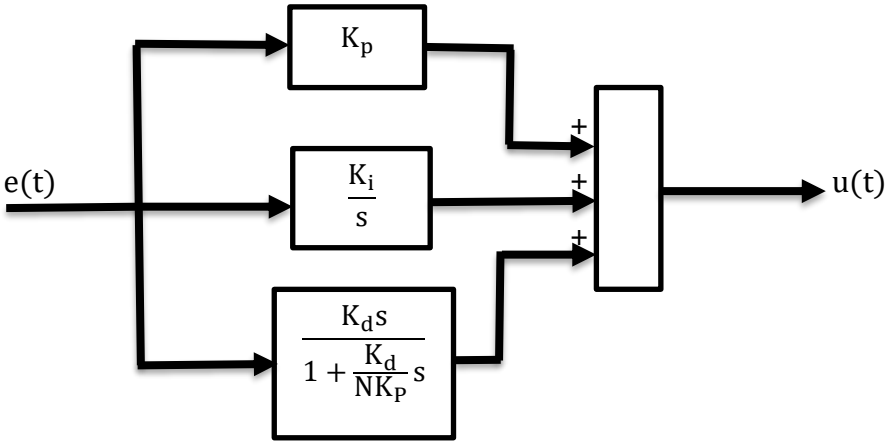

Figure 4.1: Parallel block diagram of the PID controller

A conventional feedback control loop with the parallel PID controller is represented by the block diagram in Figure 4.2.

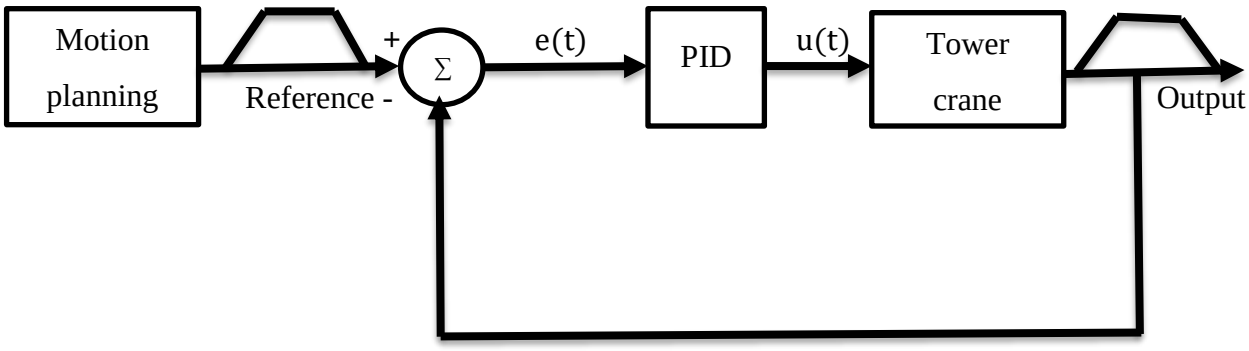

Figure 4.2: Block diagram of a parallel PID control system

For the control plant, better performance can be attained by tuning the control loop, which is adjusting the control parameters to satisfy the desired control response. For PID controller, each of the three parameters i.e. proportional gain, integral gain and derivative gain has different effect on system control which is summarized in Table 4.1 based on the situation of increasing the controller parameter individually.

Table 4.1: Effects caused by increasing the PID control parameter individually [36]

PID Control Parameters	Rise Time (t_r)	Over Shoot (M_p)	Settling Time (t_s)	Steady State Error(e_{ss})
K_p	Decrease	Increase	Small Change	Decrease
K_i	Decrease	Increase	Increase	Eliminate
K_d	Small Change	Decrease	Decrease	Small Change

In PID controller the process of adjusting of the controller parameters i.e. proportional gain, integral gain and derivative gain to the optimal values at which preferred control response is achieved is called tuning of a control loop system. For this purpose there are several tuning methods like (Z-N), (CC), (CHR) method and PID auto tuner [37]. In this thesis the PID auto tuner method is used to adjust the parameters of the controller.

4.2. Fuzzy Logic Controller

The word fuzzy refers to things which are not clear or are vague. Any event, process, or function that is changing continuously cannot always be defined as either true or false, which means that we need to define such activities in a fuzzy manner.

Fuzzy Logic resembles the human decision-making methodology. It deals with vague and imprecise information. This is gross oversimplification of the real-world problems and based on degrees of truth rather than usual true or false or 1 or 0 like Boolean logic.

In other words, fuzzy logic is not logic that is fuzzy, but logic that is used to describe fuzziness. Fuzzy Logic was introduced in 1965 by Lofti A. Zadeh in his research paper “Fuzzy Sets”. He is considered as the father of Fuzzy Logic.

Fuzzy logic is based on the mathematical theory of fuzzy sets which is extension or generalization of classical or crisp set theory. Fuzzy logic provides an inference system in which decisions are without discontinuities, flexible and non-linear i.e. closer to human brain. It looks at the world of uncertain and inaccurate terms then responds with precise action [38].

Fuzzy logic and fuzzy logic control theories added a new dimension to control systems engineering in the early 1970s. From its beginnings as mostly heuristic, somewhat ad-hoc, more recent and rigorous approaches to fuzzy logic control theory have helped make it integral part of modem control theory and produced many exciting results.

Fuzzy logic controller is a technique to embody human like thinking which is much less rigid than the calculations computer generally perform into a control system. Fuzzy logic controller can be designed to emulate human deductive thinking, that is, the process people use to infer conclusion from what they know. Meanwhile, conventional controller requires formal modeling of the physical reality of any plant. Apart from that, fuzzy logic control incorporates ambiguous human logic into computer programs. It suit control problem that can't be easily represented by mathematical model. The design of such controller leads to faster development and implementation cycles due to its unconventional approach.

There are four important elements in the fuzzy logic controller system structure which are fuzzifier, rule base, inference engine and defuzzifier. Details of the fuzzy logic controller structure can be seen in Figure 4.3. Firstly, a crisp set of input data are gathered and converted to a fuzzy set using fuzzy linguistic variables, fuzzy linguistic terms and membership functions. This step also known as fuzzification. Afterwards, an inference is made based on a set of rules. Lastly, the resulting fuzzy output is mapped to a crisp output using the membership functions, in the defuzzification step.

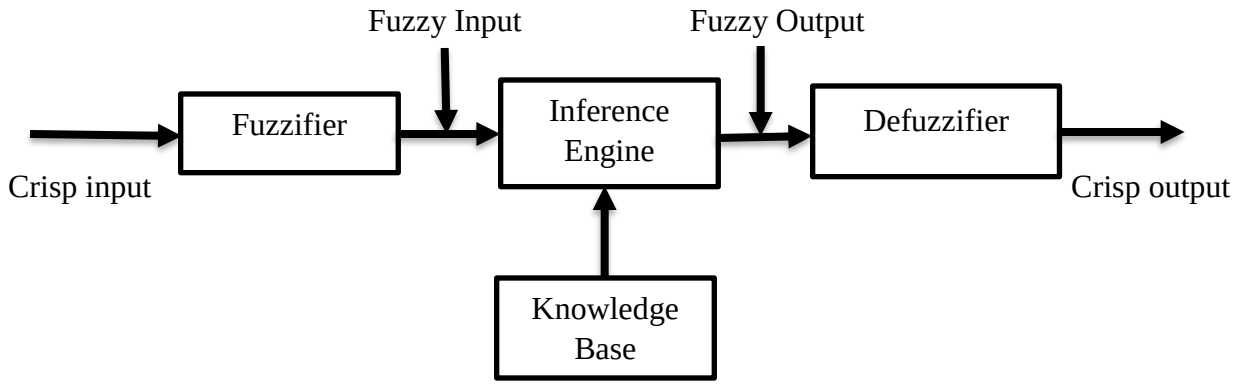

Figure 4.3: Structure of fuzzy logic controller [39]

4.2.1. Fuzzifier

The component which performs the fuzzification process i.e. converts the classical variable to fuzzy variable, is called fuzzifier. The classical variables are required to convert to fuzzy variable in order to process them in fuzzy inference engine. Fuzzification process involves two tasks: assigning membership function to input and output and representing them in linguistic variable. Linguistic variables are variables whose values are not numbers but words or sentences in a natural or artificial language. Just like an algebraic variable takes numbers as values, a linguistic variable takes words or sentences as values.

- The set of values that it can take is called its term set.
- Each value in the term set is a fuzzy variable defined over a base variable.
- The base variable defines the universe of discourse for all the fuzzy variables in the term set.

In short, the hierarchy is as follows:

Linguistic variable →fuzzy variable →base variable

A linguistic variable can be defined by the following quintuple:

$$\text{Linguistic variable} = (x, T(x), U, G, M) \tag{4.4}$$

in which x is the name of variable, T(x) is the term set of x, that is, the set of names of linguistic values of x with each value being a fuzzy number defined on U, G is a syntactic rule for generating the names of values of x and M is a semantic rule for associating with each value its meaning [40]. In order to facilitate the symbolism in what follows, some symbols will have two meanings wherever clarity allows this: x will denote the name of the variable.

Next, to map the non-fuzzy input or crisp input data to fuzzy linguistic terms, membership functions are used. In other words, a membership function is used to quantify a linguistic term. Note that, an important characteristic of fuzzy logic is that a numerical value does not have to be fuzzified using only one membership function meaning, a value can belong to multiple sets at the same time. Membership function can be measured in percentage from 0% to 100% or as a number 0 to 1. Sometimes membership function is also called as confidence factor.

Since all information contained in a fuzzy set is uniquely specified by its membership function, it is useful to develop a lexicon of terms to describe various special features of this function. The feature of the membership function is defined by three properties. They are:

(i) Core: The core of a membership function for some fuzzy set $\widetilde{A}$ is defined as that region of the universe that is characterize by complete and full membership in the set $\widetilde{A}$. Hence, core consists of all those elements x of the universe of information such that $\mu_{\widetilde{A}}(x) = 1$.

(ii) Support: The support of a membership function for some fuzzy set $\widetilde{A}$ is defined as that region of the universe that is characterize by a nonzero membership in the set $\widetilde{A}$.

Hence, support consists of all those elements x of the universe of information such that $\mu_{\widetilde{A}}(x) > 0$.

(iii) Boundary: The boundaries of a membership function for some fuzzy set $\widetilde{A}$ are defined as that region of universe containing elements that have a nonzero but incomplete membership in the set $\widetilde{A}$. That is, the boundaries comprise those elements x of the universe such that $0 < \mu_{\widetilde{A}}(x) < 1$.

These are the standard regions defined in the membership functions.

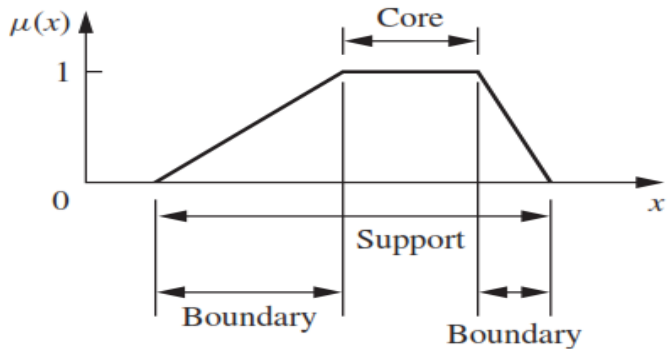

Figure 4.4: Features of membership function [41]

The membership functions are the building blocks of fuzzy set theory, that is, fuzziness in a fuzzy set is determined by its membership function. Accordingly, the shapes of membership functions are important for a particular problem since they effect on a fuzzy inference system. They may have different shapes such as triangular, trapezoidal, Gaussian, and so forth. The only condition a membership function must really satisfy is that it must vary between 0 and 1. There are different forms or shapes of membership functions such as triangular, Gaussian, trapezoidal, generalized bell and sigmoidal. The type of the membership function can be context dependent and it is generally chosen arbitrarily according to the user experience. Due to its simplicity the triangular membership function is the most commonly used type of membership functions in many applications [42-46]. This type of membership function is formed using straight line. Figure 4.5 to Figure 4.9 shows the different types of membership function shape.

Triangular MFs: A triangular membership function is specified by three parameters (a, b, c) according to:

$$\text{trimf}(x; a, b, c) = \begin{cases} 0, & x \leq 0 \\ \dfrac{x-a}{b-a}, & a \leq x \leq b \\ \dfrac{c-x}{c-b}, & b \leq x \leq c \\ 0, & c \leq x \end{cases} \tag{4.5}$$

The parameters (a, b c) or (with $a < b < c$) determine the x coordinates of the four corners of the underlying trapezoidal membership function.

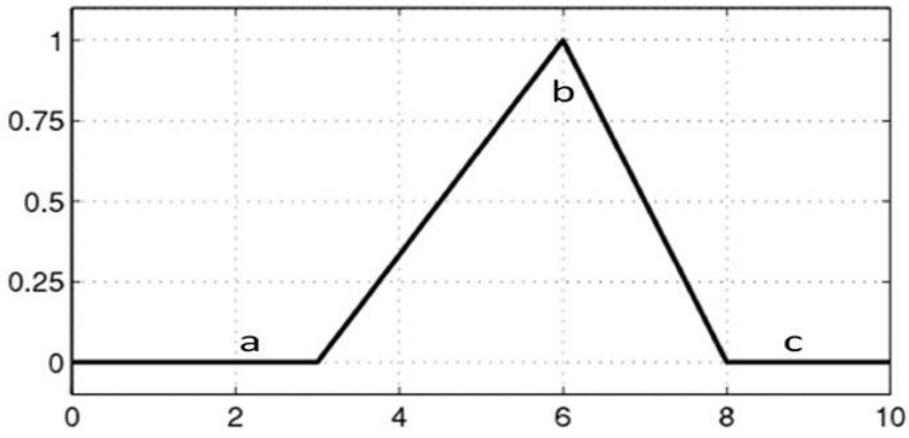

Figure 4.5: Triangular membership function shape

Gaussian MFs: A Gaussian membership function is given by two parameters (c, σ) according to:

$$\text{gaussmf}(x;\sigma,c) = e^{-\frac{1}{2}\left(\frac{x-c}{\sigma}\right)^2} \tag{4.6}$$

where c represents the membership functions center and σ determines the membership functions width.

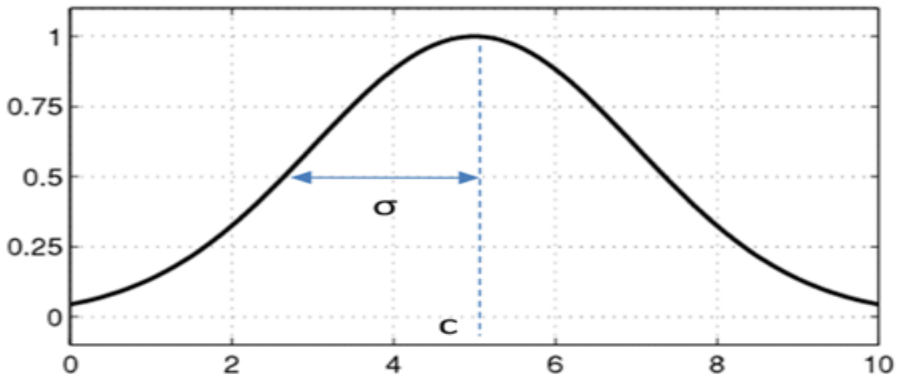

Figure 4.6: Gaussian membership function shape

Trapezoidal MFs: A trapezoidal membership function is specified by four parameters (a, b c, d) according to:

$$\text{trapmf}(x;a,b,c) = \begin{cases} 0, & x \le a \\ \dfrac{x-a}{b-a}, & a \le x \le b \\ 1, & b \le x \le c \\ \dfrac{d-x}{d-c}, & c \le x \le d \\ 0, & d \le x \end{cases} \tag{4.7}$$

The parameters (a, b c, d) or (with $a < b \le c < d$) determine the x coordinates of the four corners of the underlying trapezoidal membership function.

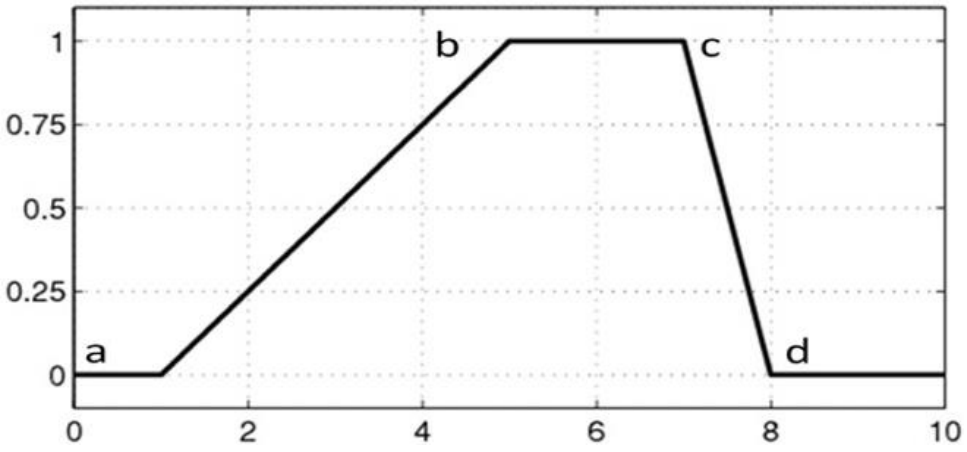

Figure 4.7: Trapezoidal membership function shape

Generalized bell MFs: A generalized bell membership function is given by three parameters (a, b, c) as follows:

$$\text{gbellmf}(x; a, b, c) = \frac{1}{1 + \left|\frac{x - c}{a}\right|^{2b}} \tag{4.8}$$

where the parameter b is usually positive. If b is negative, the shape of this membership function becomes an upside-down bell.

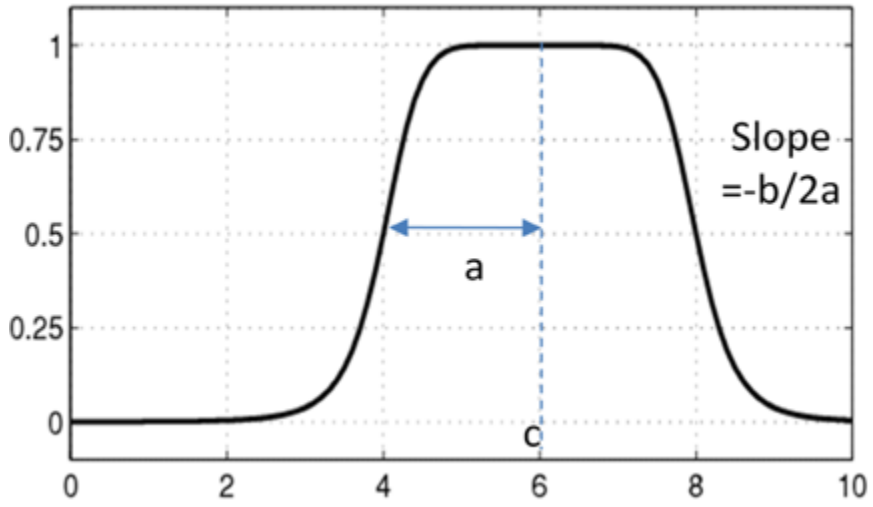

Figure 4.8: Generalized bell membership function shape

Sigmoidal MFs: A sigmoidal membership function has two parameters and is given by

$$\text{sigmf}(x; a, c) = \frac{1}{1 + e^{-a(x-c)}} \tag{4.9}$$

where a controls the slope at the crossover point x=c.

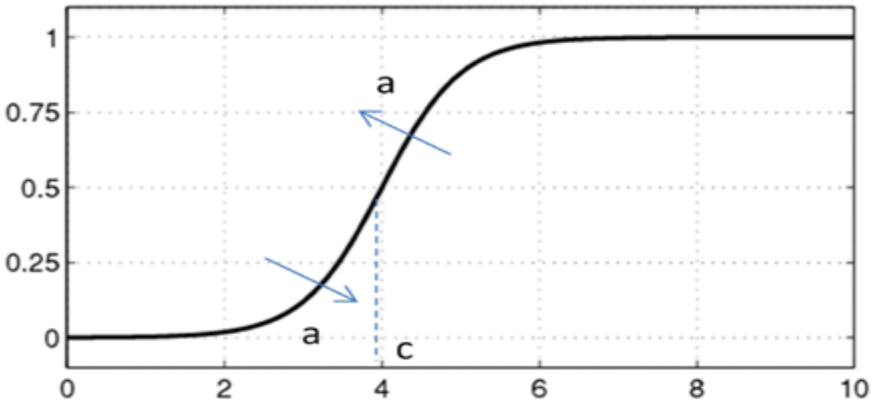

Figure 4.9: Sigmoidal membership function shape

A sigmoidal membership function is inherently open right or left and thus, it is appropriate for representing concepts such as “very large” or “very negative”. Sigmoidal membership function is mostly used as activation function of artificial neural networks.

4.2.2. Knowledge Base

The knowledge base of fuzzy logic controller consists of a data base and a rule base. The function of data base is to provide the essential information for proper functioning of the fuzzifier, defuzzifier and the rule base. The rule base provides the expert knowledge in the form of IF-THEN rules for inference engine.

4.2.3. Inference Engine

The fuzzy inference engine is the heart of FLC. According to rule base it has the capability to perform operation on fuzzy input variables. The fuzzy outputs or conclusions are the combination of input-output membership function and the fuzzy rules (IF-THEN rules). There are many methods to perform fuzzy inference method and the most common two of them are;

(i) Mamdani Fuzzy Inference System

(ii) Sugeno Fuzzy Inference System

Mamdani method was proposed by Ebrahim Mamdani as an attempt to control a steam engine and boiler in 1975. It is based on Lofti Zadeh’s 1973 paper on fuzzy algorithms for complex system and decision processes. This method uses the minimum operation as a fuzzy implication and the max-min operator for the composition. Suppose a rule base is given in the following form;

IF input x = A AND input y = B

THEN output z = C

After the aggregation process, there is a fuzzy set for each output variable that needs defuzzification. It is possible and in many cases much more efficient, to use a single spike as the output membership functions rather than a distributed fuzzy set. This is sometimes known as a singleton output membership function. It enhances the efficiency of defuzzification process because it greatly simplifies the computation required by the more general Mamdani method, which finds the centroid of two dimensional functions.

Meanwhile, Takagi-Sugeno-Kang method was introduced in 1985 and it is similar to the Mamdani method in many aspects. The first two parts of fuzzy inference processes which are fuzzifying the

inputs and applying the fuzzy operator are exactly the same. But, the main difference is that the Takagi-Sugeno-Kang output membership function is either linear or constant. A typical rule in Takagi-Sugeno-Kang fuzzy model has the form as follows;

IF input 1 = x AND input 2 = y

THEN output z = ax + by + c

For a zero order Takagi-Sugeno-Kang model, the output z is a constant (a=b=0). The output of z_i of each rule is weighted by the firing strength w_i as follows;

$$w_i = \text{AndMethod}\big(F_1(x), F_2(y)\big) \tag{4.10}$$

where $F_1(x)$ and $F_2(y)$ are the membership functions for input 1 and input 2 respectively. The final output of the system is the weighted average of all rule outputs, computed as;

$$\text{Final Output} = \frac{\sum_{i=1}^{N} w_i z_i}{\sum_{i=1}^{N} w_i} \tag{4.11}$$

The main difference between Mamdani and Sugeno is that the Sugeno output membership functions are either linear or constant. Also the difference lies in the consequents of their fuzzy rules, and thus their aggregation and defuzzification procedures differ suitably. The number of the input fuzzy sets and fuzzy rules needed by the Sugeno fuzzy systems depend on the number and locations of the extrema of the function to be approximated. In Sugeno method a large number of fuzzy rules must be employed to approximate periodic or highly oscillatory functions. The minimal configuration of the Takagi-Sugeno-Kang fuzzy systems can be reduced and becomes smaller than that of the Mamdani fuzzy systems if non-trapezoidal or non-triangular input fuzzy sets are used. Sugeno controllers usually have far more adjustable parameters in the rule consequent and the number of the parameters grows exponentially with the increase of the number of input variables. Far fewer mathematical results exist for Takagi-Sugeno-Kang fuzzy controllers than do for Mamdani fuzzy controllers, notably those on Takagi-Sugeno-Kang fuzzy control system stability. Mamdani is easy to form compared to Sugeno method. In this thesis we use the Mamdani method.

4.2.4. Defuzzifier

A defuzzifier is a module which carries out the process of de-fuzzification. The defuzzification process is meant to convert the fuzzy output back to the crisp or classical output to the control objective. The fuzzy outcomes generated cannot be used as such to the applications, hence it is necessary to convert the fuzzy quantities into crisp quantities for further processing. This can be achieved by using defuzzification process. The defuzzification has the capability to reduce a fuzzy

to a crisp single-valued quantity or as a set, or converting to the form in which fuzzy quantity is present. Defuzzification can also be called as "rounding off" method. Defuzzification reduces the collection of membership function values in to a single sealer quantity. The output or conclusion of fuzzy inference is linguistic variable and it has to be converting to classical variable or values to understand. There are many different methods for defuzzification. Some of them are listed below.

i. Centroid method
ii. Max-Membership Method
iii. Weighted Average Method
iv. Mean-Max Membership

The different methods of defuzzification are described below:

Centroid Method: This method is the most prevalent and physically appealing of all defuzzification methods [39, 47]. It is also known as center-of-area or center-of- gravity method because it computes the centroid of the composite area representing the output fuzzy term. The basic equation of Centroid of Gravity (COG) is given by;

$$x^* = \frac{\int \mu_{\tilde{A}}.x dx}{\int \mu_{\tilde{A}}.dx} \tag{4.12}$$

where, x^* is the defuzzified output.

Max-Membership Method: This method is limited to peak output functions and also known as height method. This method is given by the algebraic expression

$$\mu_{\tilde{A}}(x^*) \geq \mu_{\tilde{A}}(x), \qquad \forall x \in X \tag{4.13}$$

where, x^* is the defuzzified value.

Mean-Max Membership: This method is also known as the middle-of-the maxima. Mathematically, the defuzzified output x^* will be represented as follows:

$$x^* = \frac{\sum_{i=0}^{n} \bar{x}_i}{n} \tag{4.14}$$

where, x^* is the defuzzified value.

The mean-max membership method is closely related to the max-membership method, except that the locations of the maximum membership can be nonunique (i.e., the maximum membership can be a plateau rather than a single point).

Weighted Average Method: In this method, each membership function is weighted by its maximum membership value. Mathematically, the defuzzified output will be represented as follows:

$$x^* = \frac{\sum \mu_{\tilde{A}}(\bar{x}_i).\bar{x}_i}{\sum \mu_{\tilde{A}}(\bar{x}_i)} \tag{4.15}$$

There is no systematic procedure for choosing a good defuzzification strategy, but the selection of defuzzification procedure depends on the properties of the application. In this thesis a Centroid of Gravity (COG) is used as a defuzzification method.

4.3. Fuzzy Logic Controller Design

A basic structure of fuzzy logic controller system for anti-sway control of the tower crane system is clearly shown in Figure 4.10.

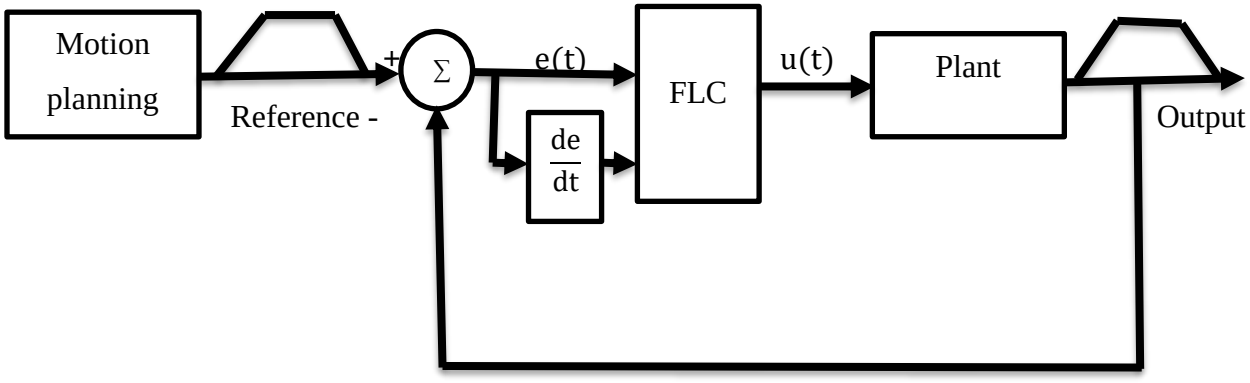

Figure 4.10: Fuzzy logic controller for a tower crane system

The most important aspect in fuzzy logic control system designs start with a process of converting the measured inputs called crisp values, into the fuzzy linguistic values used by the fuzzy reasoning mechanism. The process of reasoning mechanism will perform fuzzy logic operations and result the action according to the fuzzy inputs. A collection of the expert control rules known as knowledge needed to achieve the control goal. As shown in figure 4.10, a fuzzy logic controller input variables involves receiving the error signal and rate of change in error. These variables evaluate the fuzzy logic controller rules using the compositional rules of inference and the appropriately computed control action is determined by using the defuzzification. The essential steps in designing the fuzzy logic controller of this system are illustrated in Figure 4.11.

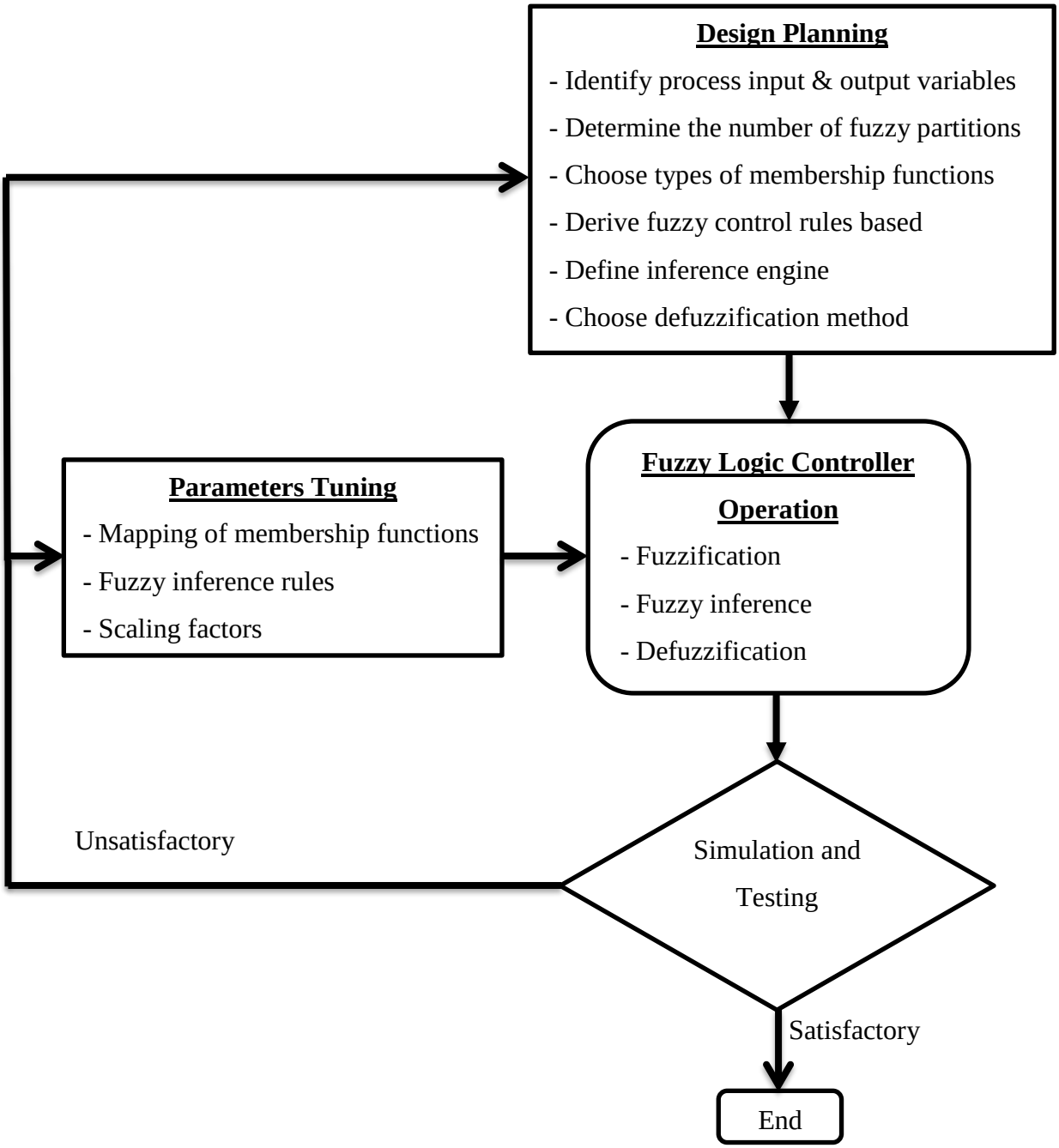

Figure 4.11: Design procedure of the fuzzy logic controller

In the design of fuzzy logic controller for velocity control of both the trolley and jib part of the tower crane system we have considered seven (7) linguistic variables (LN, MN, SN, Z, SP, MP and LP) for the inputs (error and rate of change in error) and output (control output). In case of output control output, we have considered seven (7) linguistic variables (LN, MN, SN, Z, SP, MP and LP). A triangular membership function is defined for each input and output variables which

are: error $(e(t))$, rate of change in error $(ce(t))$ and control output (u). The membership functions of the inputs and outputs are designed after the rule data base, and the controller is tested on the system to adjust any seemingly wrong parameters. The rule base works by monitoring the error and rate of change in error of the controller system. The rule base is formulated using fuzzy operators in IF – THEN statements i.e. IF (Process State – input parameters defined using fuzzy operator) THEN (Control Output).

The choice of the fuzzy operator used is the Minimum (Product) fuzzy operator. The general rules for the trolley and jib velocity control are that if trolley or jib velocity is less than the optimal velocity, then increase trolley or jib velocity and if trolley or jib velocity exceeds the optimal reference velocity, then reduce the velocity. If the error is large positive and the rate of change in error is large negative, then the output of the controller must be zero and there is no need to increase the trolley or jib velocity to meet the optimal reference velocity point which is directly proportional to the voltage of the controller. These fuzzy rules are summarized in the fuzzy rule matrix shown in Table 4.2 below.

Table 4.2: Fuzzy rule matrix table for trolley and jib velocity control

U		Ce						
		LN	MN	SN	Z	SP	MP	LP
e	LN	LN	LN	LN	LN	MN	SN	Z
	MN	LN	LN	LN	MN	SN	Z	SP
	SN	LN	LN	MN	SN	Z	SP	MP
	Z	LN	MN	SN	Z	SP	MP	LP
	SP	MN	SN	Z	SP	MP	LP	LP
	MP	SN	Z	SP	MP	LP	LP	LP
	LP	Z	SP	MP	LP	LP	LP	LP

General Interpretation of the control rules to be set to the Fuzzy control:

- If Error = 0 and rate of change in error = 0, then do not change the present setting.
- If Error is non-zero but Error is tending to zero at an acceptable rate, then do not change the present setting.
- If Error is increasing or decreasing, then make the control signal according to the magnitude and sign of the Error and rate of change in error to make the Error zero.

Illustrating the fuzzy rule matrix Table 4.2 for three valid rules,

1. IF the error (e) is Small Negative (SN) AND the rate of change in error (ce) is Large Positive (LP), THEN the control action (u) is Medium Positive (MP).

This rule quantifies the situation in which the velocity of the trolley or jib is slightly above the optimal velocity but decreasing, meaning it requires a decrease in the armature voltage which is proportional to the velocity of the trolley. So, the control signal is Medium Positive (MP) for Large Positive (LP) value of the rate of change in error.

2. IF the error (e) is Zero (Z) AND the rate of change in error (ce) is Large Negative (LN), THEN the control action (u) is Large Negative (LN).

This rule quantifies the situation in which the velocity of the trolley or jib is close to the optimal velocity but increasing slightly, meaning it requires an increase in the armature voltage which is proportional to the velocity of the trolley to correct the error.

3. IF the error (e) is Medium Positive AND the rate of change in error (ce) is Medium Negative (MN), THEN the control action (u) is Zero (Z).

The error and rate of change in error of the fuzzy controller is measured by the following formula:

$$\text{Error } e(t) = v_{ref}(t) - v_m(t) \tag{4.13}$$

$$\text{Rate of change in error } ce(t) = \frac{de(t)}{dt} = e(t) - e(t-1) \tag{4.14}$$

In equation (4.13), v_{ref} is the reference velocity of the trolley and jib and v_m is the measured velocity of the trolley and jib.

4.4. Fuzzy Logic Controller Toolbox Setup

The implementation of the FLC requires the choice of four key factors which are; the number of fuzzy sets that constitute linguistic variables, mapping the measurements into the support sets, control protocol that determines the controller behavior and the shape of the membership

functions. There are five primary graphical user interface (GUI) tools for building, editing and observing fuzzy inference systems in the toolbox. These are:

(i) Fuzzy inference system (FIS) editor
(ii) Membership function editor
(iii) Rule editor
(iv) Rule viewer
(v) Surface viewer

These GUI are dynamically linked and if changes make to the FIS to one of the toolbox, the effect can be seen in other GUIs. Figures 4.12 and 4.13 indicate the FIS editors of both trolley and jib systems and handles the high-level issues of the system. They have a command on handling basic issues of the control system such as defining of input and output variables. Fuzzy logic toolbox can hold unlimited amount of inputs but corresponding there will be a huge number of membership functions which will become difficult for us to handle. Fuzzy Logic toolbox does not limit the FIS editor displays general information about fuzzy inference system. There is a simple diagram at the top shows the name of each input variable on the left and the output on the right [48].

The trolley and jib membership function editor defines the appearance and shape of membership function as per input. These are shown in Figures 4.14, 4.15, 4.16, 4.20, 4.21 and 4.22.

Table 4.3 shows the trolley numerical range of values for the input error and its corresponding linguistic notation ranging between -0.02932 and 0.02932 with seven triangular shaped membership functions. Table 4.4 shows the trolley numerical range of values for the rate of change in error and its corresponding linguistic notation ranging between -16.07 and 16.07 with seven triangular shaped membership functions.

Table 4.5 shows the jib numerical range of values for the input error and its corresponding linguistic notation ranging between -0.2 and 0.2 with seven triangular shaped membership functions. Table 4.6 shows the jib numerical range of values for the rate of change in error and its corresponding linguistic notation ranging between -76.4 and 76.4 with seven triangular shaped membership functions.

Figures 4.14 and 4.20 illustrate the representation of the seven triangular shaped membership functions for the trolley and jib error $e(t)$ respectively.

Figures 4.15 and 4.21 illustrate the representation of the seven triangular shaped membership functions for the trolley and jib rate of change in error $ce(t)$ respectively.

Table 4.7 shows the numerical range of values for the control output of both trolley and jib and its corresponding linguistic notation ranging between -240 and 240 with seven triangular shaped membership functions. Figures 4.16 and 4.22 illustrate the representation of the seven output membership functions of trolley and jib respectively.

Table 4.3: Trolley numerical range of linguistic variable for error $e(t)$

Linguistic variable	Notation	Numerical range
Large Negative	LN	[-0.02932 -0.02932 -0.01954]
Medium Negative	MN	[-0.02932 -0.01954 -0.009786]
Small Negative	SN	[-0.01954 -0.009786 -3.634e-06]
Zero	Z	[-0.009786 -3.634e-06 0.009752]
Small Positive	SP	[-3.634e-06 0.009752 0.01955]
Medium Positive	MP	[0.009752 0.01955 0.02932]
Large Positive	LP	[0.01956 0.02932 0.02932]

Table 4.4: Trolley numerical range of linguistic variable for rate of change in error $ce(t)$

Linguistic variable	Notation	Numerical range

Large Negative	LN	[-16.07 -16.07 -10.74]
Medium Negative	MN	[-16.07 -10.74 -5.357]
Small Negative	SN	[-10.74 -5.369 -0.001114]
Zero	Z	[-5.369 -0.001114 5.348]
Small Positive	SP	[-0.001114 5.348 10.71]
Medium Positive	MP	[5.348 10.71 16.07]
Large Positive	LP	[10.73 16.07 16.07]

Table 4.5: Jib numerical range of linguistic variable for error $e(t)$

Linguistic variable	Notation	Numerical range
Large Negative	LN	[-0.2 -0.2 -0.1333]
Medium Negative	MN	[-0.2 -0.1333 -0.06675]
Small Negative	SN	[-0.1333 -0.06675 2.777e-05]
Zero	Z	[-0.06675 2.777e-05 0.06645]
Small Positive	SP	[2.777e-05 0.06645 0.1334]
Medium Positive	MP	[0.06645 0.1334 0.2]

Large Positive	LP	[0.1335 0.2 0.2]

Table 4.6: Jib numerical range of linguistic variable for rate of change in error ce(t)

Linguistic variable	Notation	Numerical range
Large Negative	LN	[-76.4 -76.4 -51.12]
Medium Negative	MN	[-76.4 -51.12 -25.4]
Small Negative	SN	[-51.12 -25.53 0.03592]
Zero	Z	[-25.53 0.03592 25.44]
Small Positive	SP	[0.03592 25.44 50.97]
Medium Positive	MP	[25.44 50.97 76.4]
Large Positive	LP	[50.97 76.4 76.4]

Table 4.7: Trolley and jib numerical range of linguistic variable for control output u(t)

Linguistic variable	Notation	Numerical range
Large Negative	LN	[-240 -240 -160.1]
Medium Negative	MN	[-240 -160.1 -79.87]
Small Negative	SN	[-160.1 -79.9 0]

Zero	Z	[-79.9 0 80.08]
Small Positive	SP	[0 80.08 160.5
Medium Positive	MP	[80.08 160.5 240]
Large Positive	LP	[160.5 240 240]

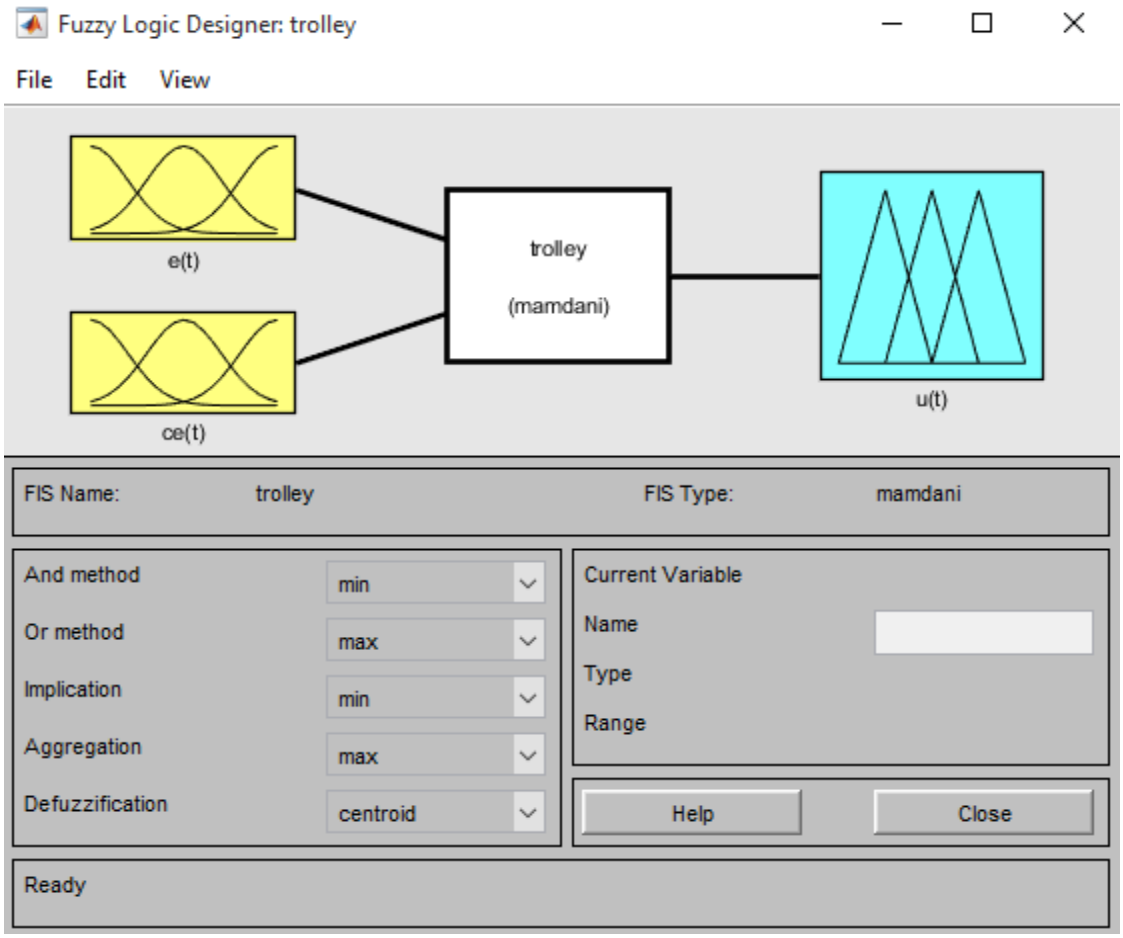

Figure 4.12: Fuzzy inference system editor for trolley system

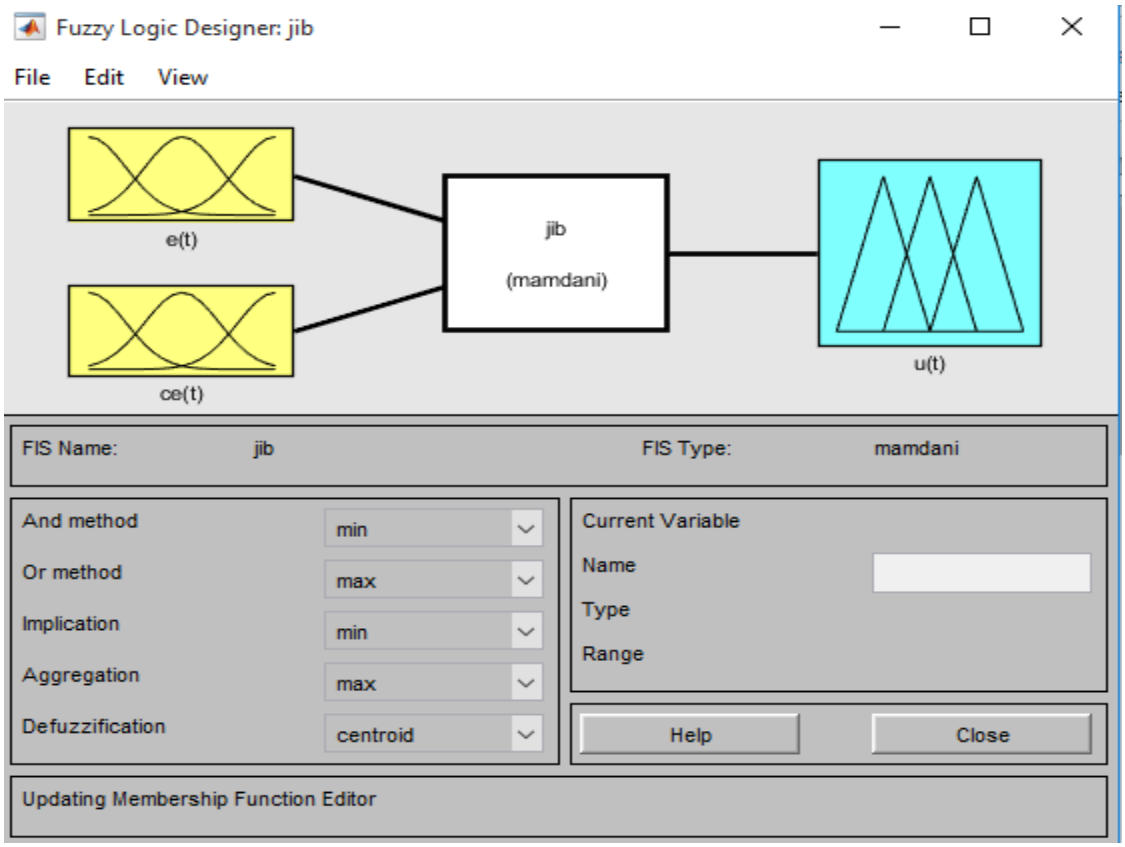

Figure 4.13: Fuzzy inference system editor for jib system

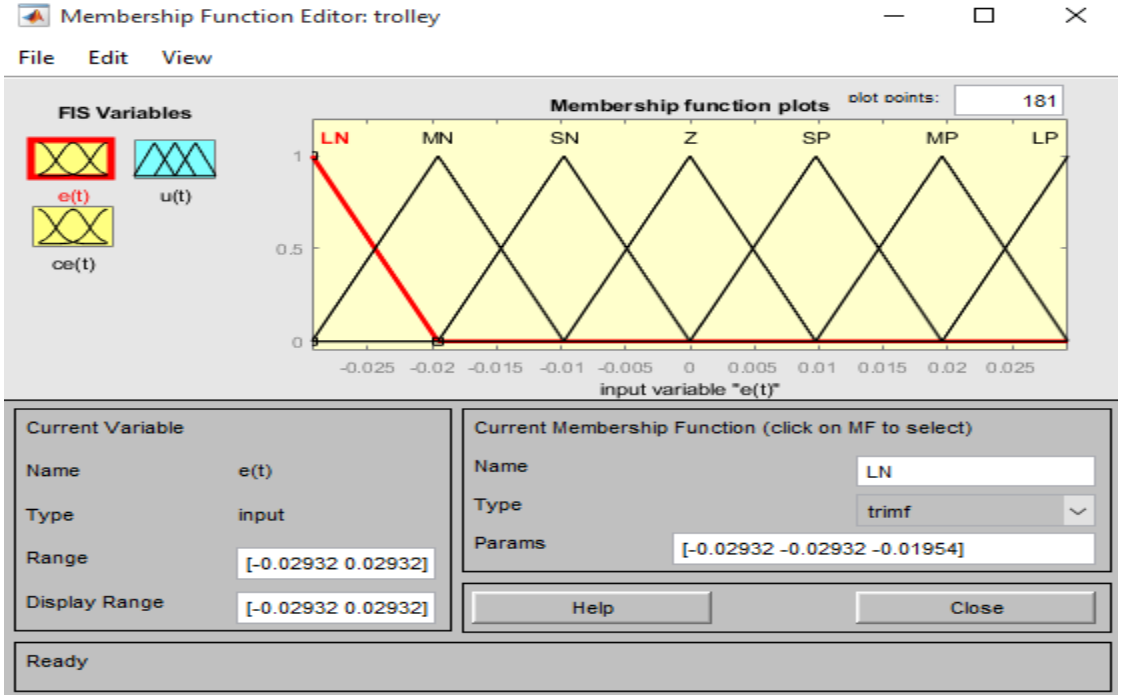

Figure 4.14: Trolley triangular membership functions for input error e(t)

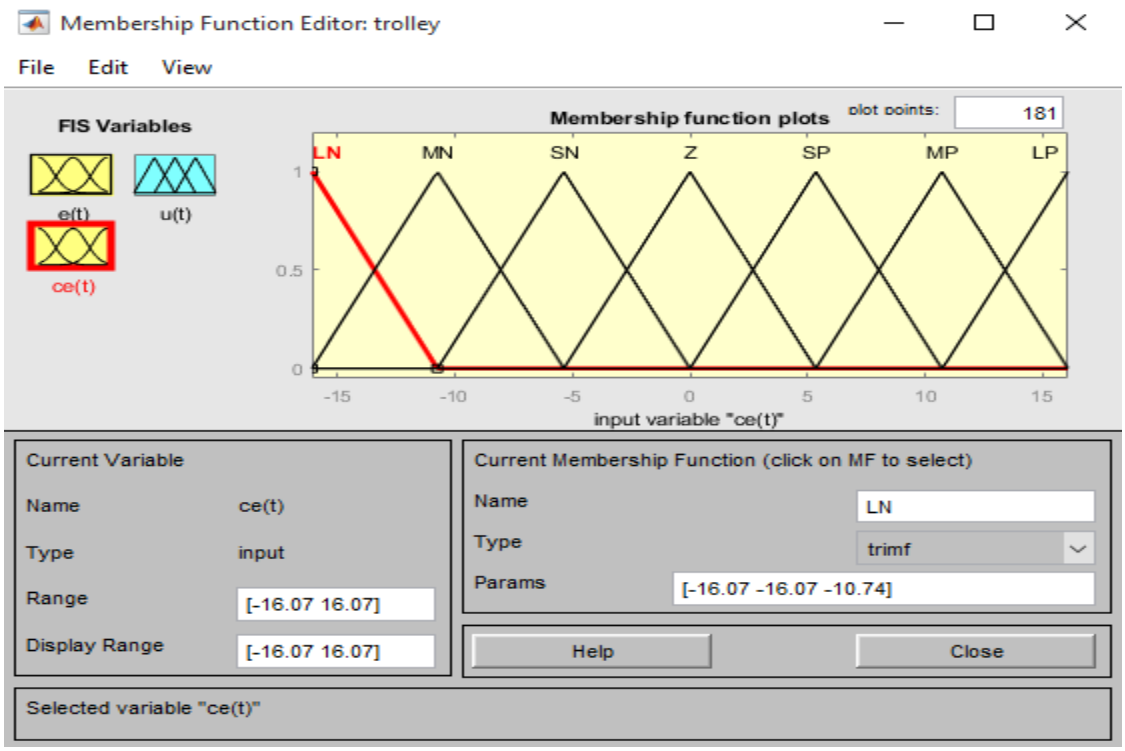

Figure 4.15: Trolley triangular membership functions for rate of change in error ce(t)

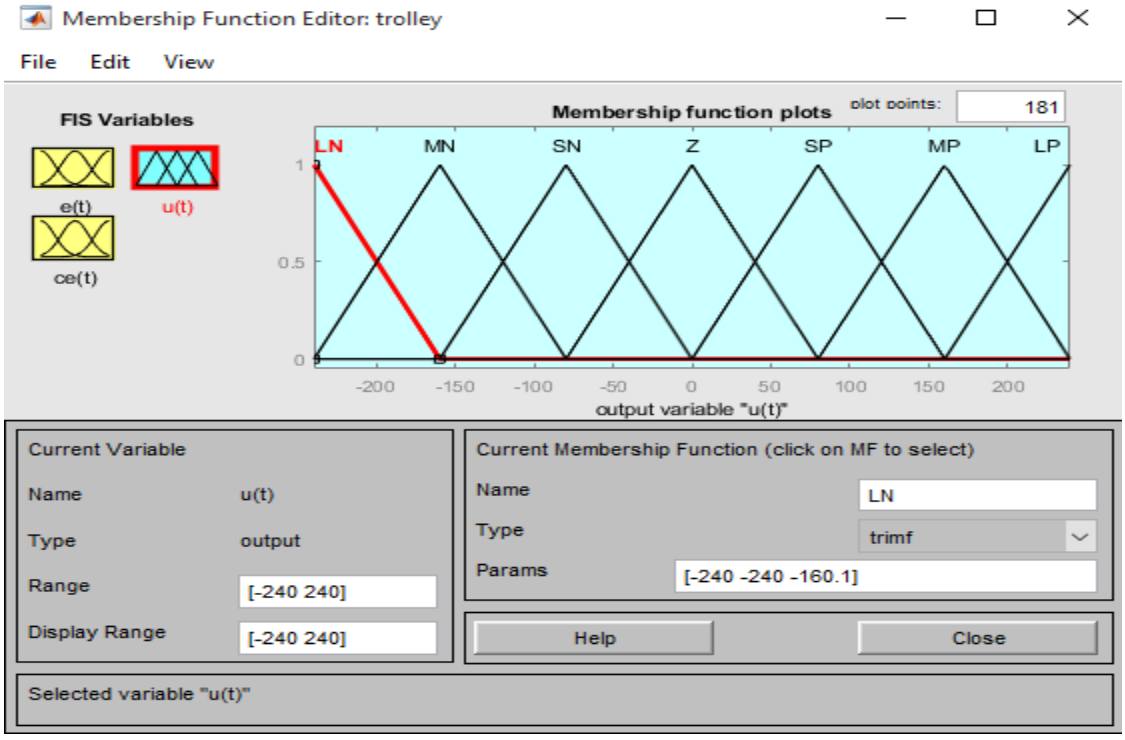

Figure 4.16: Trolley triangular membership functions for control output u(t)

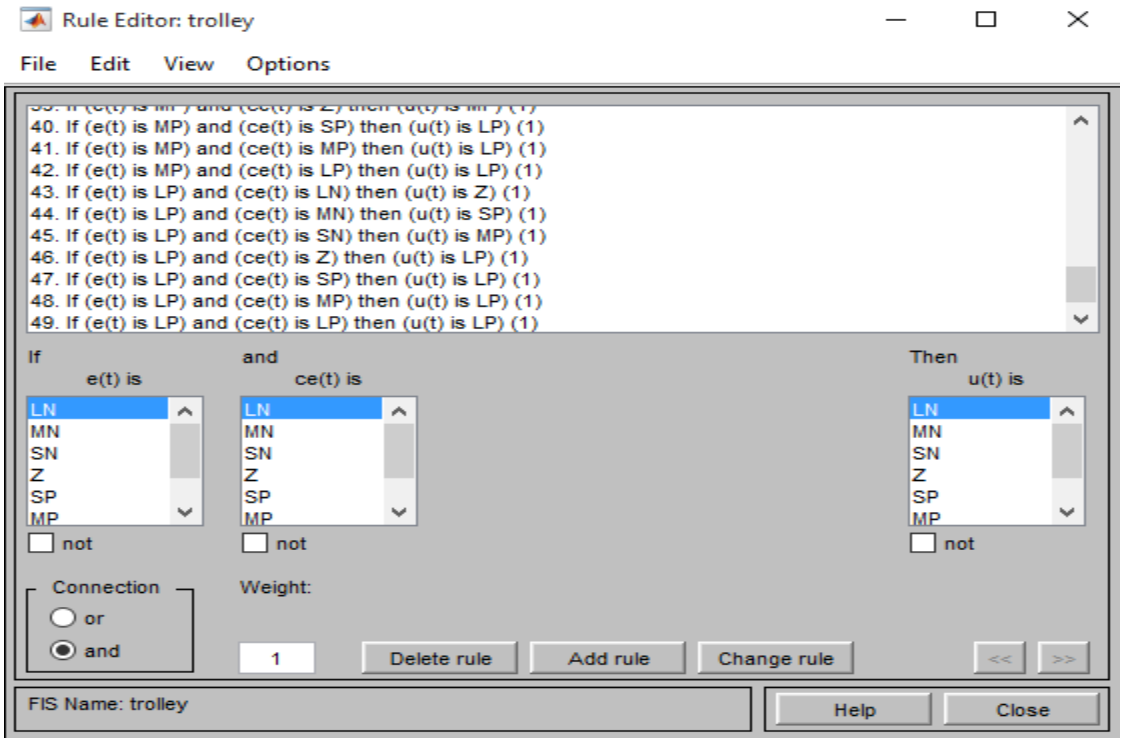

Figure 4.17: Trolley rule base editor for the fuzzy logic controller

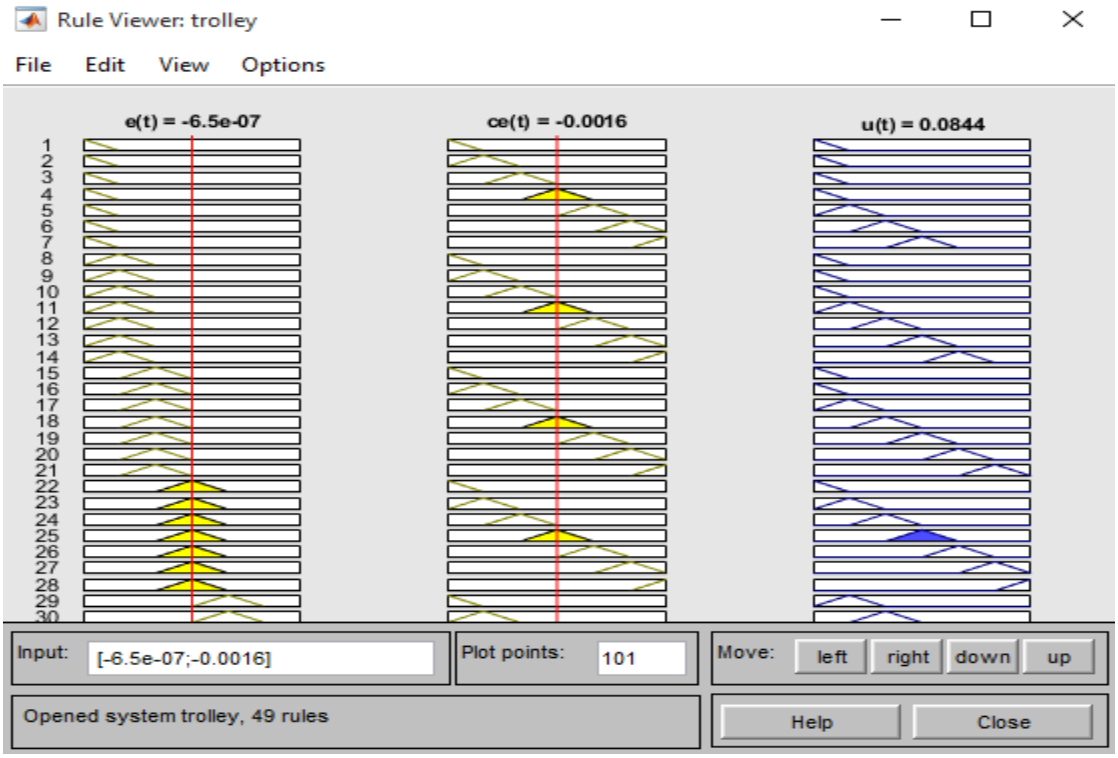

Figure 4.18: The trolley rules viewer for the fuzzy logic controller

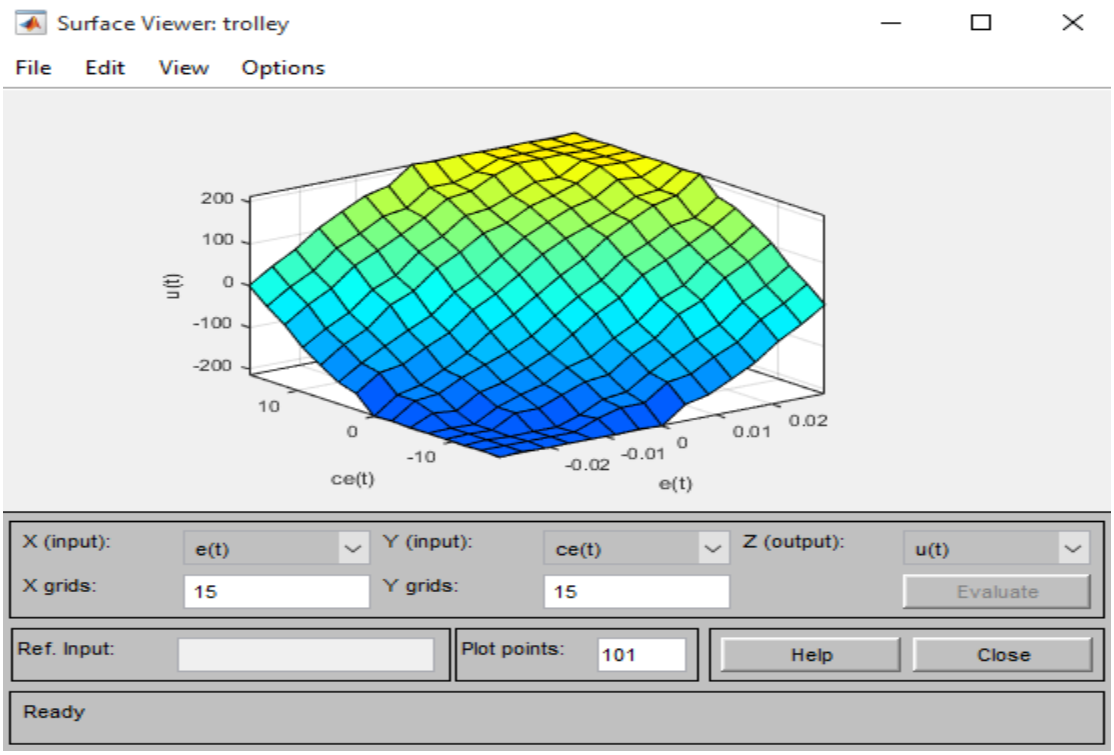

Figure 4.19: The trolley surface viewer for the fuzzy logic controller

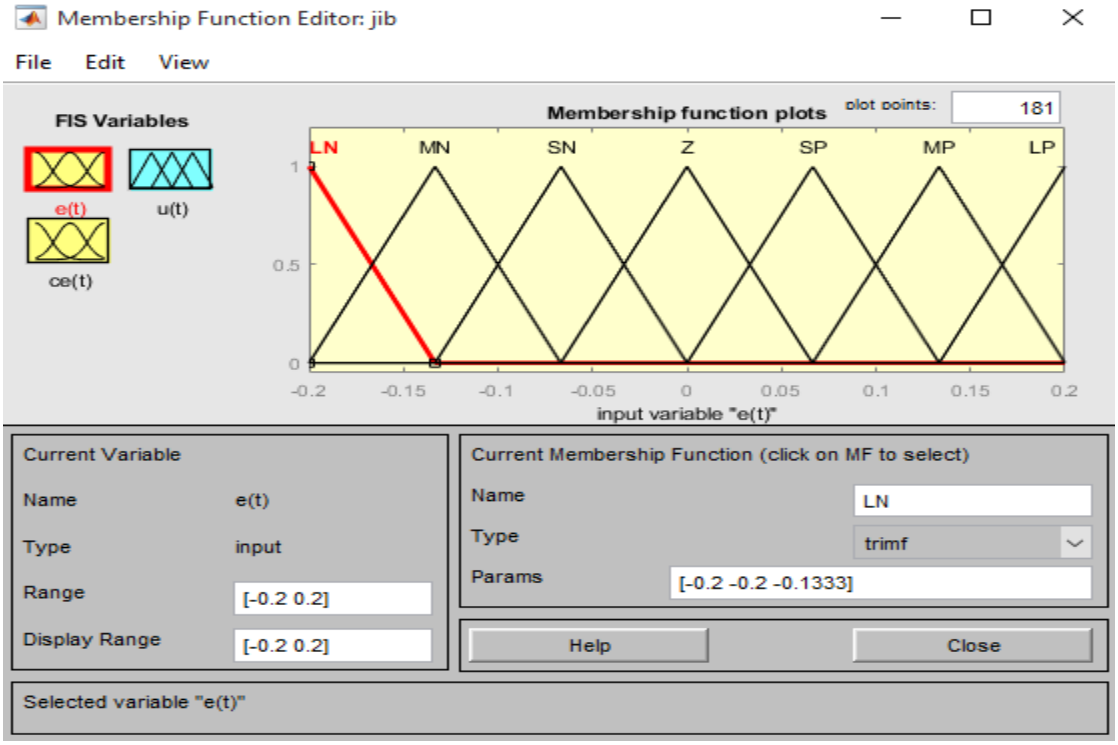

Figure 4.20: Jib triangular membership functions for input error e(t)

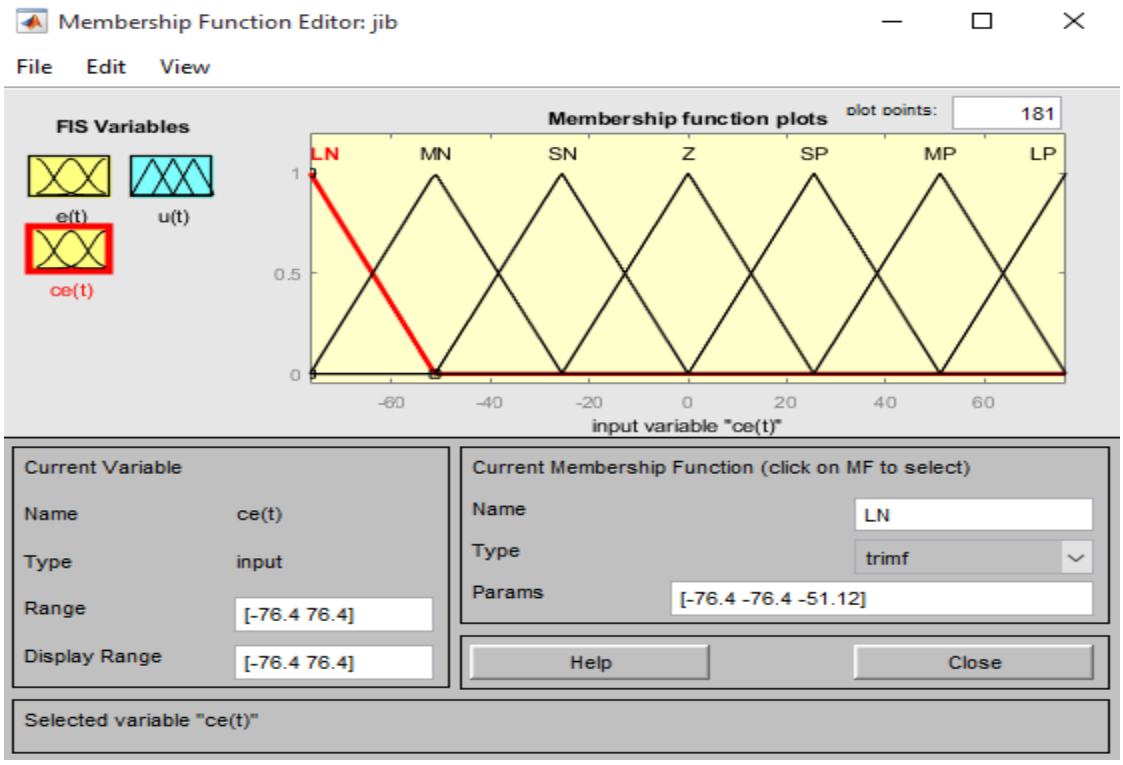

Figure 4.21: Jib triangular membership functions for rate of change in error ce(t)

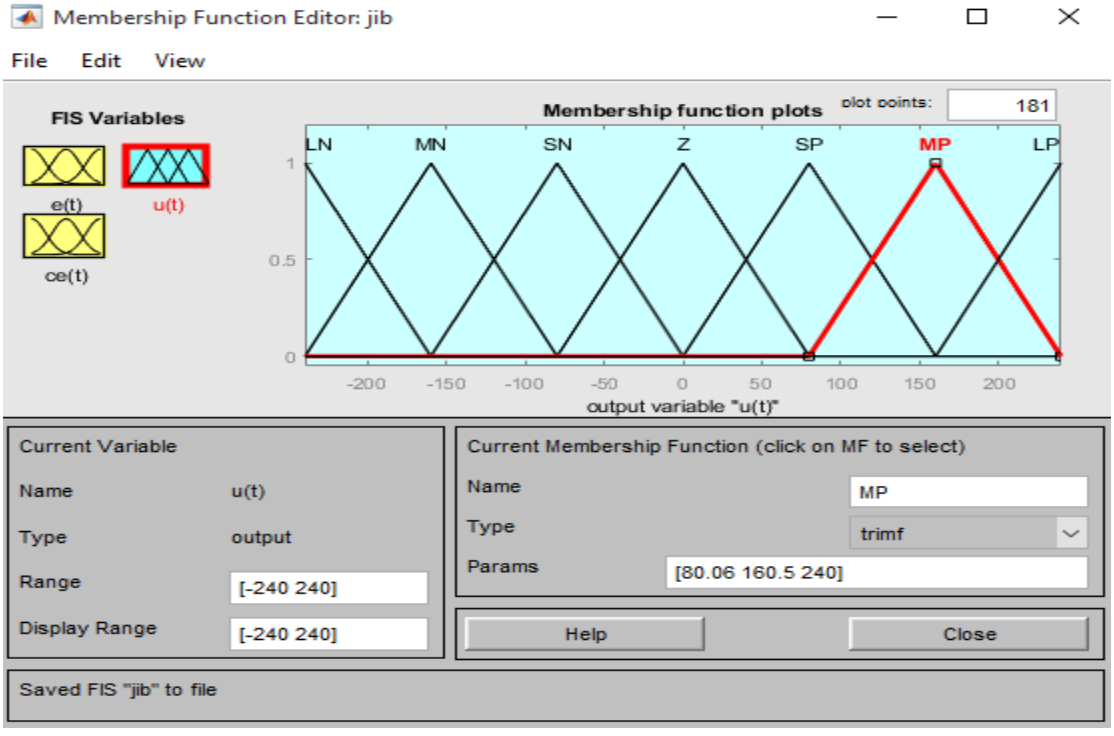

Figure 4.22: Jib triangular membership functions for control output u(t)

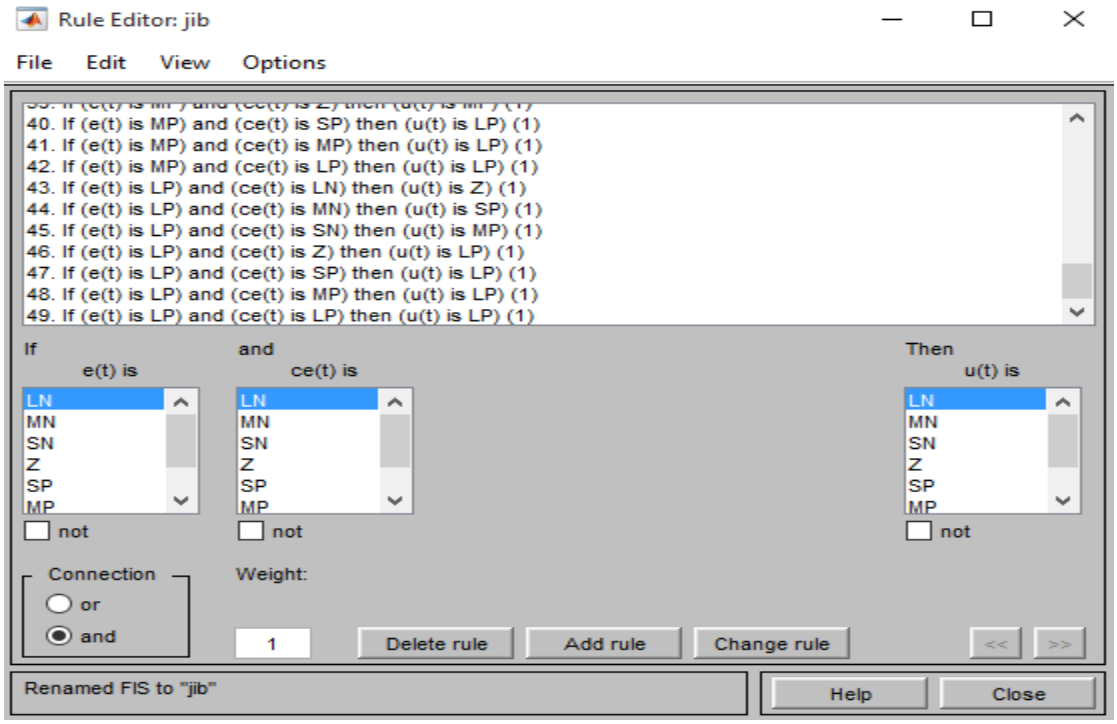

Figure 4.23: Jib rule base editor for the fuzzy logic controller

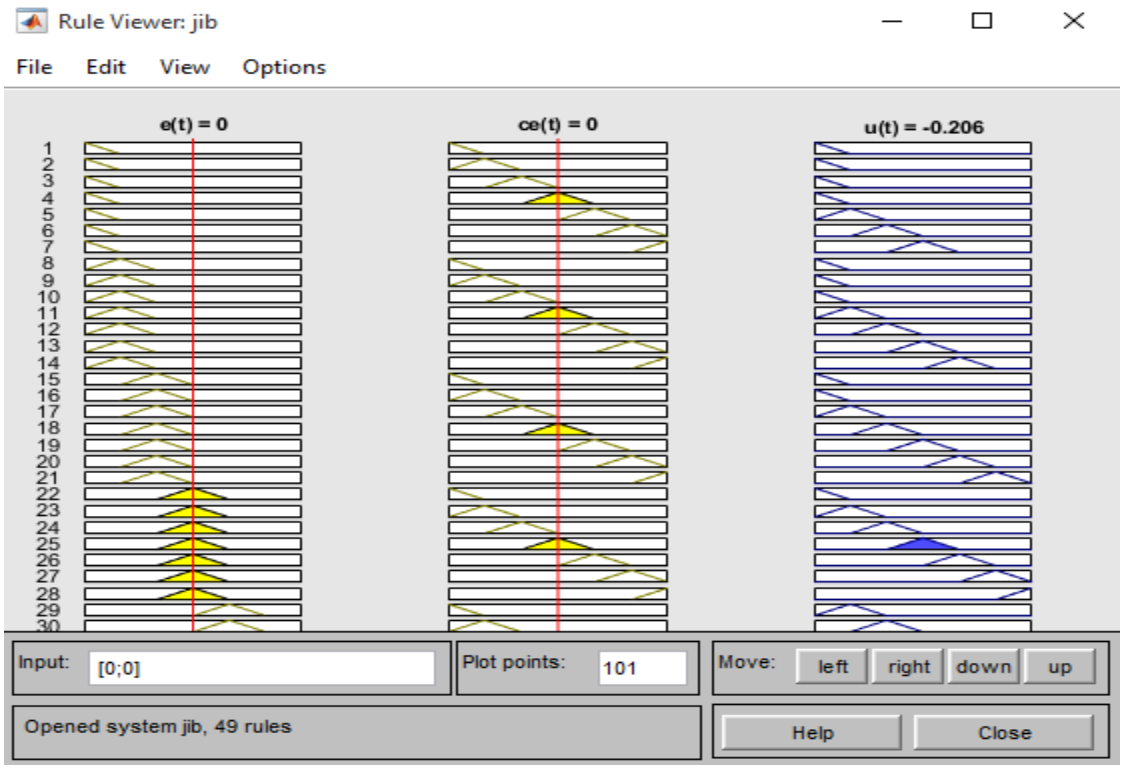

Figure 4.24: The jib rules viewer for the fuzzy logic controller

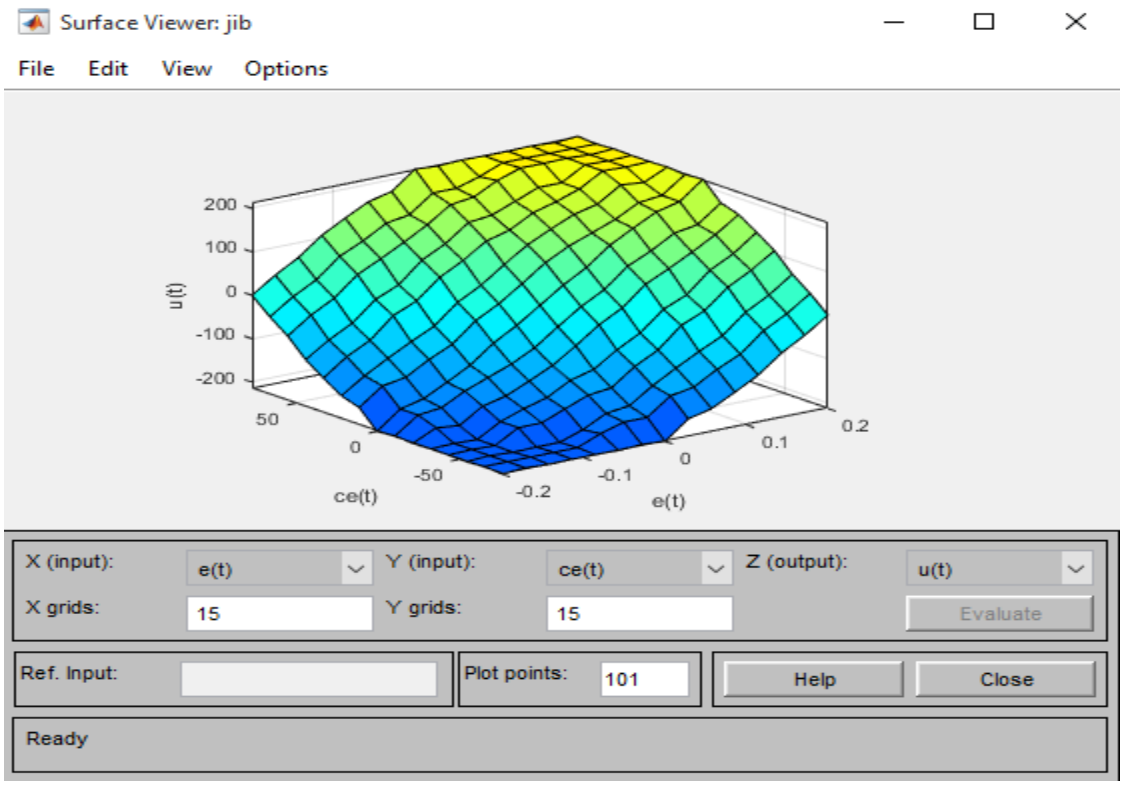

Figure 4.25: The jib surface viewer for the fuzzy logic controller

The trolley and jib rule base editor screen shown in Figures 4.17 and 4.23 locates where the FLC rules are set. That means they builds and edits the set of rules which is associated with the behavior of the system. A set of 49 rules are created for the three linguistic variables error e(t), rate of change in error ce(t) and the control output u(t) using the minimum inference rule for both trolley and jib. Figure 4.18 shows the trolley rules viewer for the fuzzy logic controller. It is used to examine and view the controller output on the basis of defined rules i.e. the rules behavior can be checked here by changing the error e(t), and changing the rate of change in error ce(t) and monitoring the control output u(t). Similarly, Figure 4.24 shows the jib rules viewer for the fuzzy logic controller. Figure 4.19 and 4.25 shows the trolley and jib surface viewer for the fuzzy logic controller. They generate a 3-D linkage of output associated with the particular number of inputs. Afterwards, a rule viewer for both the trolley and jib can be seen in Fuzzy editor, which defines set of rules for e(t) ANDed with ce(t).

CHAPTER FIVE

Result and Discussion

In this section, results of the controllers and discussion in the results will take place.

5.1. Optimal Motion Control Output

This section presents the simulation result of time optimization of velocity-time curve, acceleration- time curve, sway angle, rate of change of sway angle, direction of movement, and displacement. Therefore, the load needed to be transport is arrived at desired position with in optimal time and no sway. To generate the optimal time references, we use the following data in the simulations: Cable length 4m, trolley and jib initial position $(1\text{m}, 0^{\circ})$, final position $(10\text{m}, 90^{\circ})$ and trolley and jib maximum sway angle 36.87° (calculated using equation (3.5) for k=0.2).

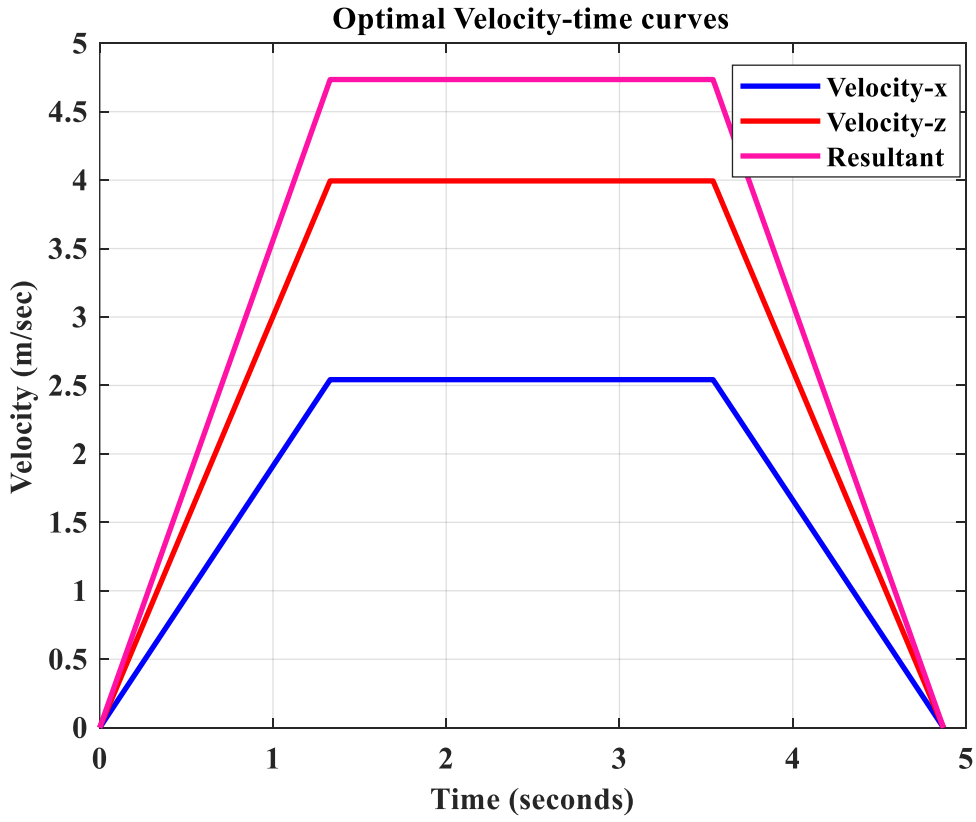

Figure 5.1: Reference velocity-time curves

The velocity of trolley, jib and load changes linearly until desired maximum velocity is reached, moves with constant velocity and when decelerates their velocity again changes linearly until it reaches zero as shown in figure 5.1. According the mathematical optimization of tower crane the

reference velocity of the trolley, the jib and the load looks like as figure 3.3 keeping the trapezoidal curve. Thus, it is expected that the system follows this reference velocity-time curves. Moreover, the tower crane optimal algorithm output of the trolley and the jib follow their respective coordinate directions but the load should follow the shortest path to the predefined coordinate destination from the take-off coordinate.

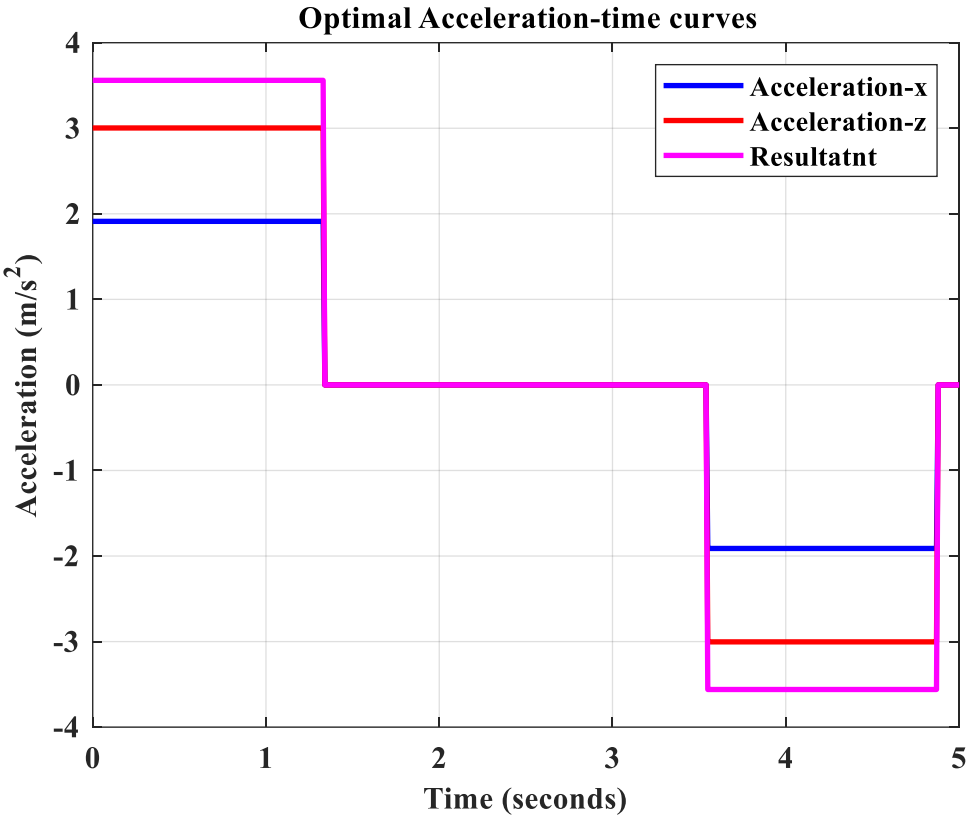

Figure 5.2: Reference acceleration-time curves

Figure 5.2 shows all the trolley, the jib and the load accelerates for the maximum time of the trolley or the jib. Moreover, all the moving parts have equal time of constant velocity and time of deceleration and also the crane accelerations attain their maximum rate change.

The trolley and jib accelerates for 1.33 seconds, moves at a constant velocity of magnitude 2.542 m/sec and 3.994 m/sec respectively for 2.21 seconds, and decelerates for another 1.33 seconds, as shown in Figure 5.1 and 5.2. The whole operation is executed within 4.87 seconds. The acceleration amplitudes of the trolley and jib are $1.912\ \mathrm{m/sec^2}$ and $3.003\ \mathrm{m/sec^2}$ respectively.

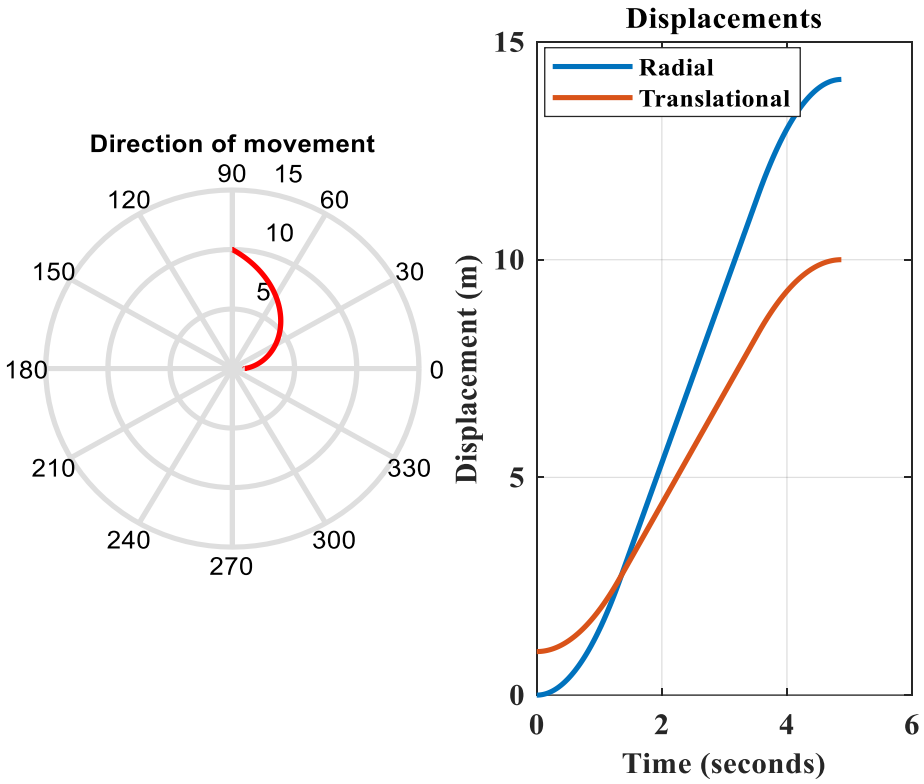

(a) (b)

Figure 5.3: Reference displacement-time curve (a) direction of movement of the jib (b) trolley and jib displacements

Figure 5.3 shows the reference displacement time curves i.e. the direction of movement of the jib and the trolley and jib displacements. Both the trolley and jib covers the required input coordinate distances. That means the trolley moves radially from 1m to 10m while the jib is rotated 90° from its initial position. Both operations execute at same time.

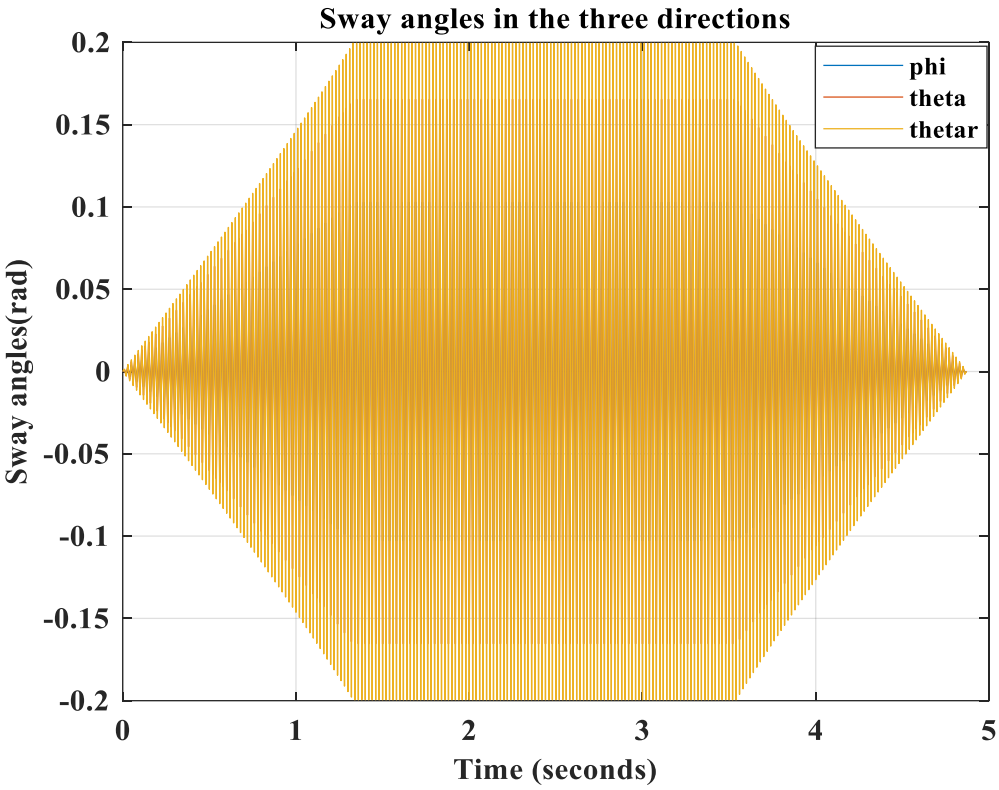

Figure 5.4: Reference sways angle-time curves

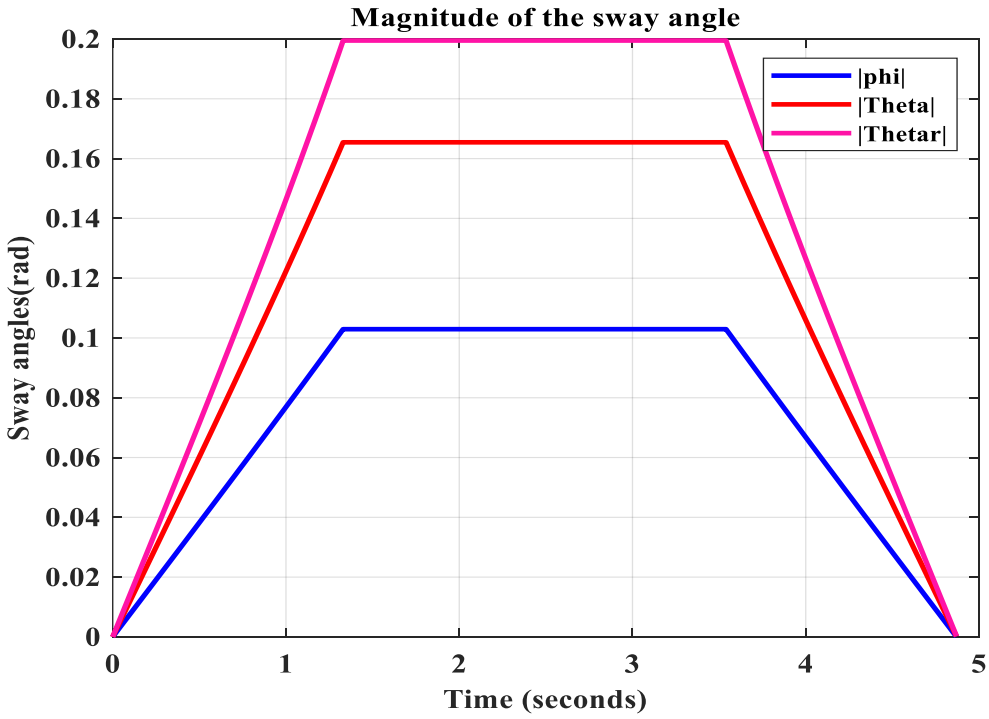

Figure 5.5: Magnitude of reference sway angle in three directions

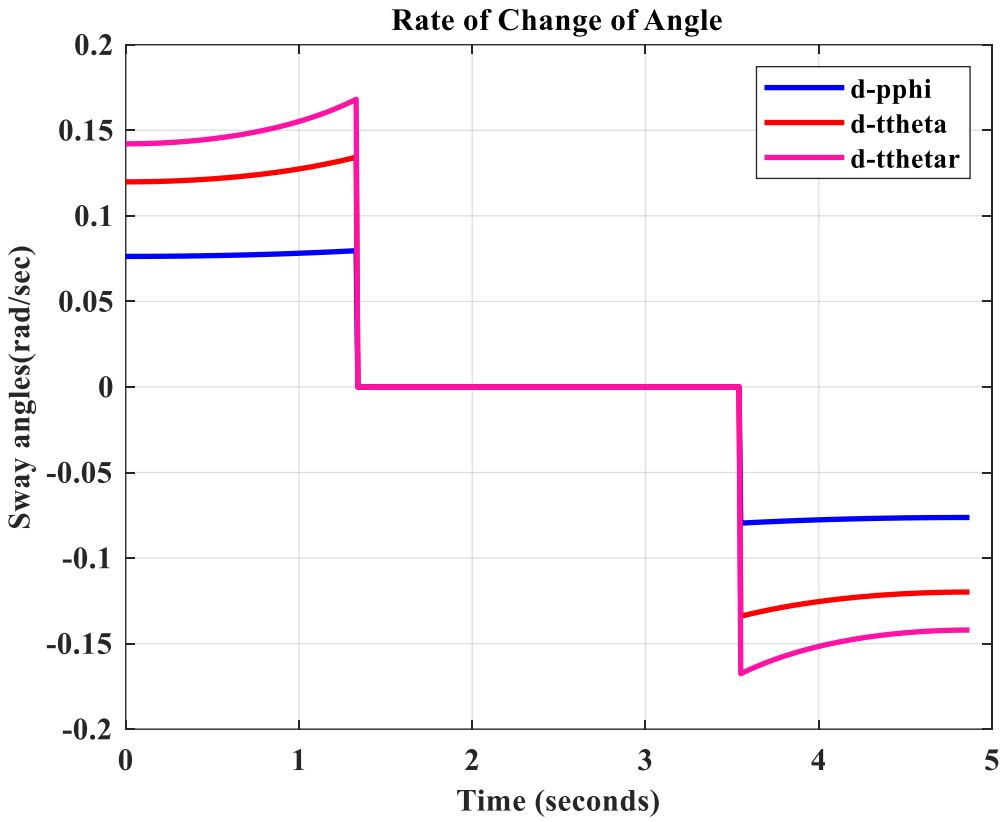

Figure 5.6: Reference rate change of sway angle-time curves

Figure 5.4 indicates that the sway angles follow the motion curve with equal rate change of angle during the acceleration and deceleration but it remains constant as long as the velocity is constant. The magnitude of the sway angle shown in figure 5.5 depends on the cable length and the acceleration of the trolley and jib. The rate of change of sway angle shown in figure 5.6 indicates that for the time of acceleration and deceleration there is a uniform change of angle but the sway angle maintained at its maximum magnitude for the constant time of velocity after it reaches its maximum rate of change of sway angle. Generally, from figure 5.5 the maximum magnitude of sway angle for both trolley and jib are 0.103 radian or 5.9° and 0.1654 radian or 9.5° respectively and becomes zero at the destination.

Radial displacement only: Initial position $(10\text{m}, 0^{\circ})$ and Final position $(10\text{m}, 90^{\circ})$

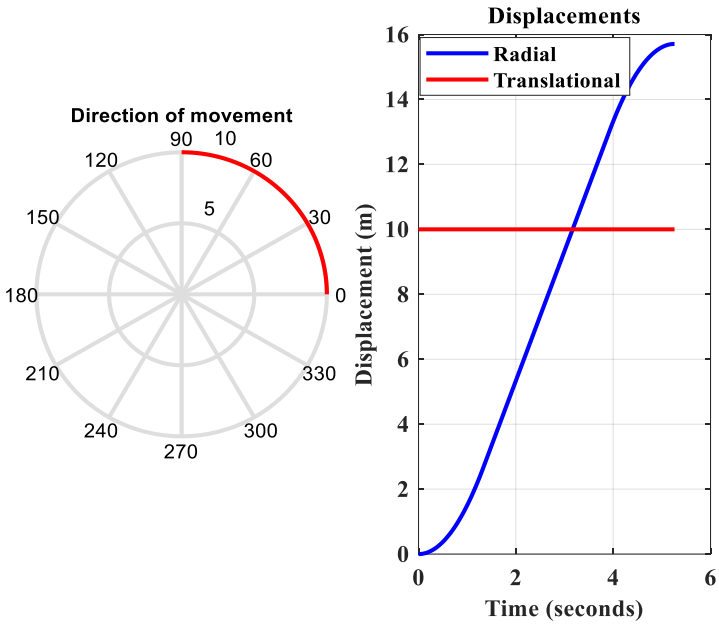

(a) (b)

Figure 5.7: Radial displacement-time curve (a) direction of movement of the jib (b) trolley and jib displacements

Translational displacement only: Initial position $(1\text{m}, 90^{\circ})$ and Final position $(10\text{m}, 90^{\circ})$

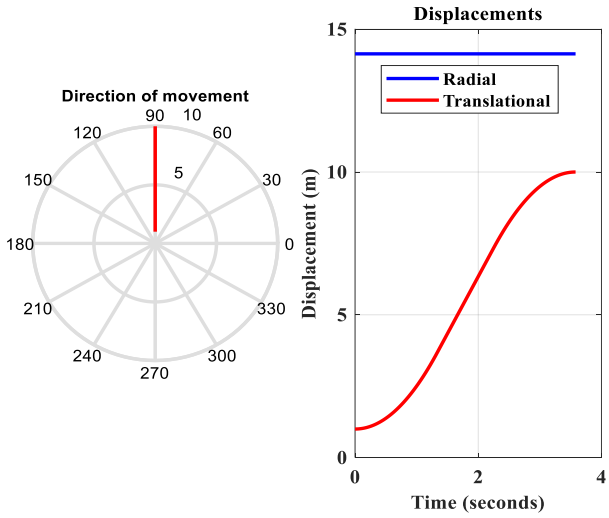

(a) (b)

Figure 5.8: Translational displacement-time curve (a) direction of movement of the jib (b) trolley and jib displacements

Negative radial displacement: Initial position $(1\text{m}, 90^{\circ})$ and Final position $(10\text{m}, 0^{\circ})$

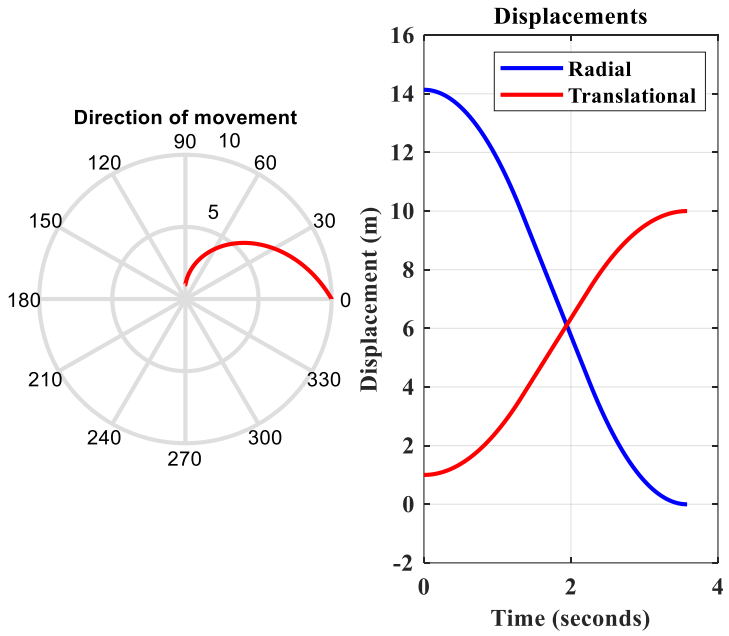

(a) (b)

Figure 5.9: Negative radial displacement-time curve (a) direction of movement of the jib (b) trolley and jib displacements

As shown in figures 5.7 to 5.9 the optimal algorithm is checked for radial, translational and negative radial displacement cases. The algorithm covers the required displacements.

5.2. Closed Loop Control Response

Control system in which the output has an effect on the input quantity in such a manner that the input quantity will be adjusted based on the output generated to attain the required set value. Therefore, this feedback automatically makes the suitable changes in the output due to the system dynamics and external disturbance. In this way closed loop control system is called automatic control system. In this thesis a simple unity feedback is used. The outputs of all optimal motion planning are shown in figures 5.1 to 5.9. Thus, all outputs of closed loop control systems as shown in Figures 5.11 and 5.12 are not tracked the optimal time references. This indicates that the closed loop control system is not efficient to control the tower crane system at optimal time that is why PID and FLC controllers are considered.

Figure 5.12 indicates that both the trolley and jib are not covered the required distance with in optimal time. This indicates that, they are stopped before arrived at the predefined destinations. That means, they require additional excitation to cover the remaining distances. The sway angle is also not reduced to zero at the destination.

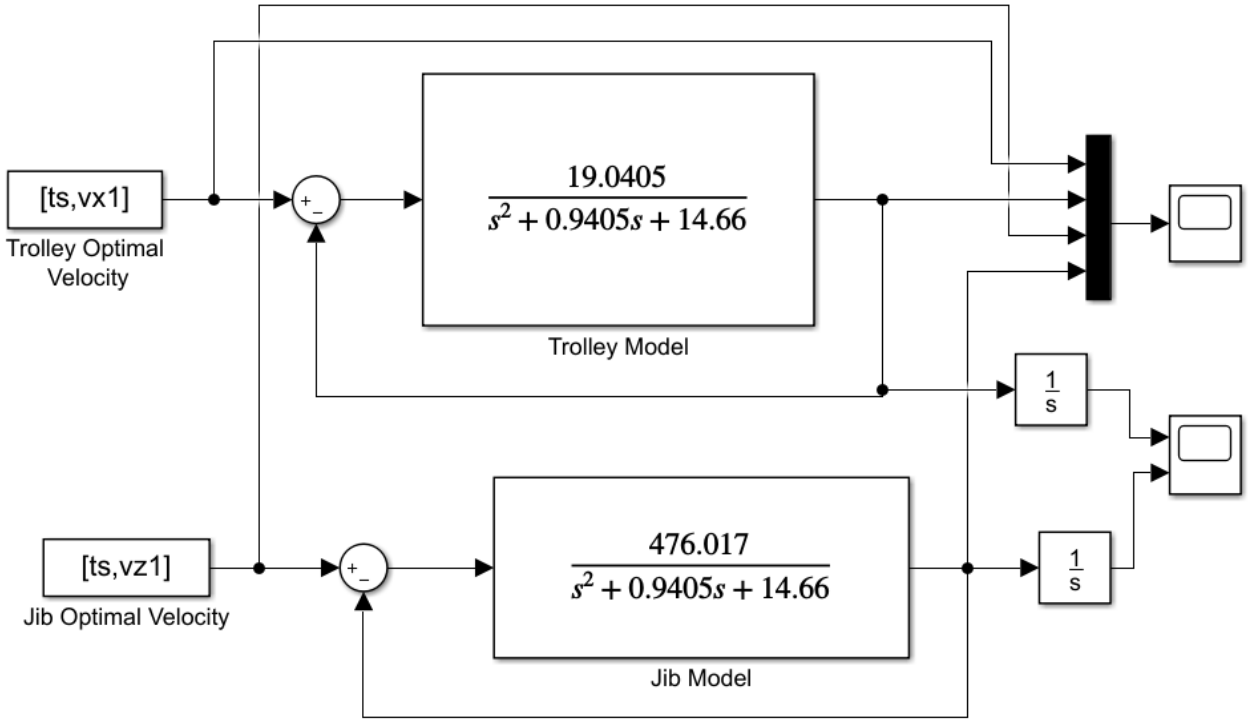

Figure 5.10: Simulink diagram of trolley and jib velocity under closed loop system

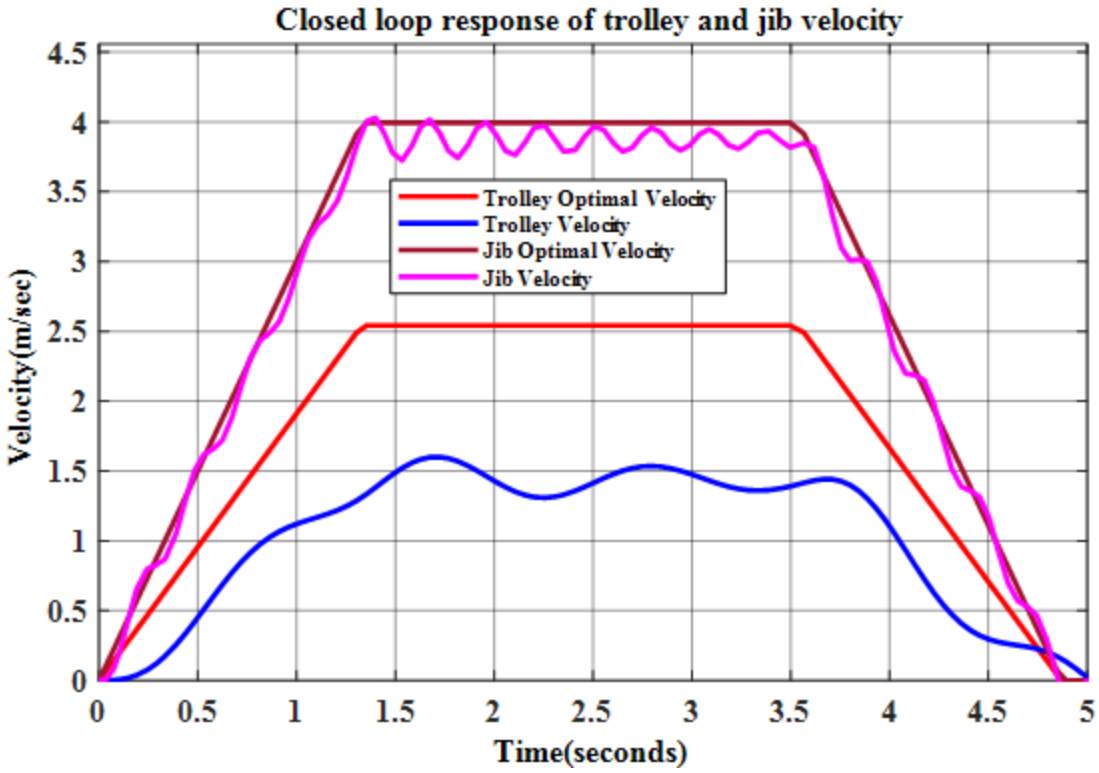

Figure 5.11: Closed loop response of trolley and jib velocity

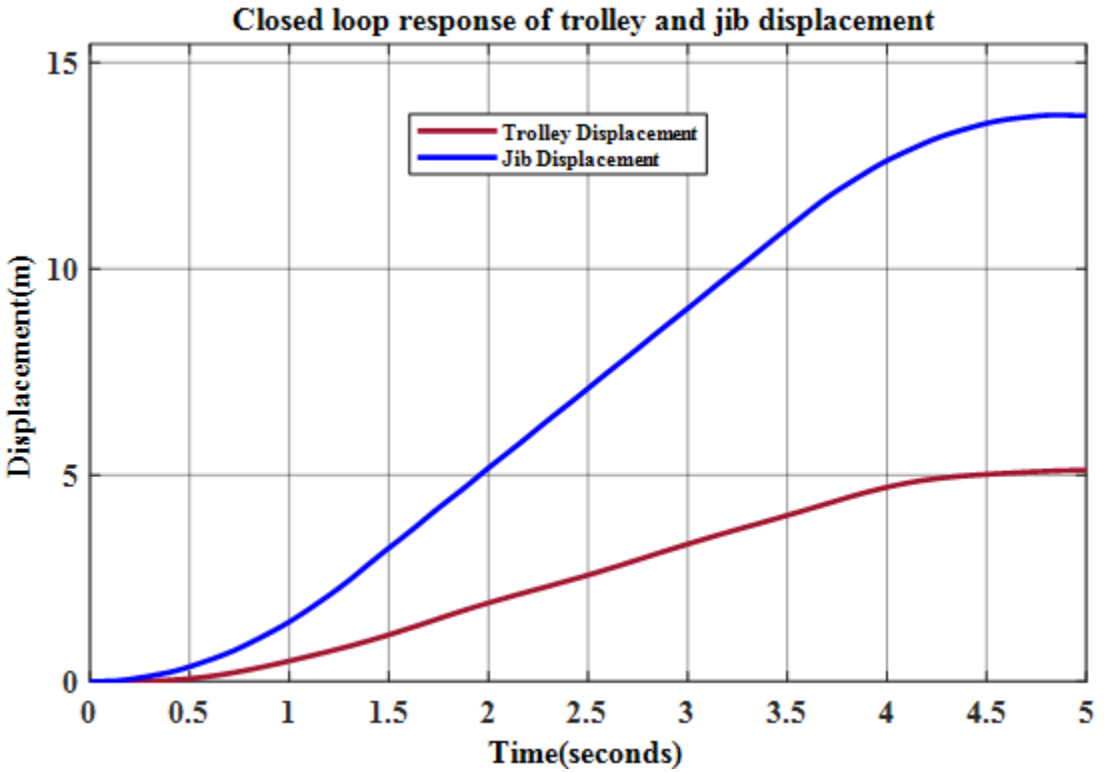

Figure 5.12: Closed loop response of trolley and jib displacement

5.3. PID Controller Response

The Matlab/Simulink implementation of both the trolley and jib velocity model using PID controller is shown in Figure 5.13. The parameters of PID Controller are tuned automatically using Matlab PID auto tuner. Using the PID auto tuner at 0.6 robustness for the trolley we get the values of PID controller parameters K_p, K_i, K_d and N as 6.4536, 8.547, 0.84685 and 2046.36 respectively. Similarly, for the jib we get the values of PID controller parameters K_p, K_i, K_d and N as 0.258, 0.342, 0.034 and 2046.36 respectively. PID controller solves the problems of both open loop and closed loop control systems.

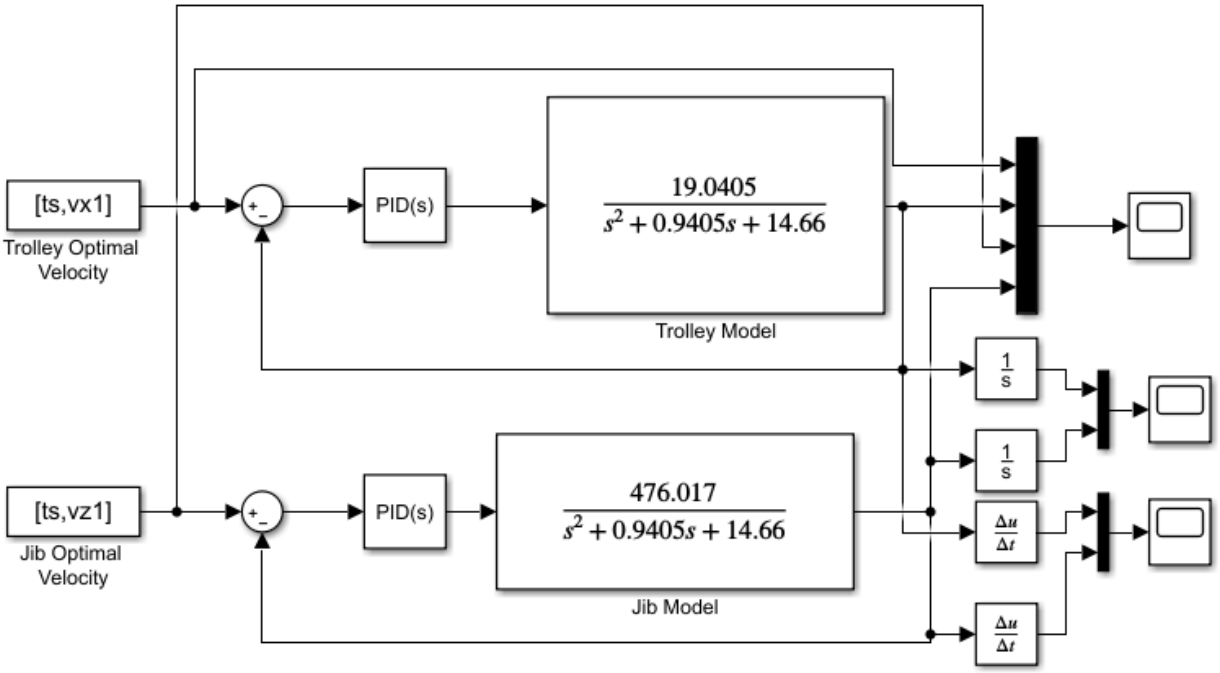

Figure 5.13: Simulink diagram of trolley and jib velocity under PID controller

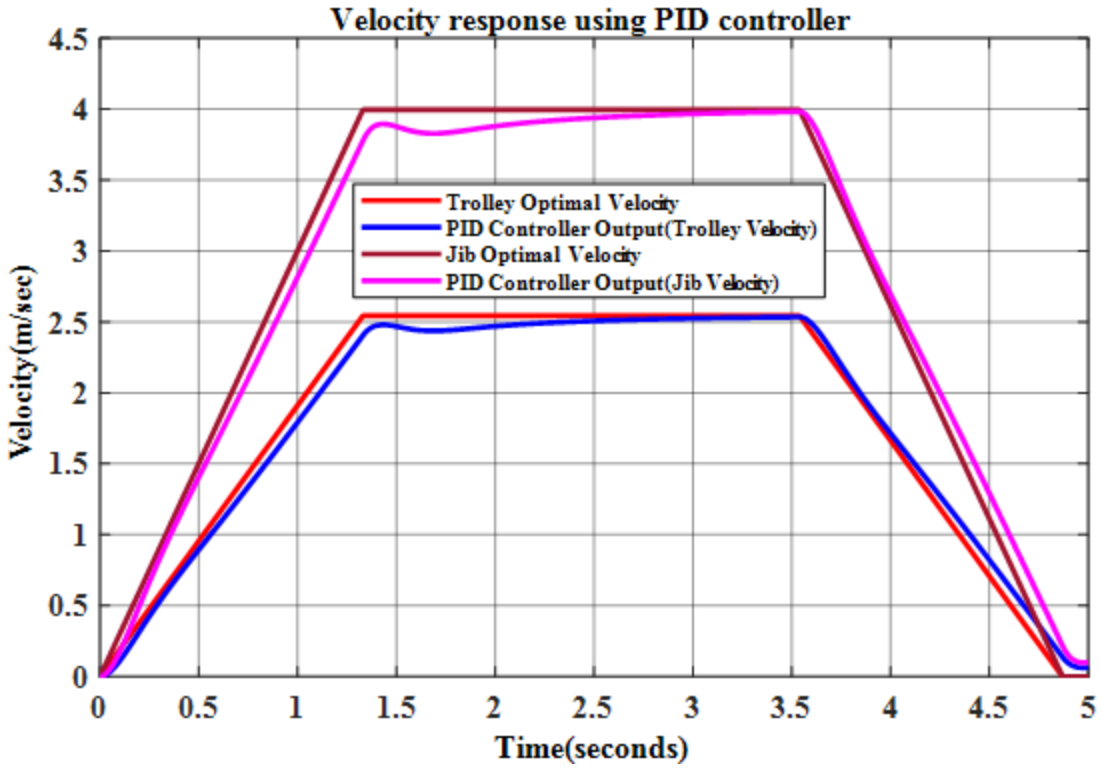

Figure 5.14: Trolley and jib velocity response using PID controller

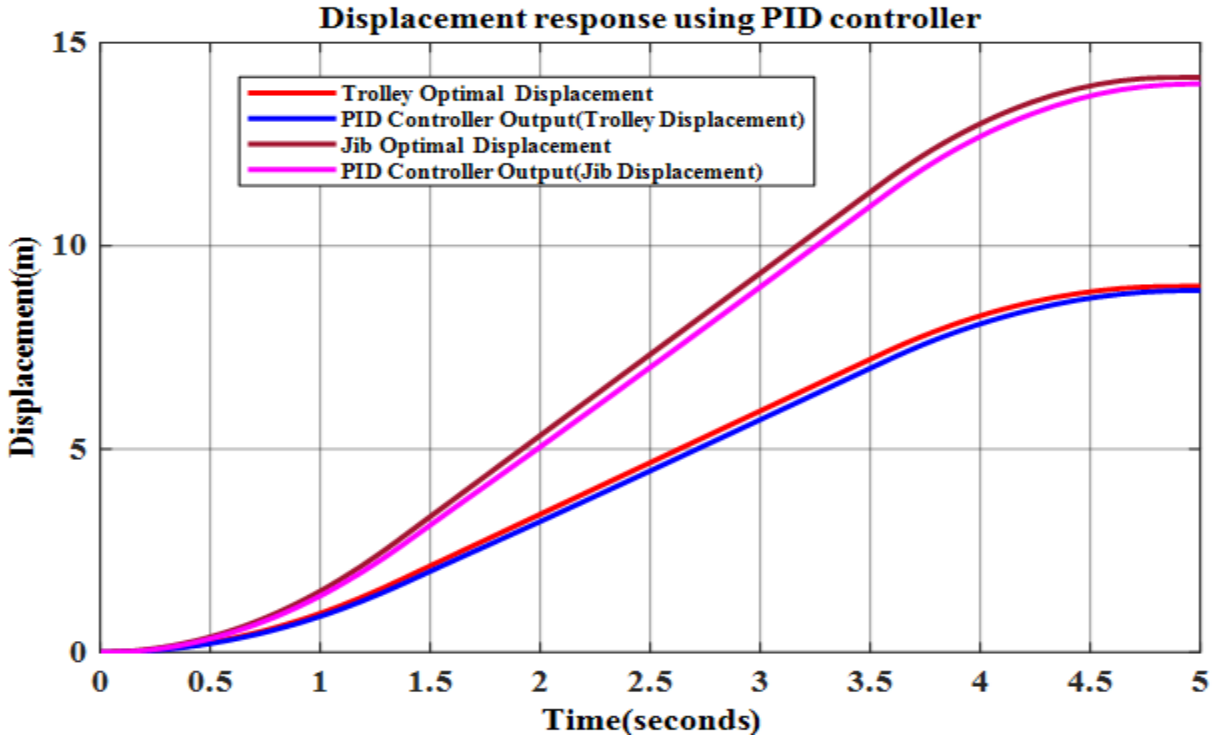

Figure 5.15: Trolley and jib displacement response using PID controller

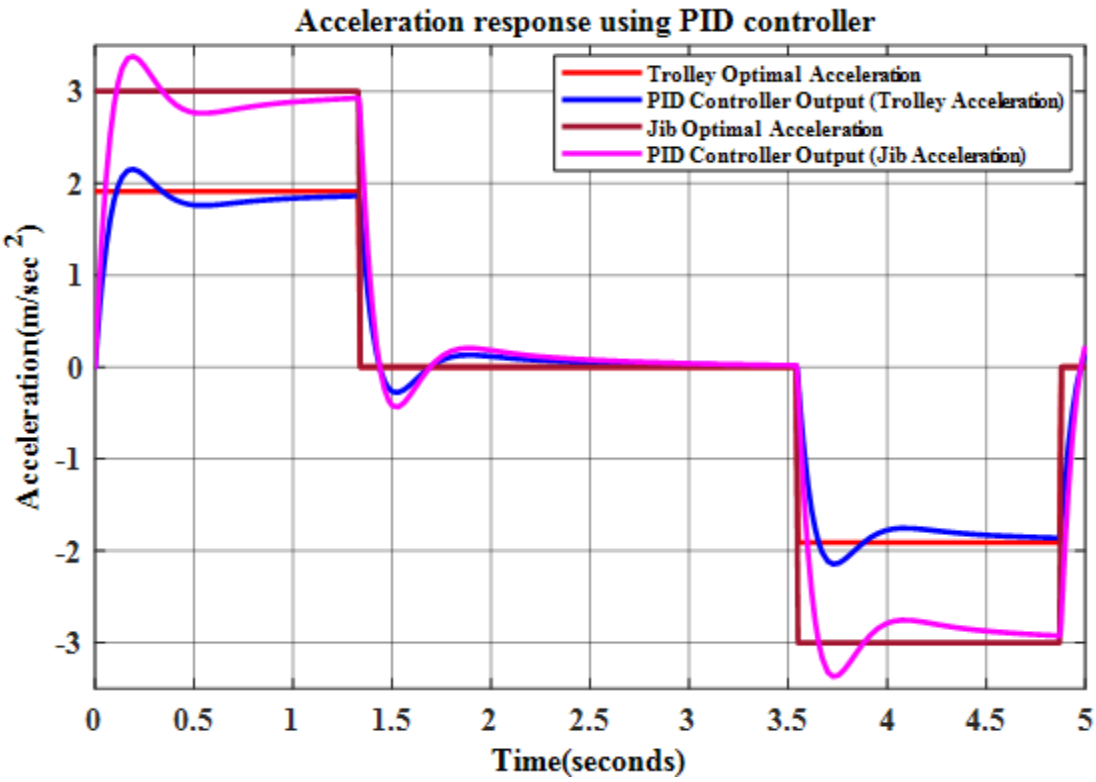

Figure 5.16: Trolley and jib acceleration response using PID controller

The outputs of PID controller are smoothly tracked the optimal time velocity, displacement and acceleration within short time as shown in Figures 5.14 to 5.16 respectively. That means PID controller have better tracking performance of optimal time references as compared to both open loop and closed loop control system. But, it is clear that PID controller response is slower than the optimal value. As shown in Figure 5.14 the given distances of the moving parts are not covered completely within optimal time. So, the sway angles are not suppressed to zero at the destination i.e. the crane will not arrive at its destination at the predetermined optimal time. Therefore, the output shows that PID controllers can give better performance if they are properly tuned. But, one of the draw back with PID controller is that manual tuning method when there is any system parameter change due to different reasons.

5.4. Fuzzy Logic Controller Response

All the responses of open loop control system, closed loop control system and PID controllers are not tracked the generated optimal time references. However, the responses of PID controller are better velocity, acceleration, displacement and magnitude of sway angle tracking performances than both open loop and closed loop control systems. To solve all the drawbacks of open loop

control system, closed loop control system and PID controllers' fuzzy logic controller is developed. The Matlab/Simulink implementation of the velocity control of both trolley and jib using FLC controller is presented in Figure 5.17 shown below. The FLC design procedures are presented in chapter four sections 4.3.

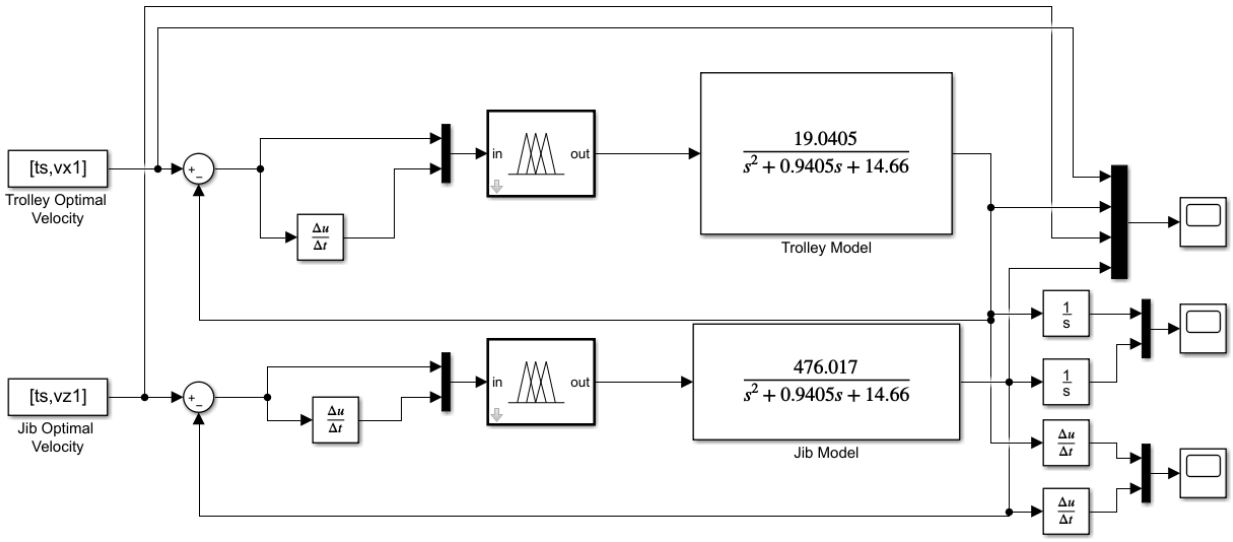

Figure 5.17: Simulink diagram of trolley and jib velocity using FLC

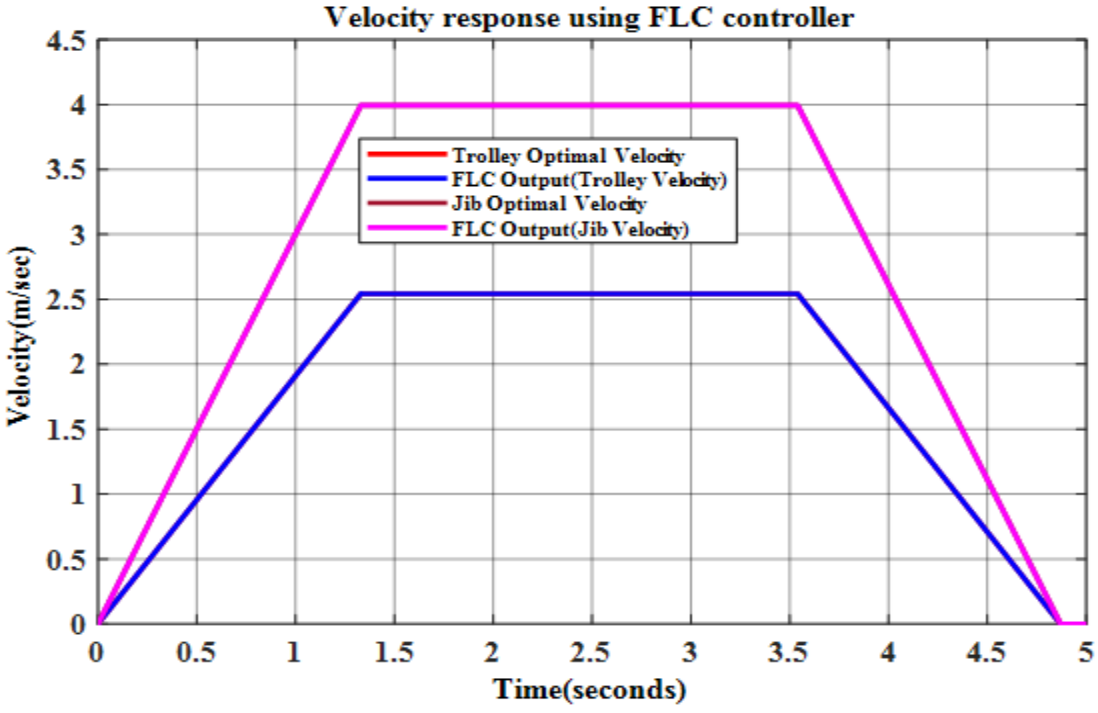

Figure 5.18: Trolley and jib velocity response using FLC

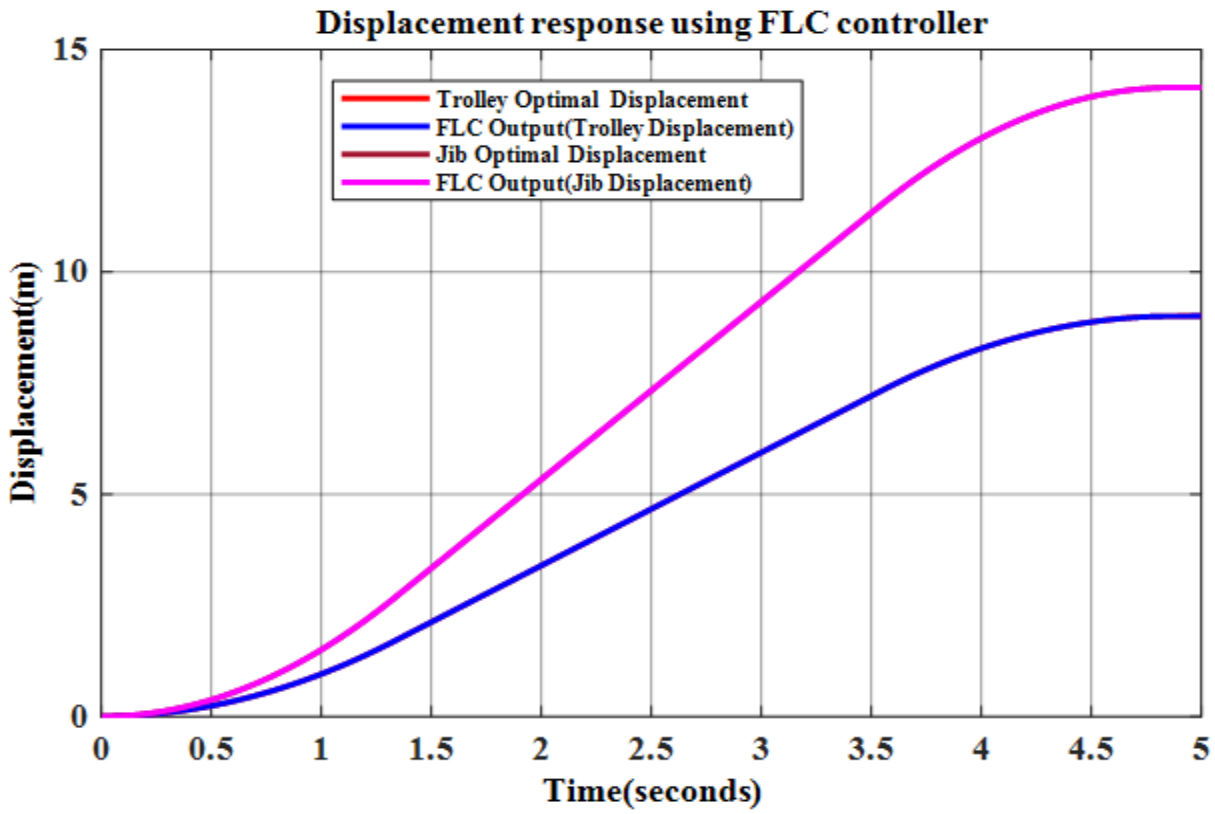

Figure 5.19: Trolley and jib displacement response using FLC

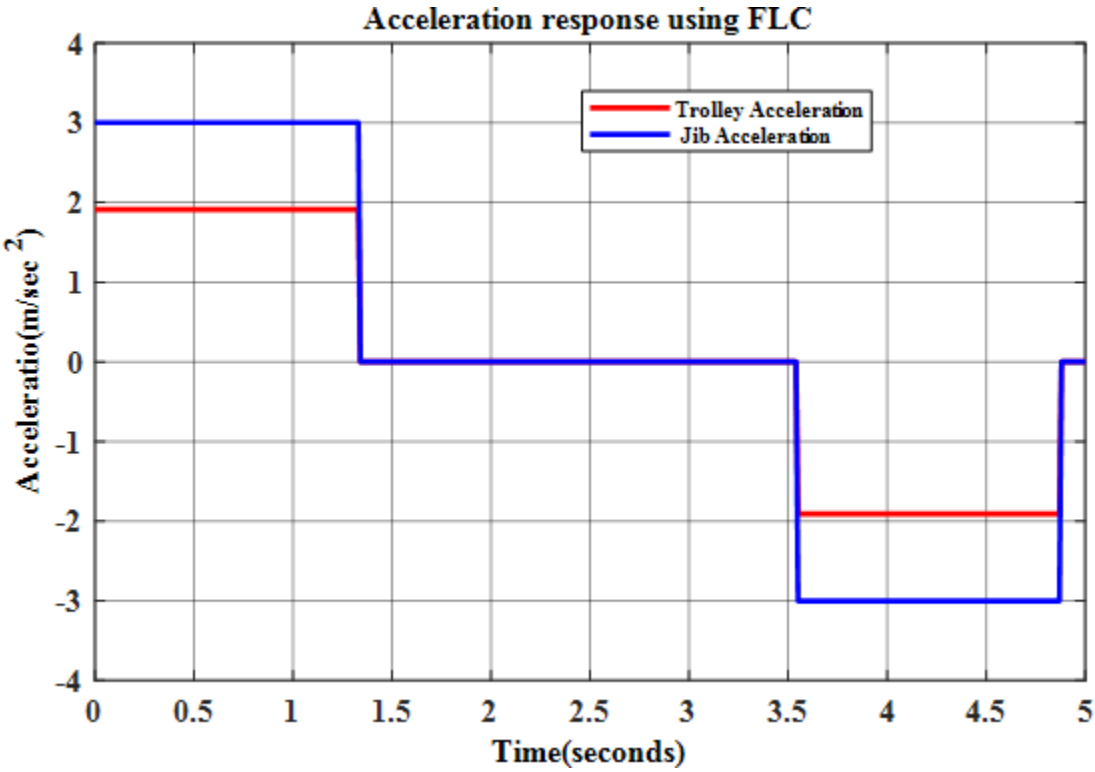

Figure 5.20: Trolley and jib acceleration response using FLC

As shown in Figure 5.18 the trolley and jib accelerates for 1.33 seconds, moves with a constant velocity of magnitude 2.542 m/sec and 3.994 m/sec respectively for 2.21 seconds, and they decelerates for 1.33 seconds. The final velocity of the trolley and jib at the destination becomes zero. The whole operation is executed within 4.87 seconds which is optimal. Similarly, the sway angle becomes zero at the destination.

Figure 5.19 shows both trolley and jib covers the given displacements at optimal time. That is, the trolley moves 9m from its initial position while the jib is rotated by 90° from its initial position or radially from 0m to 14.14m. FLC tracks the given optimal time references. Therefore, FLC is better velocity, displacement and sway angle tracking performances than open loop control system, closed loop control system and PID controllers. For all cases the acceleration magnitude of the trolley and jib are $1.912\ \mathrm{m/sec^2}$ and $3.003\ \mathrm{m/sec^2}$ respectively as shown Figure 5.20.

5.5. FLC Response under Different Trolley Displacements

Let's see the tracking performance of fuzzy logic controller for the velocity control of the trolley and jib which in turn controls the sway angles by varying the trolley displacement. Figures 5.21 and 5.22 indicates that the trolley is moved 11m from r=1m to r=12m while the jib is rotated by 90° from its initial position. Both the trolley and jib accelerates for 1.33 seconds, moves with a constant velocity of magnitude 2.54 m/sec and 3.991 m/sec respectively for 3 seconds and decelerates for 1.33 seconds. The whole operation is executed within 5.66 seconds. In this case the maximum magnitude of sway angle that occurs due to trolley displacement and jib rotations are 0.1028 radian or $5.89^{\circ}$and 0.1653 radian or 9.47° respectively and they become zero at the target point. For this case the acceleration magnitude of the trolley and jib are $1.91\ \mathrm{m/sec^2}$ and $3.001\ \mathrm{m/sec^2}$ respectively.

Figures 5.23 and 5.24 indicates that the trolley is moved 13m from r=1m to r=14m while the jib is rotated by 90° from its initial position (radially from 0m to 20.42m). Both the trolley and jib accelerates for 1.33 seconds, moves with a constant velocity of magnitude 2.544 m/sec and 3.996 m/sec respectively for 3.78 seconds and decelerates for 1.33 seconds. The whole operation is executed within 6.44 seconds. For this case the acceleration magnitude of the trolley and jib are $1.913\ \mathrm{m/sec^2}$ and $3.0045\ \mathrm{m/sec^2}$ respectively and the maximum magnitude of sway angle that

occurs due to trolley displacement and jib rotation are 0.103 radian or 5.9°and 0.1655 radian or 9.48° respectively and they become zero at the target point within the optimal time.

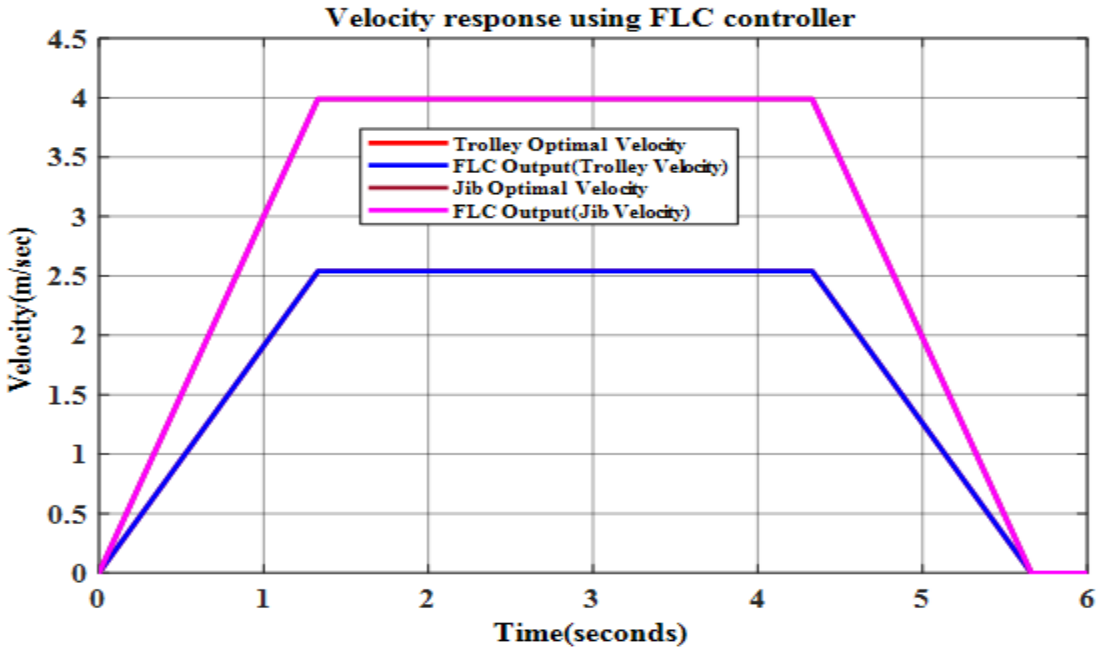

Figure 5.21: Jib and trolley velocity response using FLC when the trolley moves from 1m to 12m

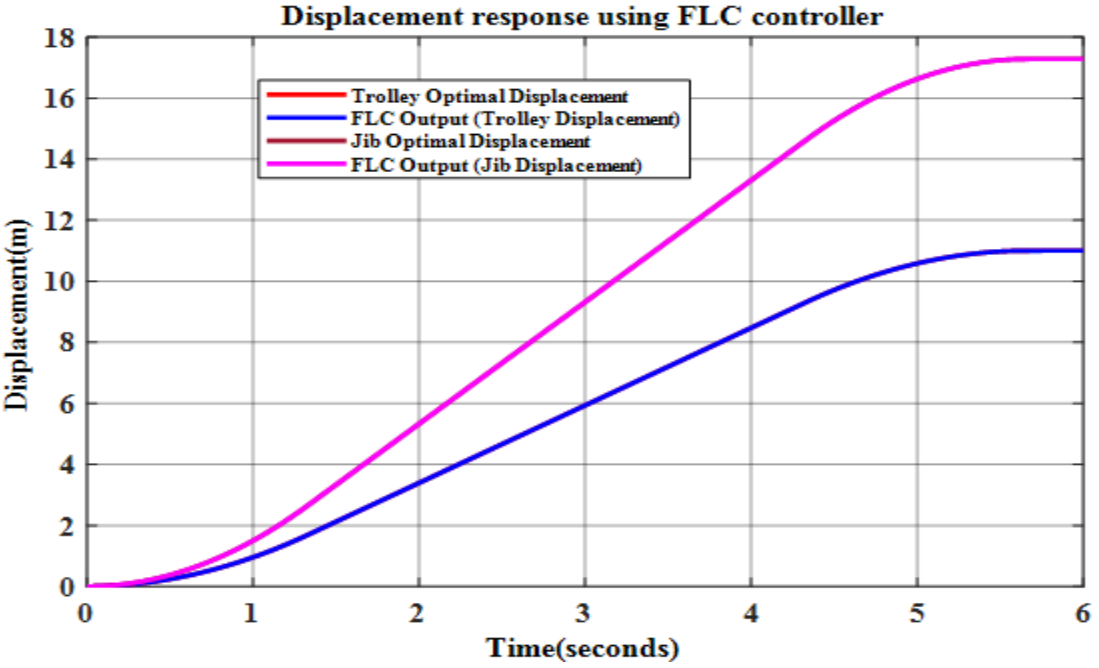

Figure 5.22: Jib and trolley displacement response using FLC when the trolley moves from 1m to 12m

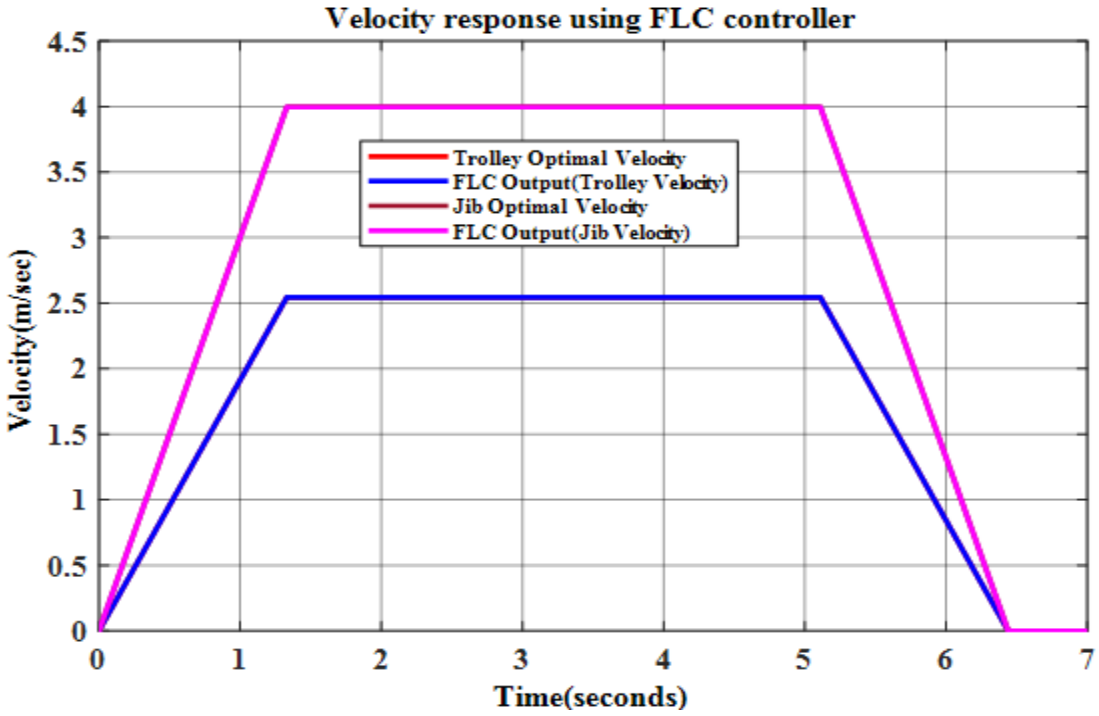

Figure 5.23: Jib and trolley velocity response using FLC when the trolley moves from 1m to 14m

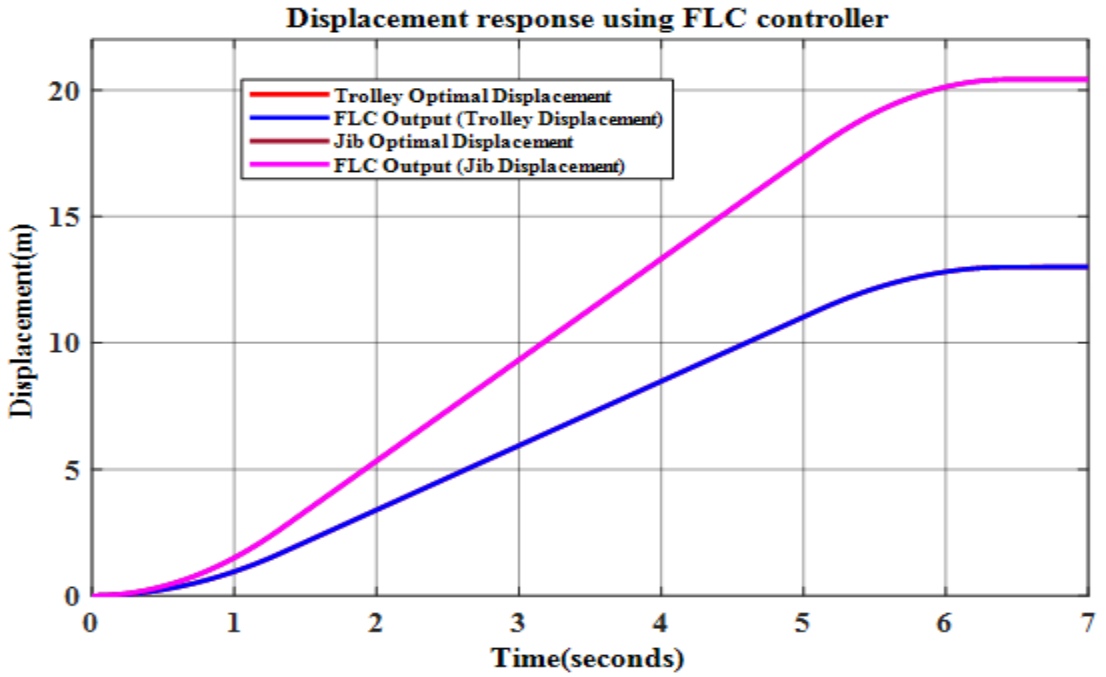

Figure 5.24: Jib and trolley displacement response using FLC when the trolley moves from 1m to 14m

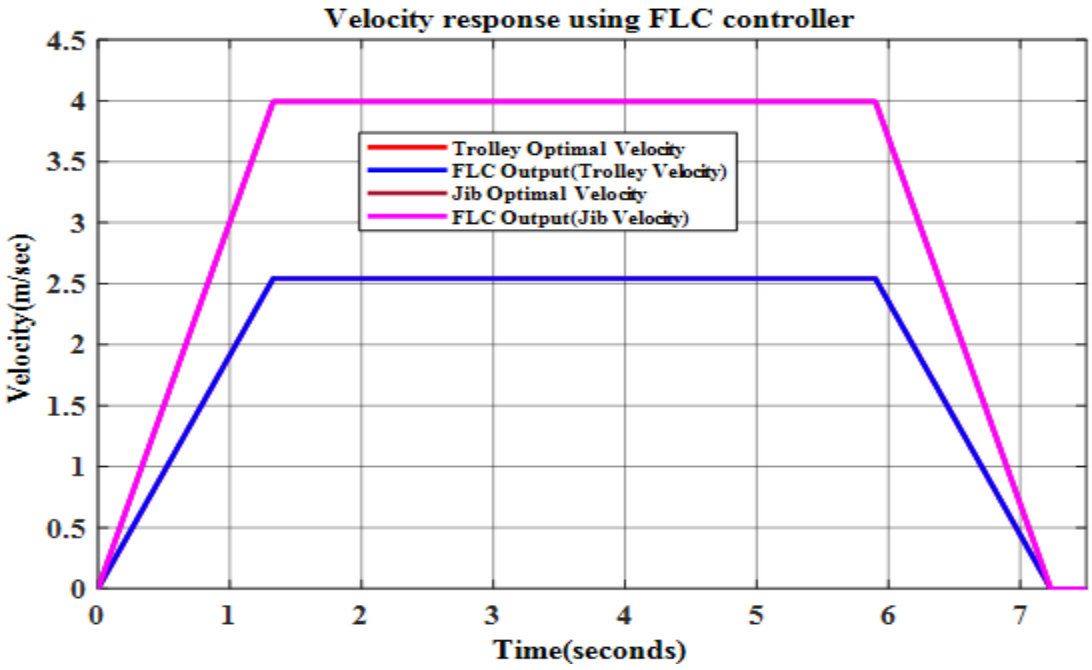

Figure 5.25: Jib and trolley velocity response using FLC when the trolley moves from 1m to 16m

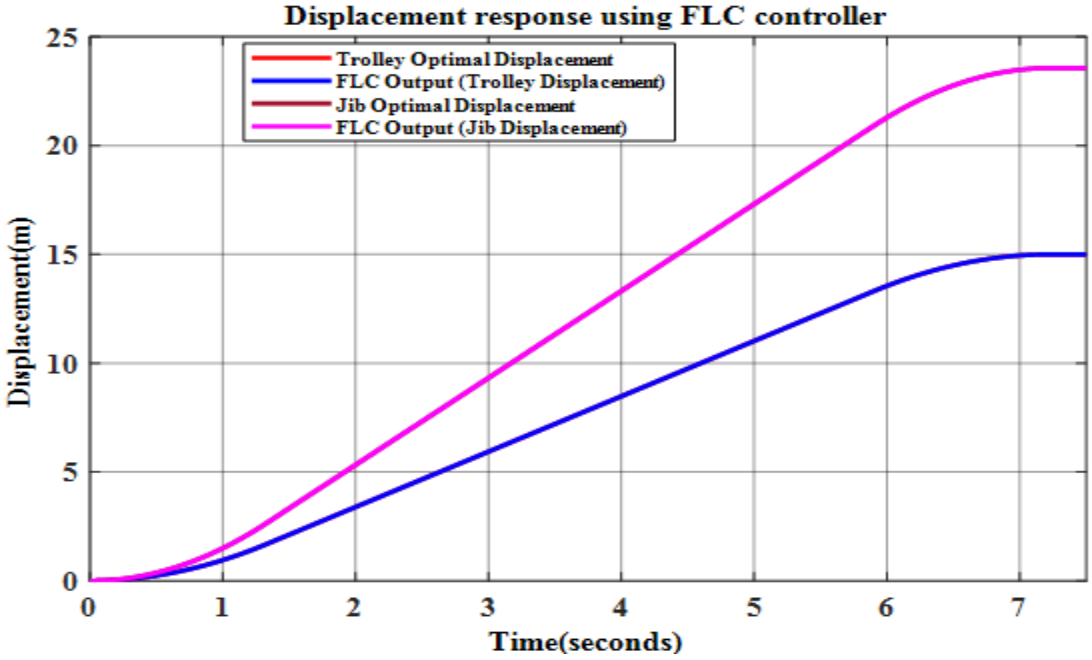

Figure 5.26: Jib and trolley displacement response using FLC when the trolley moves from 1m to 16m

Figures 5.25 and 5.26 indicates that the trolley is moved 15m from r=1m to r=16m while the jib is rotated by 90° from its initial position or radially from 0m to 23.56 m. Both the trolley and jib

accelerates for 1.33 seconds, moves with a constant velocity of magnitude 2.542 m/sec and 3.993 m/sec respectively for 4.57 seconds and decelerates for 1.33 seconds. The whole operation is executed within 7.23 seconds. In this case the maximum magnitude of the sway angle due to the trolley movements and jib rotations are 0.1029 and 0.1654 radians respectively and reduces to zero at the destination. Therefore, fuzzy logic controller tracks the given optimal references without error at the optimal time. This indicates that the tracking performance of FLC is not affected due to trolley displacement variations.

As shown in Figure 5.27 the trolley and jib accelerates for 1.33 seconds, moves with a constant velocity of magnitude 4 m/sec and -6.284 m/sec respectively for 0.92 seconds, and they decelerates for 1.33 seconds. The final velocity of the trolley and jib at the destination becomes zero. The whole operation is executed within 3.58 seconds which is the optimal. The jib rotates from 90° to 0° while the trolley moves 1m to 10m as show in Figure 5.28. Figures 5.27 and 5.28 illustrate the negative radial velocity or displacement presented in Figure 5.9.

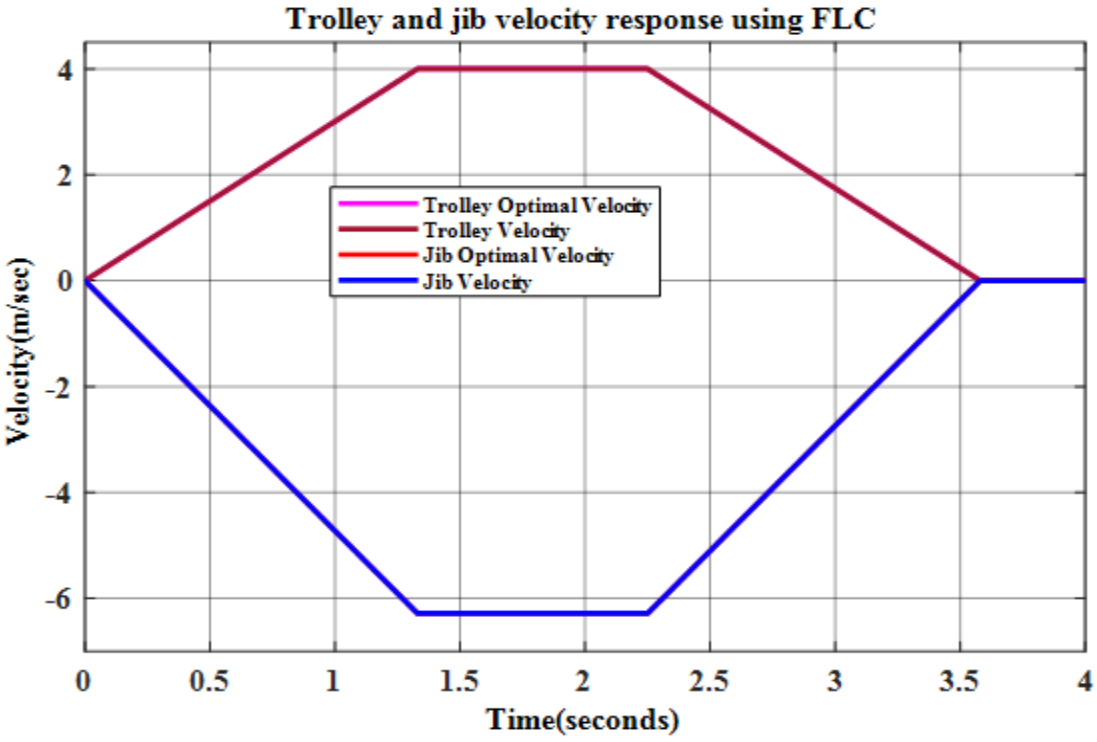

Figure 5.27: Jib and trolley velocity response using FLC

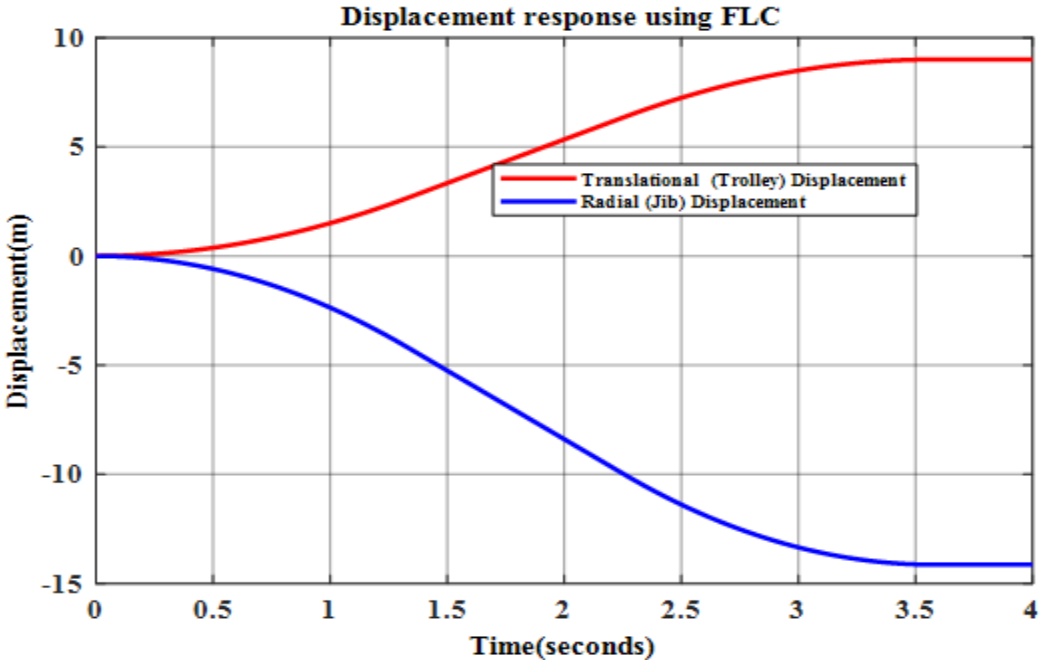

Figure 5.28: Jib and trolley displacement response using FLC

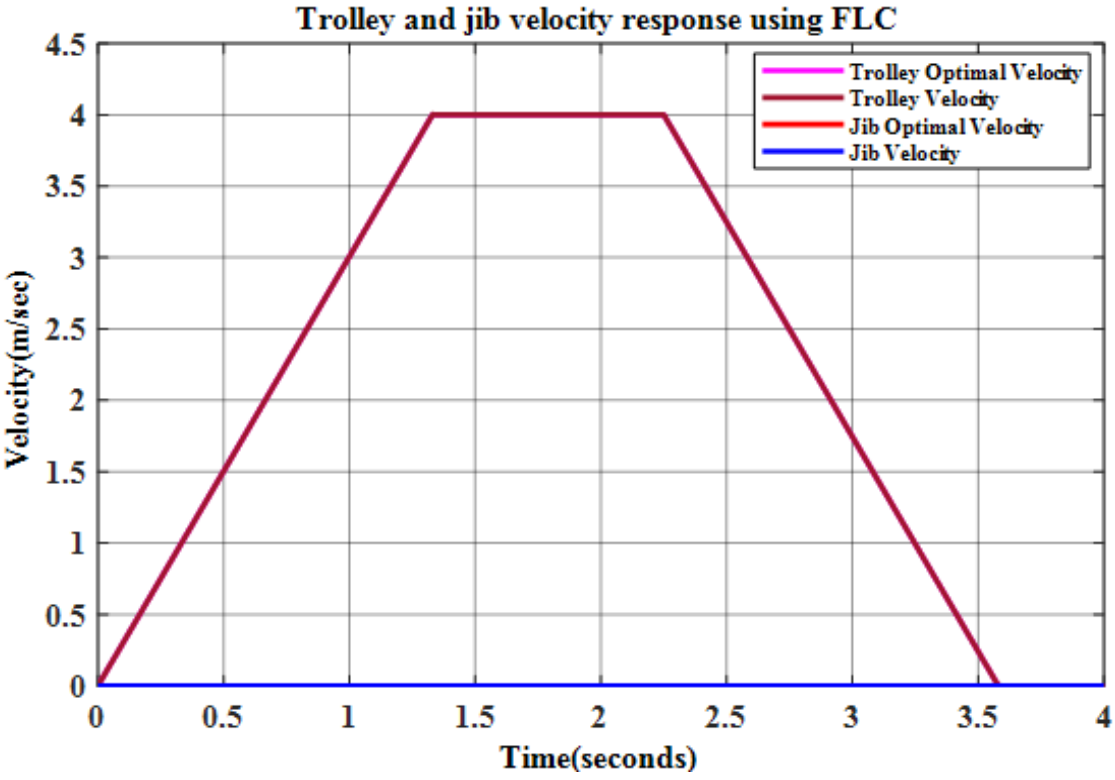

Figure 5.29: Trolley velocity response using FLC while the jib is not rotating

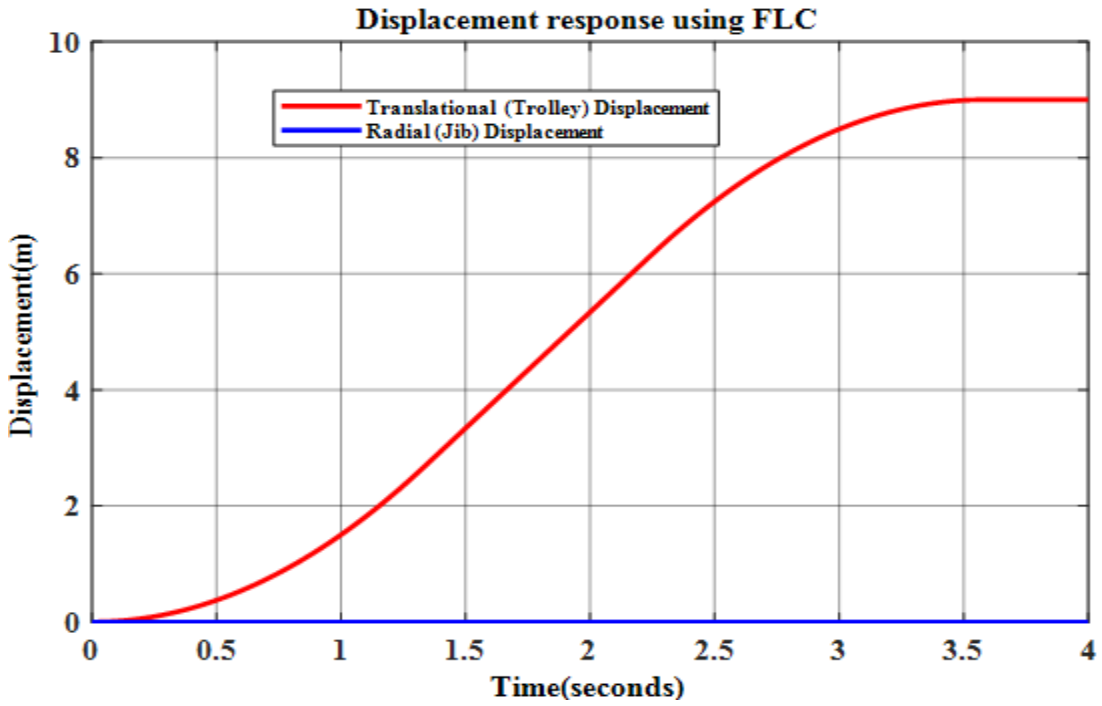

Figure 5.30: Trolley displacement response using FLC while the jib is not rotating

As shown in Figure 5.29 the trolley accelerates for 1.33 seconds, moves with a constant velocity of magnitude 4 m/sec for 0.92 seconds and decelerates for 1.33 seconds. The operation takes 3.58 seconds which is optimal. Figure 5.30 illustrates that the trolley or cart moves 9m from its initial position i.e. from r=1m to r=10m while the jib is not rotated. The trolley covers the given distances within the optimal time of 3.58 seconds.

5.6. Comparison of FLC, PID, and Closed Loop Control Systems In Terms of Optimal Motion Tracking Performance

This section presents the comparison of different controllers in terms of optimal motion tracking performance. The Matlab/Simulink model of the trolley and jib velocity with FLC, PID controller, open and closed loop control system are shown in Figures 5.31 and 5.34 respectively.

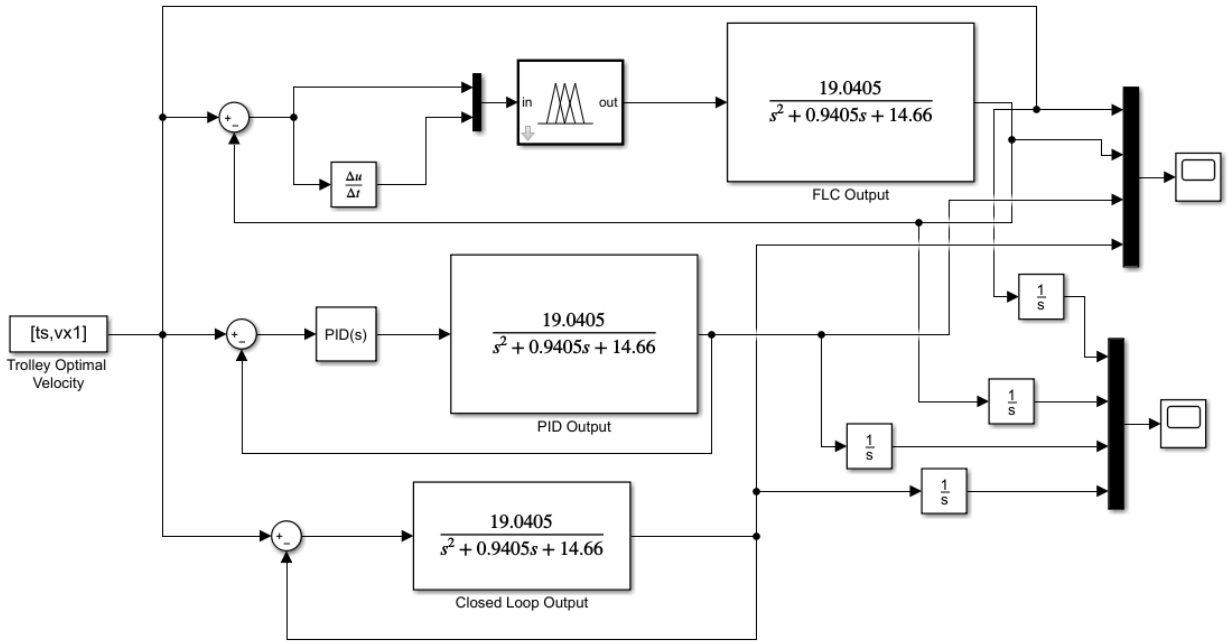

Figure 5.31: Simulink diagram of trolley velocity using FLC, PID and closed loop control

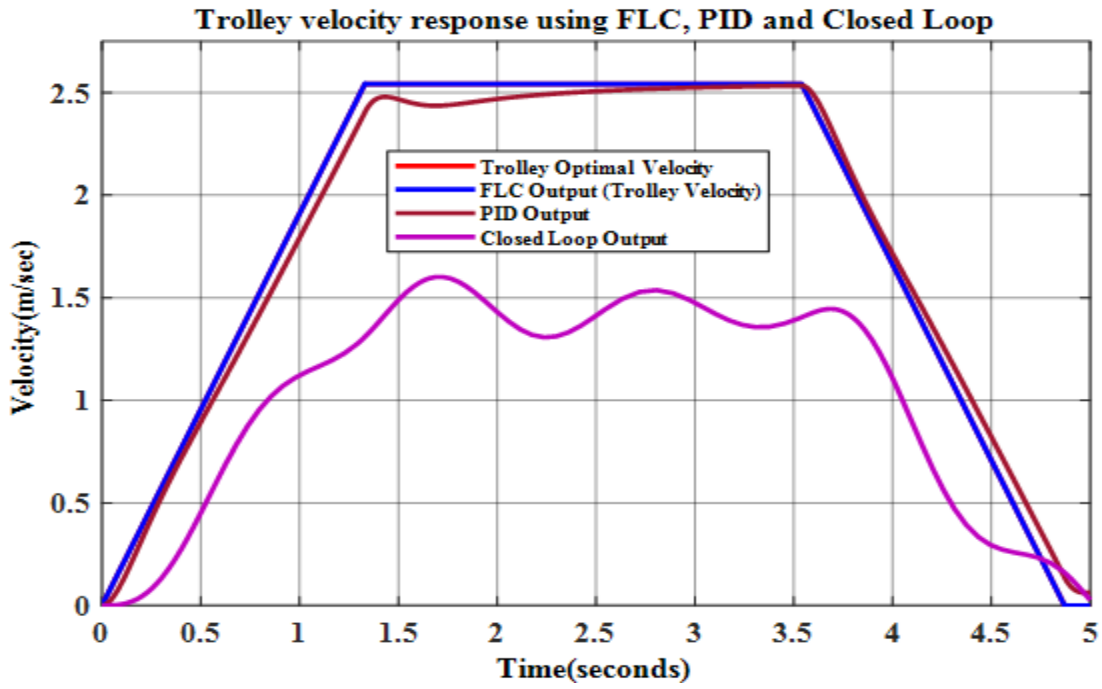

Figure 5.32: Response of FLC, PID, Closed loop control system in terms of trolley optimal velocity tracking performance

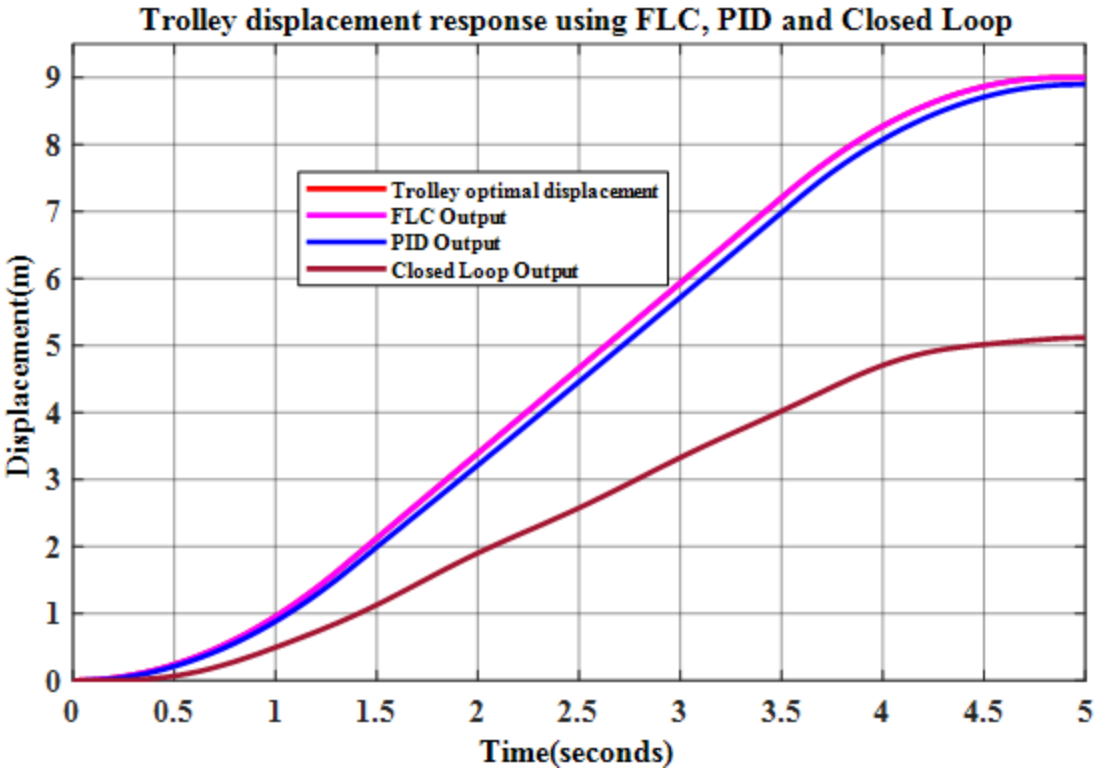

Figure 5.33: Response of FLC, PID and Closed loop control system in terms of trolley optimal displacement tracking performance

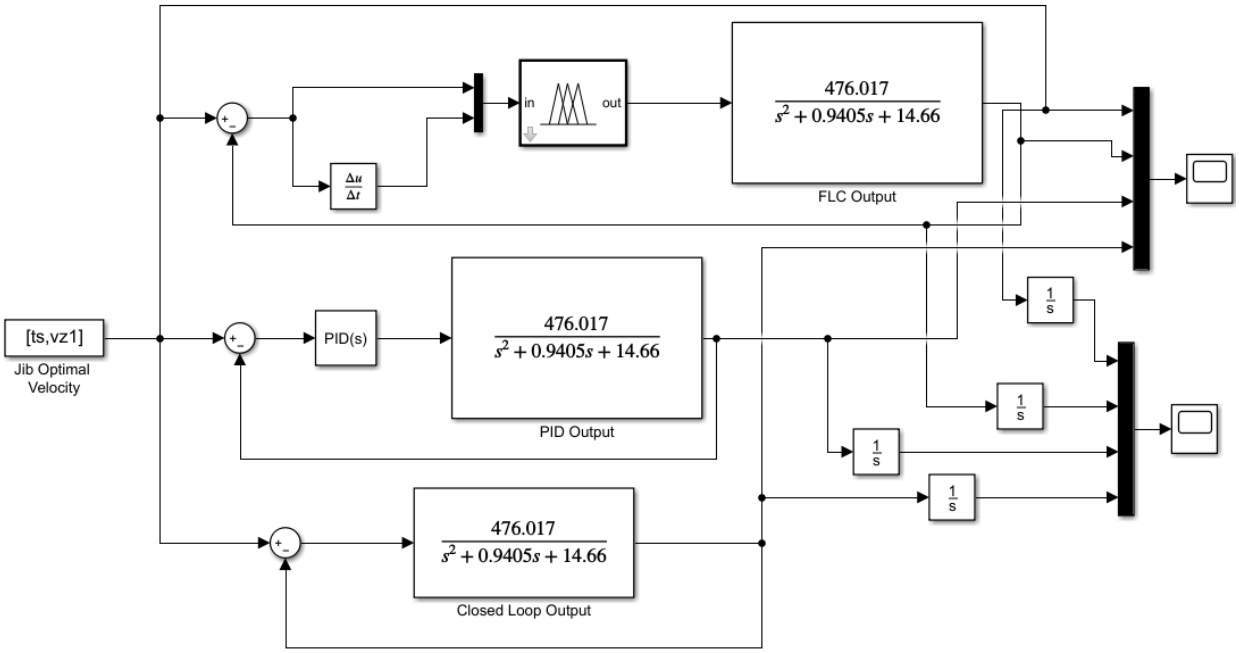

Figure 5.34: Simulink diagram of jib velocity using FLC, PID and closed loop control system

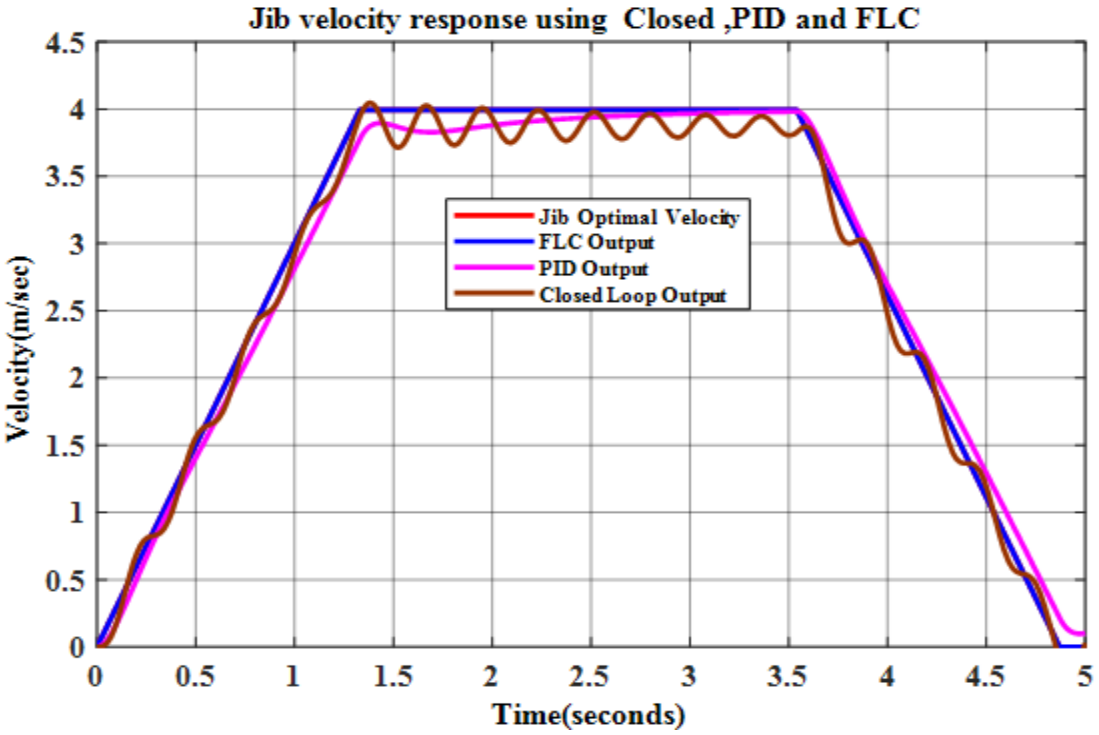

Figure 5.35: Response of FLC, PID and Closed control system in terms of jib optimal velocity tracking performance

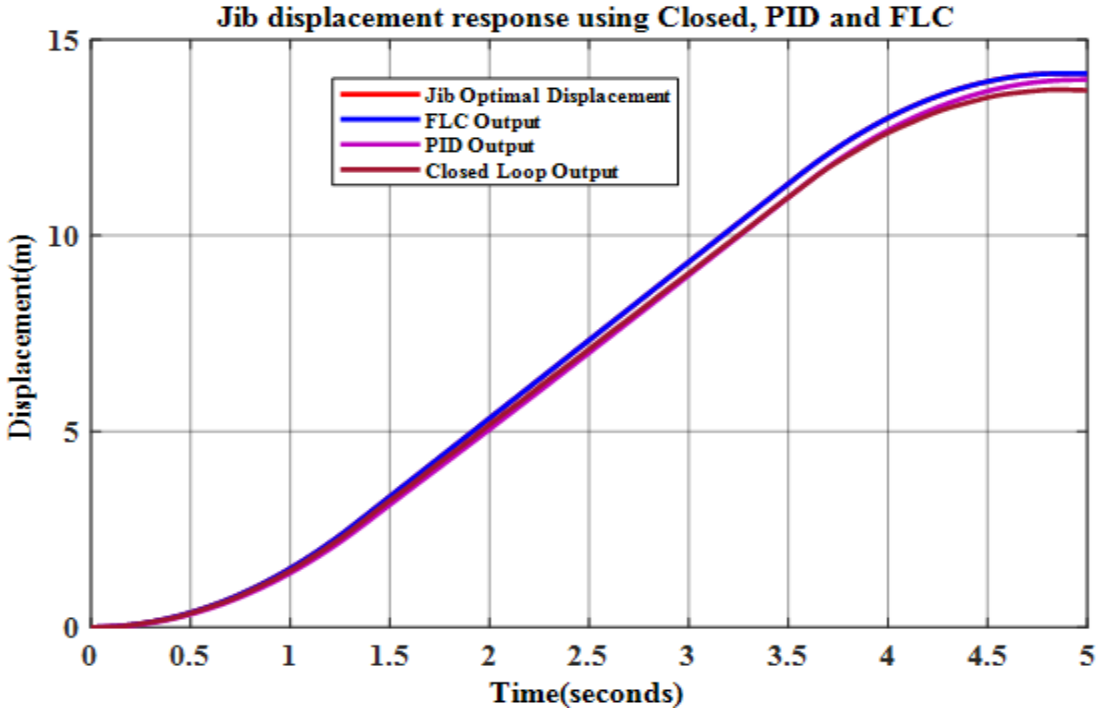

Figure 5.36: Response of FLC, PID and Closed control system in terms of jib optimal displacement tracking performance

Figure 5.32 and 5.35 shows a comparison between fuzzy logic controller, PID controller, and closed loop control systems in terms of trolley and jib optimal velocity tracking performance. It can be noted that fuzzy logic controller has better tracking performance compared with the other control techniques. From this it can be concluded that fuzzy logic controller tracks the desired velocity faster than the other control techniques i.e. PID controller, and closed loop control systems. The fuzzy logic controller forces the output velocity of the trolley and jib to follow the optimal time reference input velocity as shown in Figure 5.36 and 5.39. That means, all the parameters of the trolley and jib i.e. trolley velocity, jib velocity and the load velocity exactly tracked its optimal time reference inputs.

Figures 5.33 and 5.36 illustrates a comparison between FLC, PID controller and closed loop control systems in terms of trolley and jib optimal displacement tracking performance. The responses of PID controller and closed loop control systems are not covered the required displacement but the response of fuzzy logic controller is covered the desired displacement within optimal time. It can be noted that fuzzy logic controller and PID controller have better tracking performance compared with closed loop control system techniques. But, PID has very small deviation about optimal reference position tracking. The fuzzy logic controller follows exactly the optimal time reference input. From this it can be concluded that fuzzy logic controller has better position tracking performance compared with the other control techniques.

Table 5.1: Distances covered by the moving parts of tower crane using different controllers

Controllers	Distances covered by trolley at the optimal time 4.87 second	Distances covered by jib at the optimal time 4.87 second	Trolley distance Error (reference-observed)
Closed loop control system	5.103m	13.73m	3.897m
PID controller	8.89m	13.97m	0.11m
Fuzzy logic controller	9m	90° (14.14m)	0m

5.7. FLC and PID Controller Response In The Presence of Random Disturbances

Let's see the effect of external disturbance such as wind on the response of both fuzzy logic controller and PID controller under the assumption that our plant is certain. The Simulink representation of the velocity model of both trolley and jib with external disturbance is shown in Figure 5.37 and 5.38.

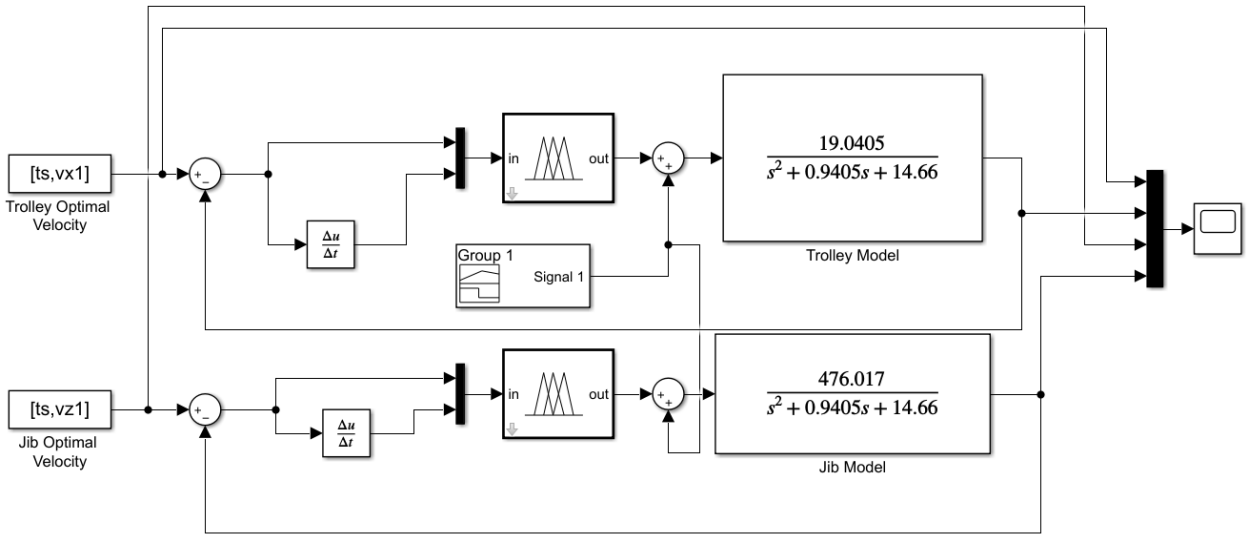

Figure 5.37: Simulink diagram of trolley and jib velocity using FLC under external disturbance

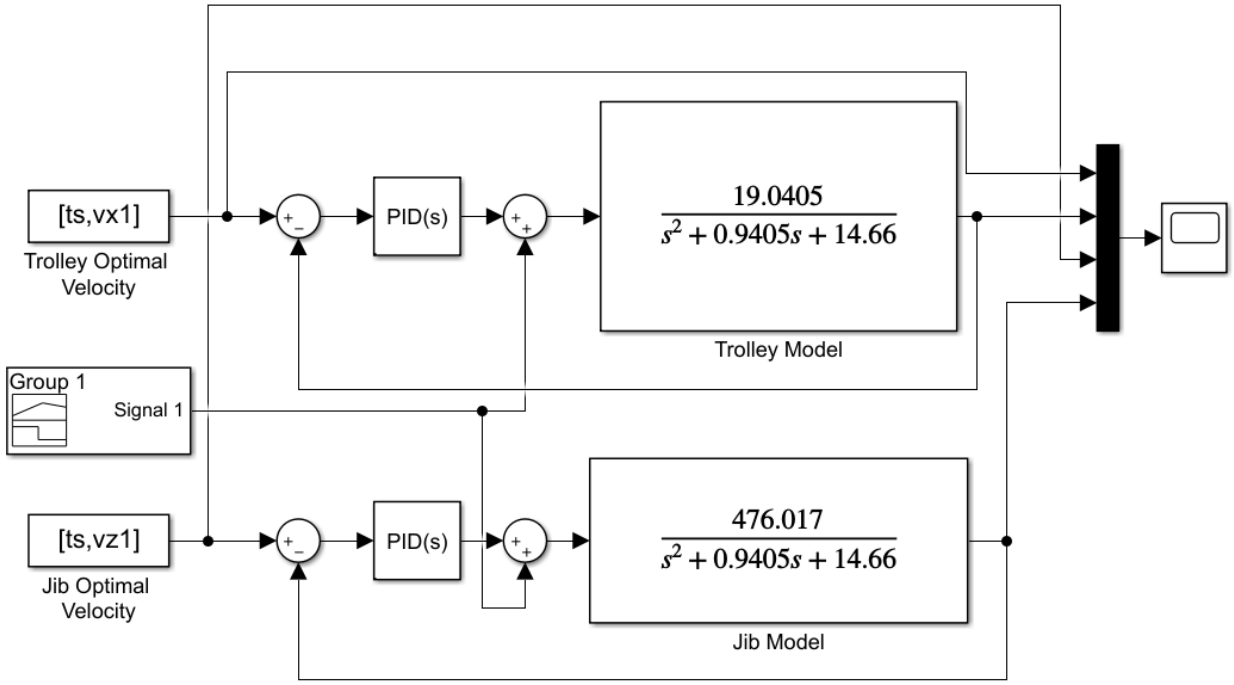

Figure 5.38: Simulink diagram of trolley and jib velocity using PID under external disturbance

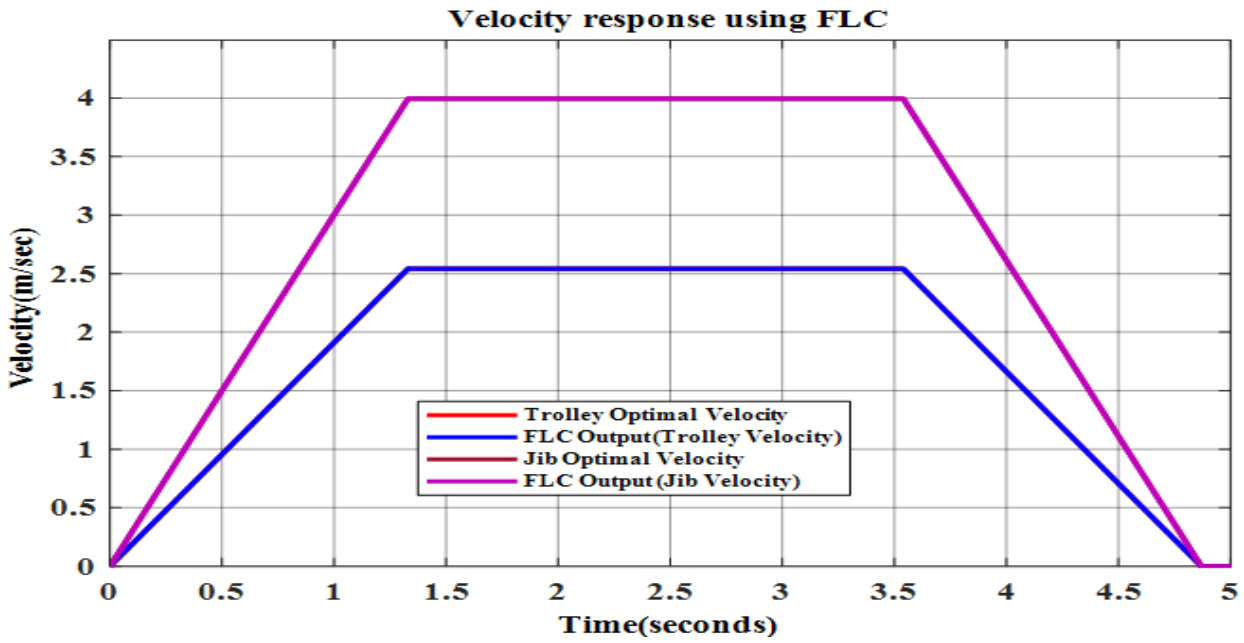

Figure 5.39: Response of FLC for trolley and jib velocity control under external disturbance

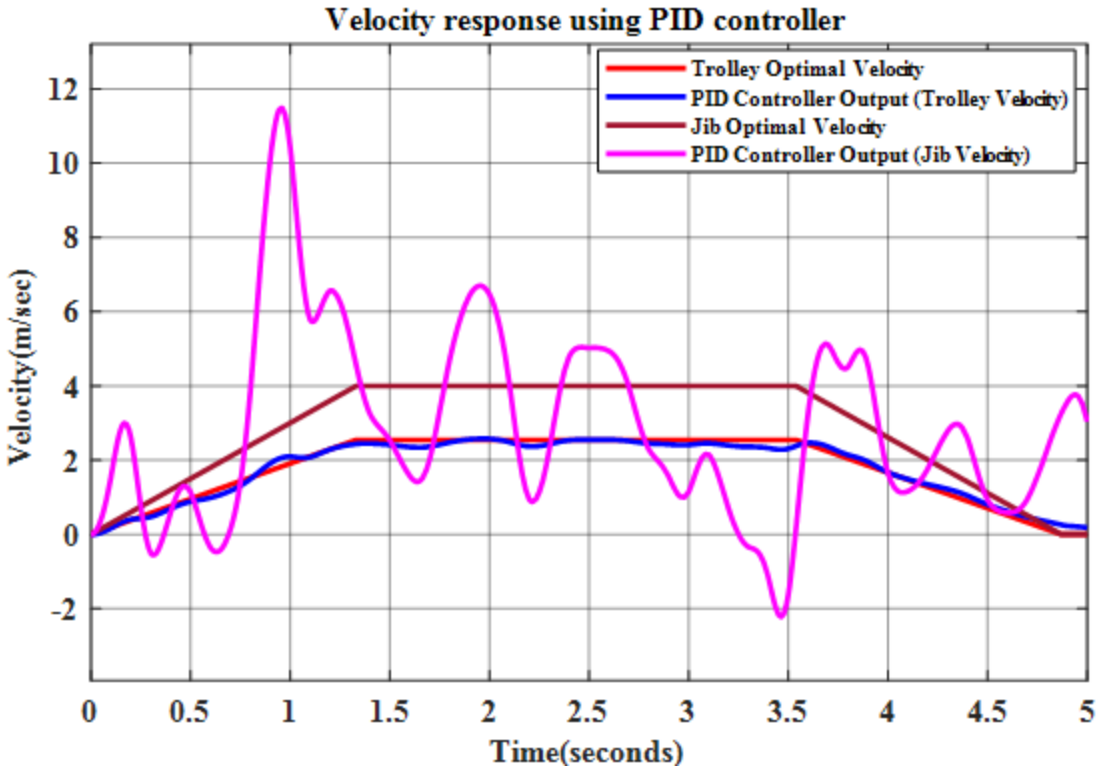

Figure 5.40: Response of PID for trolley and jib velocity control under external disturbance

Here, we compare the two controllers' i.e. fuzzy logic controller and PID controller in terms of external disturbance rejection ability under the assumption that the plant is certain. Both Figures 5.39 and 5.40 shows the velocity response of trolley and jib using fuzzy logic controller and PID

controller. The responses of FLC are tracked the optimal reference (velocity) in the presence of external disturbance. That means, fuzzy logic controller is not affected by the random disturbance. However, the responses of PID controller are deviated from the optimal value i.e. velocity due to the presence of random external disturbance. Therefore, PID controller needs manual tuning to reject the effect of the external disturbance. From this we can conclude that fuzzy logic controller is more robust than PID controller because of the capability to cover a huge range of operating conditions. The fuzzy logic controller rejects the external disturbance by changing error and rate of change of error and monitoring the armature input voltage to the motor.

CHAPTER SIX

Conclusion and Recommendation

6.1. Conclusion

The main target of this thesis is to ensure safety of the tower crane system and improves time efficiency during transportation of the load. Moreover, both the trolley and jib parts of the tower crane system are needed to be arrived at the desired position quickly with minimum sway angle of the load. These objectives of the tower crane system have been achieved based on two step design phases which are a systematic anti-sway optimal motion planning and controller design. The optimal motion planning is mainly focused on generating an optimal time reference inputs for the controllers and they are done on Matlab based on the system nature. Based on this design stage the trolley sway angle is reduced to 0.103 radian or 5.9° and jib sway angle is reduced to 0.1654 radian or 9.5° with fast motion. Furthermore, the sway angles of both the trolley and jib at the desired position are reduced to zero. The controller design stages are based on two approaches. In the firs approach, a PID controller is designed to track the desired optimal time reference inputs generated using an optimal motion planning algorithm developed in Matlab workspace. The parameters of the PID controller are tuned automatically in Matlab/Simulink using PID auto tuner method. In the second approach, a fuzzy logic controller is designed to track the desired optimal time reference inputs generated using an optimal motion planning algorithm developed in Matlab workspace. The fuzzy logic controller is designed based on Mamdani FIS, COG defuzzification method and trapezoidal membership function to track the optimized reference inputs. The performances of the control schemes have been evaluated in terms of load sway angle suppression, trolley and jib optimal time velocity and displacement tracking capability by varying the trolley displacements. Acceptable performance in sway angle suppression, trolley and jib optimal time velocity and displacement tracking control has been achieved with fuzzy logic controller. A comparative assessment of the control schemes has shown that the fuzzy logic controller performs better than the PID controller in respect of trolley and jib trajectory tracking performance and sway angle reduction. It can be conclude that fuzzy logic controller has fast response and better velocity and displacement tracking performance compared to PID controllers. That means the considered controller in this thesis satisfies the design objectives i.e. the optimum time, optimal sway angle, maintained the destination terminal and zero sway at the target point.

6.2. Recommendation

The FLC presented in this thesis can be used for other types of cranes. In the anti-sway control of the tower crane system the dynamics of the cable is not considered. Therefore, future researcher can include the dynamics of a cable.

The membership function parameter range for input and output variables of the fuzzy logic controller are selected by users or designers. In this thesis we select the value of these parameters using trial and error method. In addition to this the anti-sway fuzzy logic controller performance can be improved by a proper tuning of the parameters of the membership functions. The future researcher can be used optimization methods such as genetic algorithm, particle swarm optimization, etc. to determine the optimum value for these parameters.

References

[1] V. Renuka, A. T. J. I. J. o. T. Mathew, and A. R. i. M. Engineering, "Precise modelling of a gantry crane system including friction, 3d angular swing and hoisting cable flexibility," vol. 2, no. 1, pp. 117-123, 2013.

[2] N. Zrnić, V. Gašić, S. J. A. o. C. Bošnjak, and M. Engineering, "Dynamic responses of a gantry crane system due to a moving body considered as moving oscillator," vol. 15, no. 1, pp. 243-250, 2015.

[3] K.-E. J. I. J. o. S. S. Kurrer, "The history of the theory of structures: from arch analysis to computational mechanics," vol. 23, no. 3, pp. 193-197, 2008.

[4] H. I. Jaafar, Z. Mohamed, J. Jamian, A. F. Z. Abidin, A. M. Kassim, and Z. J. P. T. Ab Ghani, "Dynamic behaviour of a nonlinear gantry crane system," vol. 11, pp. 419-425, 2013.

[5] R. Amstel. (2016, 27 June). *Overhead Crane System*. Available: https://ellsenoverheadcrane.wixsite.com/ellsenoverheadcrane/blog/category/Overhead%20Crane%20System

[6] A. A. Al-Mousa, "Control of rotary cranes using fuzzy logic and time-delayed position feedback control," Virginia Tech, 2000.

[7] Crane and Machinery. (2020, January 16). *GANTRY CRANE*. Available: https://www.gruasyaparejos.com/en/gantry-crane/

[8] E. M. Abdel-Rahman, A. H. Nayfeh, and Z. N. J. M. A. Masoud, "Dynamics and control of cranes: A review," vol. 9, no. 7, pp. 863-908, 2003.

[9] Crane and Machinery. (2020, January 16). *Tower crane parts*. Available: https://www.gruasyaparejos.com/en/tower-crane/tower-crane-parts/

[10] YMV Crane and Winch Systems. *Boom crane*. Available: https://www.nauticexpo.com/prod/ymv-crane-winch-systems/product-63904-505120.html

[11] J. Yoon, S. Nation, W. Singhose, and J. E. J. I. T. o. C. S. T. Vaughan, "Control of crane payloads that bounce during hoisting," vol. 22, no. 3, pp. 1233-1238, 2013.

[12] W. J. I. j. o. p. e. Singhose and manufacturing, "Command shaping for flexible systems: A review of the first 50 years," vol. 10, no. 4, pp. 153-168, 2009.

[13] W. Blajer, K. J. J. o. t. Kołodziejczyk, and a. mechanics, "Dynamics and control of rotary cranes executing a load prescribed motion," vol. 44, pp. 929-948, 2006.

[14] A. Kaur, S. K. Priyahansha, T. J. I. J. o. A. R. i. E. Singh, Electronics, and I. Engineering, "Position control of overhead cranes using fuzzy controller," vol. 3, no. 5, pp. 9341-9350, 2014.

[15] G. G. Parker, B. Petterson, C. R. Dohrmann, and R. D. Robinett III, "Vibration suppression of fixed-time jib crane maneuvers," in *Smart Structures and Materials 1995: Industrial and Commercial Applications of Smart Structures Technologies*, 1995, vol. 2447, pp. 131-140: International Society for Optics and Photonics.

[16] G. G. Parker, B. Petterson, C. Dohrmann, and R. D. Robinett, "Command shaping for residual vibration free crane maneuvers," in *Proceedings of 1995 American Control Conference-ACC'95*, 1995, vol. 1, pp. 934-938: IEEE.

[17] A. D. Smith, "Comparison of Filtering Methods for Vibration Reduction," 2009.

[18] A. R. Golafshani and J. Aplevich, "Computation of time-optimal trajectories for tower cranes," in *Proceedings of International Conference on Control Applications*, 1995, pp. 1134-1139: IEEE.

[19] A. H. HAILU, "OPTIMAL MOTION–PLANNING AND HYBRID (ADAPTIVE-PID) ANTI-SWAY CONTROL OF 3D OVERHEAD CRANE," 2019.

[20] A. A. El-Badawy and M. M. G. Shehata, "Anti-sway control of a tower crane using inverse dynamics," in *2014 International Conference on Engineering and Technology (ICET)*, 2014, pp. 1-6: IEEE.

[21] H. M. Omar, "Control of gantry and tower cranes," Virginia Tech, 2003.

[22] R. E. Samin, Z. Mohamed, J. Jalani, and R. Ghazali, "A hybrid controller for control of a 3-DOF rotary crane system," in *2013 1st International Conference on Artificial Intelligence, Modelling and Simulation*, 2013, pp. 190-195: IEEE.

[23] H. M. Omar and A. H. J. M. A. Nayfeh, "Gain scheduling feedback control for tower cranes," vol. 9, no. 3-4, pp. 399-418, 2003.

[24] F. Altaf, "Modeling and Event-Triggered Control ofMultiple 3D Tower Cranes over WSNs," ed, 2010.

[25] W. Wahyudi and J. Jalani, "Design and implementation of fuzzy logic controller for intelligent gantry crane system," 2005.

[26] R. Ruslee, "Anti-swing control strategy for automatic 3 DOR crane system using FLC," Universiti Tun Hussein Onn Malaysia, 2008.

[27] R. Hurteau and R. M. Desantis, "Microprocessor-based adaptive control of a crane system," in *The 22nd IEEE Conference on Decision and Control*, 1983, pp. 944-947: IEEE.

[28] M. J. Nalley, M. B. J. J. o. I. Trabia, and F. Systems, "Control of overhead cranes using a fuzzy logic controller," vol. 8, no. 1, pp. 1-18, 2000.

[29] M. Akar, I. J. I. J. o. A. M. Temiz, and Informatics, "Motion controller design for the speed control of dc servo motor," vol. 4, no. 1, pp. 131-137, 2007.

[30] P. Pratumsuwan, S. Thongchai, and S. J. E. R. J. Tansriwong, "A hybrid of fuzzy and proportional-integral-derivative controller for electro-hydraulic position servo system," vol. 1, no. 2, pp. 62-67, 2010.

[31] O. Wahyunggoro and N. B. Saad, "Development of fuzzy-logic-based self tuning PI controller for servomotor," in *2008 10th International Conference on Control, Automation, Robotics and Vision*, 2008, pp. 1545-1550: IEEE.

[32] K. Ogata, "Modern Control Engineering, Prectice-Hall," ed: Inc, 1990.

[33] K. Ogata and Y. Yang, "Modern control engineering," 1970.

[34] D. O. J. J. o. C. T. Aborisade and Informatics, "DC Motor with Load Coupled by Gears Speed Control using Modified Ziegler-Nichols Based PID Tunings," vol. 4, no. 5, pp. 58-67, 2014.

[35] H. Ahmed, G. Singh, V. Bhardwaj, S. Saurav, and S. Agarwal, "Controlling of DC Motor using Fuzzy logic controller," in *Proceedings of the Conference on Advances in Communication and Control Systems-2013*, 2013: Atlantis Press.

[36] K. H. Ang, G. Chong, and Y. J. I. t. o. c. s. t. Li, "PID control system analysis, design, and technology," vol. 13, no. 4, pp. 559-576, 2005.

[37] V. Chopra, S. K. Singla, and L. J. A. P. h. Dewan, "Comparative analysis of tuning a PID controller using intelligent methods," vol. 11, no. 8, pp. 235-249, 2014.

[38] R. Langari and J. Yen, "Fuzzy Logic: intelligence, control, and information," ed: Prentice-Hall Inc, 1999.

[39] C.-C. J. I. T. o. s. Lee, man, and cybernetics, "Fuzzy logic in control systems: fuzzy logic controller. II," vol. 20, no. 2, pp. 419-435, 1990.

[40] R. Fullér, "Neural fuzzy systems," 1995.

[41] S. Ghosh, *Control Systems: Theory and Applications*. Pearson India, 2013.

[42] P. J. I. J. o. A. M. Czekalski and C. Science, "Evolution-fuzzy rule based system with parameterized consequences," vol. 16, pp. 373-385, 2006.

[43] T. J. J. 한. Ross, "Fuzzy logic with engineering applications," vol. 25, no. 4, pp. 71-71, 2013.

[44] A. J. J. o. A. I. Rutkowska and S. C. Research, "Influence of membership function's shape on portfolio optimization results," vol. 6, no. 1, pp. 45-54, 2016.

[45] D. Wu, "Twelve considerations in choosing between Gaussian and trapezoidal membership functions in interval type-2 fuzzy logic controllers," in *2012 IEEE International Conference on Fuzzy Systems*, 2012, pp. 1-8: IEEE.

[46] J. Zhao and B. K. Bose, "Evaluation of membership functions for fuzzy logic controlled induction motor drive," in *IEEE 2002 28th Annual Conference of the Industrial Electronics Society. IECON 02*, 2002, vol. 1, pp. 229-234: IEEE.

[47] M. J. I. s. Sugeno, "An introductory survey of fuzzy control," vol. 36, no. 1-2, pp. 59-83, 1985.

[48] I. MathWorks and W.-c. Wang, *Fuzzy Logic Toolbox: for Use with MATLAB: User's Guide*. Mathworks, Incorporated, 1998.

Appendix

This appendix shows the Matlab programs developed for generating optimal time reference inputs to the controller as shown in Figures 5.1 to 5.9.

```
clc
clear
x1 =1;
x2 =10;
z1=0;
z2=90;
K=0.2;
ax=3;
az=3;
l=4;
%L1=[x1,z1];    % Previous location
%L2=[x2,z2];    % New location
zs=sign(z2-z1);        % sign of Z
xs=sign(x2-x1);        % sign of X
mx=(x1+x2)/2;
g=9.81;
Sx=x2-x1; % Displacement in translational motion
Sz=round(pi*(Sx+(1-xs)*mx)*(z2-z1)/180,2); % Displacement in the radial direction
if Sx+Sz==0&& abs(Sx*Sz)>0
   Sz=Sz+0.0001;
else
   Sz=Sz;
end
%====================== Determination of times t1 and t2======================
% Enter the acceleration in the x and z directions ax,az
t1x=sqrt(abs(Sx/ax));  % value of s over ax
t1z=sqrt(abs(Sz/az));       % value of s over az
```

```
dt=0.01;              % Decimal Range
W=1/dt;               % Weight to determine the decimal number
%==================== Time optimization ============================
%==================== Condition for t1 and t2 ================
t11=max((abs(Sx)*t1x+abs(Sz)*t1z)/(abs(Sx)+abs(Sz)));
t12=sqrt(2*K*g*l)*(Sx/(ax*(Sx+Sz))+Sz/(az*(Sx+Sz)));
t01=min(t11,t12);
t1=ceil(t01*W)/W;   % Time of acceleration/ deceleration
t02x=Sx/(ax*t1)-t1;
t02z=Sz/(az*t1)-t1;
t02=max(t02x,t02z);
t2=floor(W*t02)/W;   % time of constant velocity
%---------------- Correction on acceleration ----------------------
ax=Sx/(t1*(abs(t1)+abs(t2)));
az=Sz/(t1*(abs(t1)+abs(t2)));
%============================================================
%Determination of the necessary variables in x & z-directions
%============================================================
v1(1)=0;    v2(1)=0;          % Initial velocity
acx(1)=ax; acz(1)=az;         % Initial acceleration
acr(1)=sqrt(ax^2+az^2);       % Initial resultant acceleration
tj1 = 0:dt:t1;
tj2 = 0:dt:t2;
tj3 = 0:dt:t1;
tj4 = 0:dt:t1;
v11 = v1(1)+zeros(1,length(tj1));
v21 = v2(1)+zeros(1,length(tj1));
acx1 = zeros(1,length(tj1));
acz1 = zeros(1,length(tj1));
acr1 = zeros(1,length(tj1));
v12 = v1(1)+zeros(1,length(tj2));
```

```
v22 = v2(1)+zeros(1,length(tj2));
acx2 = zeros(1,length(tj2));
acz2 = zeros(1,length(tj2));
acr2 = zeros(1,length(tj2));
v13 = v1(1)+zeros(1,length(tj3));
v23 = v2(1)+zeros(1,length(tj3));
acx3 = zeros(1,length(tj3));
acz3 = zeros(1,length(tj3));
acr3 = zeros(1,length(tj3));
v14= v1(1)+zeros(1,length(tj4));
v24= v2(1)+zeros(1,length(tj4));
acx4= zeros(1,length(tj4));
acz4= zeros(1,length(tj4));
acr4= zeros(1,length(tj4));
for i=1:length(tj1)
    acx1(i) = ax;
    acz1(i) = az;
    acr1(i) = sqrt(ax^2+az^2);
    v11(i) = v1(1)+ax*tj1(i);
    v21(i) = v2(1)+az*tj1(i);
end
for i=1:length(tj2)
    acx2(i)=0;
    acz2(i)=0;
    acr2(i)=0;
    v12(i)= v1(1)+ ax*t1;
    v22(i)= v2(1)+az*t1;
end
for i=1:length(tj3)
    acx3(i)= -ax;
    acz3(i)= -az;
```

```
        acr3(i)= -sqrt(ax^2+az^2);
        v13(i)= v1(1)+ ax*t1 - ax*tj3(i);
        v23(i)=(v2(1)+ az*t1)- az*tj3(i);
end
for i=1:length(tj4)
        acx4(i) = 0;
        acz4(i) = 0;
        acr4(i) = 0;
        v14(i) = 0;
        v24(i) = 0;
end
T1=tj1';   % change tj1 from a row to a column vector tj1'
T2=tj2(2:end)' + t1;   % shift bounds and drop first vector element
T3=tj3(2:end)' + t1 + t2;
T4=tj4(2:end)' + t1 + t2 + t1;
t =[T1;T2;T3];
ts = [T1;T2;T3;T4];    % sample time
v11=v11';
v12=v12(2:end)';
v13=v13(2:end)';
v14=v14(2:end)';
vx = [v11;v12;v13];
vx1 = [v11;v12;v13;v14];
v21=v21';
v22=v22(2:end)';
v23=v23(2:end)';
v24=v24(2:end)';
vz = [v21;v22;v23];
vz1 = [v21;v22;v23;v24];
vr1=sqrt(v11.^2+v21.^2);
vr2=sqrt(v12.^2+v22.^2);
```

```
vr3=sqrt(v13.^2+v23.^2);
vr4=sqrt(v14.^2+v24.^2);
vr = [vr1;vr2;vr3];
vrr = [vr1;vr2;vr3;vr4];
acx1=acx1';
acx2=acx2(2:end)';
acx3=acx3(2:end)';
acx4=acx4(2:end)';
a1 = [acx1;acx2;acx3];
a11 = [acx1;acx2;acx3;acx4];
acz1=acz1';
acz2=acz2(2:end)';
acz3=acz3(2:end)';
acz4=acz4(2:end)';
a2 = [acz1;acz2;acz3];
a22 = [acz1;acz2;acz3;acz4];
acr1=acr1';
acr2=acr2(2:end)';
acr3=acr3(2:end)';
acr4=acr4(2:end)';
a3 = [acr1;acr2;acr3];
a33 = [acr1;acr2;acr3;acr4];
Ssx(1)=x1;
Ssz(1)=z1*pi*(Sx+(1-sign(Sx))*x1)/180;
Ssr(1)=sqrt(Ssx (1)^2+Ssz (1)^2);
for i=2:length(a1)
   Ssx(i)=Ssx(i-1)+(vx(i)+vx(i-1))*dt/2;
   Ssz(i)=(Ssz(i-1)+(vz(i-1)+vz(i))*dt/2);
   Ssr(i)=sqrt(Ssx (i)^2+Ssz (i)^2);
   Ssr1(i)=Ssx(i-1)+(Ssx(i)-Ssx(i-1))*cos(Ssz(i)-Ssz(i-1));
end
```

```
h1= vx.^2/(2*g); %square of v1 divided by 2g
h2= vz.^2/(2*g);  %square of v2 divided by 2g
h3= vr.^2/(2*g);  %square of vr divided by 2g
y1= l*sqrt(g*(l-h1));   % square root of h1
y2= l*sqrt(g*(l-h2));   % square root of h2
y3= l*sqrt(g*(l-h3));   % square root of h3
dpphi=(a1./y1);
dttheta=(a2./y2);
dtthetar=(a3./y3);
yyy =[t dtthetar];
p1=[t dpphi];
p2=[t dttheta];
p3=[t dtthetar];
pphi(1)=0; ttheta(1)=0; tthetar(1)=0;
dtt =2:length(ttheta);
tt=dtt';
for i=2:length(t)
   pphi(i)=pphi(i-1)+dpphi(i);
   ttheta(i)=ttheta(i-1)+dttheta(i);
   tthetar(i)=tthetar(i-1)+dtthetar(i);
end
   pphi=dt*pphi;
   ttheta=dt*ttheta;
   tthetar=dt*tthetar;
   pphii=pphi';
   tthetaa=ttheta';
   ym=[t,pphii];
%======================  Angle theta  ============================
for i=1:length(t)
   phi(i)=pphi(i)*(-1)^i;
   theta(i)=ttheta(i)*(-1)^i;
```

```
   thetar(i)=tthetar(i)*(-1)^i;
end
p4= phi';
p5=[t theta'];
p6=[t thetar'];
figure(1);   % opens a figure window
plot(t,vx);     % plots trajectory versus time
hold on
plot(t,vz);
plot(t,vr);
title('Optimal Velocity-time curves')
legend('Velocity-x', 'Velocity-z', 'Resultant')
xlabel('time (seconds)')
ylabel('Velocity (m/sec)')
grid on
figure(2);
plot(ts,a11)
hold on
plot(ts,a22)
plot(ts,a33)
title(' Optimal Acceleration-time curves')
legend('Acceleration-x', 'Acceleration-z', 'Resultatnt')
xlabel('Time (seconds)')
ylabel('Acceleration (m/s^2)')
grid on
figure(3)
subplot 121
polar(Ssz/(Sx+(1-abs(sign(Sx)))*x1),(Ssx),'r')
title('Direction of movement')
subplot 122
plot(t,Ssz)
```

```
hold on
plot(t,Ssx)
grid on
title('Displacements')
legend('Radial','Translational')
grid on
xlabel('Time (seconds)')
ylabel('Displacement (m)')
figure(4)
subplot(221)
plot(t,Ssz*180/(pi*(Sx+(1-abs(sign(Sx)))*x1)))
grid on
title(' Angular Displacement')
legend('Angle in z-dir')
xlabel('Time (seconds)')
ylabel('Angular (deg)')
subplot(222)
plot(t,Ssx)
title(' Translational Displacement')
legend('Translation')
grid on
xlabel('Time (seconds)')
ylabel('Displacement (m)')
subplot(223)
plot(t,Ssz)
title('Radial Displacement')
legend('Radial in z')
xlabel('Time (seconds)')
ylabel('Displacement (m)')
grid on
subplot(224)
```

```
plot(t,Ssr,'r-.')
hold on
plot(t,Ssr1,'g-')
legend('resultant 1','resultant 2')
grid on
title(' Two types of total Displacements.')
xlabel('Time (seconds)')
ylabel('Displacement (m)')
figure(5)
plot(t,phi)
hold on
plot(t,theta)
plot(t,thetar)
title('Sway angles in the three directions')
legend('phi', 'theta', 'thetar')
xlabel('Time (seconds)')
ylabel('Sway angles(rad)')
grid on
figure(6)
plot(t,pphi)
hold on
plot(t,ttheta)
plot(t,tthetar)
title('Magnitude of the sway angle')
legend('|phi|', '|Theta|', '|Thetar|')
xlabel('Time (seconds)')
ylabel('Sway angles(rad)')
grid on
figure(7)
plot(t,dpphi)
hold on
```

```
plot(t,dttheta)
plot(t,dtthetar)
title('Rate of Change Angle')
legend('d-pphi', 'd-ttheta', 'd-tthetar')
xlabel('Time (seconds)')
ylabel('Sway angles(rad/sec)')
grid on
```